AD 682062

FOREIGN TECHNOLOGY DIVISION

ADVANCES IN THE MECHANICS OF AEROSOLS
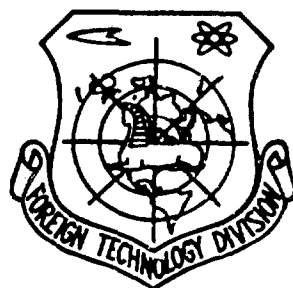
by

N. A. Fuks

FEb 17 1959

201

EDITED MACHINE TRANSLATION

ADVANCES IN THE MECHANICS OF AEROSOLS

By: N. A. Fuks

TM8501040

USPEKHI
MEKHANIKI
AEROZOLEY

Izdatel'stvo

Akademii Nauk SSSR

Moskva

1961

159 pages

DATA HANDLING PAGE

01-ACCESSION NO.	98-DOCUMENT LOC	39-TOPIC TAGS
TM8501040		aerosol, aerosol chemistry, adhesion, coagulation, electrostatic acceleration, laminar flow heat diffusion, particle collision, particle motion, thermal diffusion separation, turbulent flow, sound absorption
09-TITLE ADVANCES IN THE MECHANICS OF AEROSOLS		
47-SUBJECT AREA 07, 20		

42-AUTHOR/CO-AUTHORS		10-DATE OF INFO
FUKS, N. A.		54---59
43-SOURCE USPEKHI MEKHANIKI AEROZOLEY. MOSCOW, IZD-VO AN SSSR (RUSSIAN)		68-DOCUMENT NO. FTD-MT-24-4-68
		69-PROJECT NO. 72302-74

63-SECURITY AND DOWNGRADING INFORMATION	64-CONTROL MARKINGS	97-HEADER CLASN
UNCL, 0	NONE	UNCL

76-REEL/FRAME NO.	77-SUPERSEDES	78-CHANGES	40-GEOGRAPHICAL AREA	NO. OF PAGES
1884 1962			UR	192

CONTRACT NO.	X REF ACC. NO.	PUBLISHING DATE	TYPE PRODUCT	REVISION FREQ
94-00	65-	.	Translation	NONE

STEP NO.	ACCESSION NO.
02-UR/0000/61/000/000/0001/0159	TM8501040

ABSTRACT This is a second edition of an earlier book by the author "Mechanics of Aerosols" (1955). It digests the literature on the subject published between 1954 and 1959. During this time the mechanics of aerosols have been developed very erratically: on some problems--thermophoresis, diffusion-phoresis, inertial settling of particles at large Reynolds numbers, sound absorption by aerosols, gravitational coagulation--great successes have been achieved, on other problems--theory of sound coagulation, experimental study of coagulation in a turbulent flux--almost nothing has been done. So much new theoretical and experimental data has been collected in this area that the need arose for this book. Location of material and designations in the survey are the same as in the previous book, however for the Stokes number we have taken that presently accepted by the majority of authors, Stk = $\frac{1}{R}$ instead of Stk = $\frac{1}{2R}$. The footnotes give corrections of errors in this book which were detected after its publication. The text is broken down into the following chapters: 1. Dimensions and form of aerosol particles; 2. Uniform rectilinear movement of aerosol particles; 3. Nonuniform rectilinear movement of aerosol particles; 4. Curvilinear-rectilinear movement of aerosol particles; 5. Brownian movement and diffusion in aerosols; 6. Turbulent diffusion of aerosols; 7. Coagulation of aerosols; and 8. Transition of powders to aerosols.

TABLE OF CONTENTS

PREFACE

In the five years which have passed since the publication of the author s book "Mechanics of Aerosols," a great many works have appeared which pertain directly or indirectly to this field of knowledge. During this time the mechanics of aerosols have been developed very erratically: on some problems — thermophoresis, diffusion-phoresis, inertial settling of particles at large Reynolds numbers, sound absorption by aerosols, gravitational coagulation — great successes have been achieved, on other problems — theory of sound coagulation, experimental study of coagulation in a turbulent flux — almost nothing has been done. In any case, so much new theoretical and experimental data has been collected in this area that the need arose for "Advances in the Mechanics of Aerosols."

The survey of material published under this name envelops the literature published approximately from 1954 to the end of 1959, and also a small number of earlier works, omitted in the above-mentioned book. Location of material and designations in the survey are the same as in that book, however for the Stokes number we have taken that presently accepted by the majority of authors, $Stk = \ell_1/R$ instead of $Stk = \ell_1/2R$. Since in an account of new works it is necessary to constantly refer to older works, then for the convenience of the readers in these references in addition to the original articles we have also shown the corresponding places in the book

"Mechanic of Aerosols." Furthermore, the footnotes give corrections of errors in this book which were detected after its publication. The author expresses his sincere gratefulness to G. L. Natanson and L. M. Levin, who critically reviewed certain chapters of the survey, and I. B. Stechkina who performed a series of necessary calculations and computations.

C H A P T E R   1

DIMENSION AND FORM OF PARTICLES IN AN AEROSOL

At present the basic method for the determination of size of very small aerosol particles is electron microscopy which, however, inapplicable to particles of liquid and volatile substances. With the help of electron microsocope aerosol particles with $r \approx$ $\approx 10^{-7}$ cm [1] have been revealed. Another very important method of measuring the size of particles in highly dispersed aerosols is the so-called diffusion method (see p. 82). With it it has been established that in aerosols just formed in the corona discharge from a metallic point the radius of particles is equal to $0.5 \cdot 10^{-7}$ cm [2].

Since the time of Aitken meteorologists have determined the computing concentration of atmospheric aerosols, preliminarily condensing on particles of moisture, in counters of "nuclei of condensation," as these particles are usually called. Apparently only a very small portion of particles contained in the atmosphere (badly moistened by water) cannot be detected by this method. Junge [3], in investigating the distribution of dimensions of nuclei of condensation by different methods — with an impactor for large particles and based on electrical mobility for small particles — established that for particles with dimensions greater than 0.1 μm this distribution is expressed best of all by the formula

$$f(r) = C/r'.$$

(1.1)

FTD-MT-24-4-68

1

where C — constant.

Junge arrived at this formula in a lax way from the theory of coagulation of aerosols.

At present nuclei of condensation with r > 1 μm are called gigantic with a radius lying between 1 and 0.1 μm — large, and with r < 0.1 μm — Aitken.

Questions about the distribution of particle grades, about different average values, etc., are examined very thoroughly in the book by Herdan [4].

Here it is appropriate to touch upon the question about advantages of working with isodispersed aerosols. As is shown by an analysis of experimental works on filtration of aerosols, their precipitation in different apparatuses, in the respiratory system, etc., work conducted with isodispersed aerosols as a rule gives more exact and reliable results. This is explained by the fact that when working with polydispersed aerosols it is necessary to determine not only the distribution of particle grades before and after precipitation, but also the absolute number of particles in each fraction, and for this it is necessary to count (usually with the help of a microscope) a very large number of particles in each fraction. Such measurements usually made visually (only the first steps in their autoautomation have been taken), are so labor-consuming that only a few authors carry them out to the required extent.

Switching to the complex question about the nature of the degree of dispersion of aerosols with nonspherical particles, let us note that recently in connection with the appearance of photoelectrical apparatuses for the automatic counting and measuring of particles precipitated on transparent sublayers [5], singular importance has been acquired by the "projected" radius introduced by Heywood [6], i.e., the radius of a circle, the area of which is equal to the area of projection of a particle on the surface of the sublayer,

since in the majority of these apparatuses it is exactly this value
which is being determined. Furthermore, in the well-known visual
method of determining particle grade under a microscope with the
help of ocular discs, discs will also be selected with an area
approaching the area of image of the particle.

We will not dwell on other methods of expressing the grade of
particles with an irregular shape. We will only note that the
important problem of determination of vertical dimensions of
particles, lying on a base layer, in optical and electron microscopy
is presently being resolved by means of subshadowing [Editor's NOTE:
podteneniye, Russian word not confirmed] of particles in a vacuum
at a very small angle to horizontal. The question about the influence
of the method of precipitation of particles with an irregular shape
on results of their microscopic examination is examined on page 7.

In connection with the observations by I. Artemov [7] about the
influence of humidity on the rate of coagulation is NH_4Cl mists, we
will mention the observations by Dallavalle and Orr [8], according
to whom the rate of sedimentation of aerosols of MgO and, especially,
NH_4Cl is considerably increased in a humid atmosphere. Microscopic
examination shows that aggregates of particles become more compact
under these conditions. In all probability this is caused by
capillary constriction of aggregates by the condensed water film.

C H A P T E R   2

RECTILINEAR UNIFORM MOVEMENT OF AEROSOL PARTICLES

Resistance of a Medium to Movement
of Spherical Particles

For new technology there is great interest in the question of resistance of a medium at very high speeds of motion of particles. For particles, the size of which is considerably less than the length of free path of gas molecules, and at velocities V, comparable with the average velocity of molecules $\overline{G}_g$, Tsien [9] and Krzywoblowski [10] derived the formula

$$F_M = -\tfrac{1}{2}\pi r^2 n_g m_g V^2 f (V, \overline{G}_g).\qquad (2.1)$$

In which f is a rather composite function. At $V \gg \overline{G}_g$

$$F_M \approx -\pi r^2 n_g m_g (V^2 + \overline{G}_g^2).\qquad (2.2)$$

We will define the question about the value of constants A, Q and b in the Millikan expression for resistance of a medium

$$F_M = -6\pi\eta r V \left[1 + A l/r + Q\,(l/r)\,e^{-br/l}\right]$$

Millikan took in the formula for viscosity of gas $\eta = \theta n_g m_g G_g l$ $\theta = 0.350$, whence for air at 760 mm Hg column and room temperature it follows that $l = 0.942 \cdot 10^{-5}$ cm.

At present the value θ 0.499 is generally accepted and, accordingly, $\ell = 0.653 \cdot 10^{-5}$ cm. Here the Millikan values of constants should change in the following way: $A = 1.246$, $Q = 0.42$ and $b = 0.87$. The data mentioned below are relative to $\ell = 0.653 \cdot 10^{-5}$ cm.

For oil drops in the air Mattach [11] found $A = 1.300$, $Q = 0.45$, $b = 3.42$. Schmitt [12] worked with drops of silicone oil ($r = 0.7-1.2$ μm) in different gases at pressures of 10-760 mm Hg column and in nitrogen obtained $A = 1.45 \pm 3\%$, $Q = 0.40 \pm 10\%$ and $b = 0.9 \pm 20\%$. These values for Q and b are very close to Millikan; the values of A and sums of A + Q are considerably larger than for Millikan and theoretically are possible only with a very large ($\sim$50%) percentage of specular reflection of gas molecules from the surface of the droplets [13].

Investigating water droplets with $r = 0.4-1.0$ μm in Millikan a condenser filled with water vapor saturated air, Gokhale and Gatha [14] found $A = 1.032$.

For certain aerosol investigations there is interest in the problem of resistance to motion of a spherical particle along the axis of a cylindrical capillary. The expression [15] derived by Faxen

$$F_u = -6\pi\eta r V/[1 - 2.104\, r\, R + 2.09\,(r\,R)^3 - 0.95\,(r\,R)^5].$$
(2.3)

where r/R − ratio of radii of particle and capillary, according to model experiments by Bacon [16] is observed accurately at Re $\leq$ 0.02 and r/R < 1/3.

Rotation of Particles in a Gradient Flow

From the general formula for velocity of rotation of an ellipsoidal particle, found in a laminar flow with gradient of velocity Γ [17]

$$\frac{d\theta}{dt} = \frac{\Gamma\,(a^2\cos^2\theta + c^2\sin^2\theta)}{a^2 - c^2}$$
(2.4)

It follows that for spherical particles

$$\frac{d\eta}{dt} = \frac{\Gamma}{2}.$$
(2.5)

This formula was accurately confirmed in model experiments with glass balls (r = 75-140 μm) in corn molasses at Γ = 0-1.6 s^{-1} [18].

Based on the experiments by Sharkey [19], following the isokinetic introduction of a thin stream of soot suspension into a laminar current of water through a tube, the stream gradually shifts to the axis of the tube. The further the point of issue of the stream from the axis and the greater the speed of flow, then the faster the shift. In the opinion of the author this phenomenon is caused by the Magnus force, induced by the rotation of particles of soot in the gradient flow. It is necessary to note that for the development of the Magnus effect it is necessary that the rotating particle possess forward motion with respect to the medium. This was absent in the experiments by Sharkey. Actually, based on the experiments of Manley and Mason [20] no transverse forces act on spherical particles moving in a gradient flow. Furthermore, the Magnus formula is obviously applicable only at fairly large Re numbers. At small Re, according to the calculations of Garstang [21], the frontal force acting on a spherical particle which is rotating around an axis perpendicular to the direction of forward motion does not differ from the force in the absence of rotation. Lateral force is most probably equal to zero or is directed to the side opposite the Magnus force.

An analogous explanation is given by Tollert [22] with his observations, according to which during the settling of a system of spherical particles in a vertical tube with liquid or air (at Re = = 500-7000) the density of the deposit forming on the bottom of the tube increases from the periphery to center. In this case only beads falling near the wall have to rotate, but the direction of rotation is apparently such that the Magnus force should be directed not to the axis, but to the wall of the tube.

Resistance of Medium to Motion Nonspherical Particles

The question of orientation of moving nonspherical particles is of great importance during microscopic examination of precipitated aerosols. According to the observations of Cruize [23], confirmed also by other authors [24], in the deposits obtained in a thermoprecipitator the particles are oriented randomly. During sedimentation under the effect of force of gravity in a fixed medium or in a laminar flow the majority of particles descends on the surface in the stablest position (flat). Unfortunately the particle size in the experiments by Cruize is not given. According to data by Timbrell [25], random orientation of particles also takes place during sedimentation. Apparently the reason for this difference is the fact that in one case the experiments were conducted with larger and in the other with smaller particles, i.e., at different Re numbers. The fact that in a conifuge [Editor's NOTE: Konifug, Russian word not confirmed] [26] the particles fall flat [27] is also understandable, since here the settling rate is great.

Switching to the sedimentation rate of nonspherical particles, let us note that the term "Sedimentational radius" is more preferable than the commonly used term "Stokes radius," since this idea is not connected with the Stokes formula and is fully applicable to those large and small particles for which the Stokes formula is clearly unsuitable. In certain cases, for example, in aerosols consisting of particles with a different density, it is useful to apply another value, which we will call the "reduced sedimentation radius" of particle. This is the radius of a spherical particle with a density equal to 1 and with the same rate of sedimentation.

Timbrell [28] proposed a convenient method for measuring the sedimentation radius r_S of aerosol particles with an irregular shape. For this spherical particles from glass, polystyrene, etc., are added to the aerosol. A narrow stream of the aerosol is introduced isokinetically into the middle (by height) of the horizontal plane-parallel channel, through which the laminar flow of air is taking

place. On the bottom of the channel is a transparent sublayer, on which the particles are collected. Then they are examined under a microscope. Based on the size of beads they determine r_S of particles of irregular shape, aggregates, etc., which have settled side by side with them. In order not to make a very long channel for precipitation of small particles, they use a channel which expands to the sides. For determining the radius of very small particles this method is apparently unsuitable since it is exceedingly difficult to completely remove thermal convection in the channel. Furthermore, observance of one more important condition is necessary — a sufficiently small concentration by weight of the aerosol in order to avoid settling of the stream as a whole [29].

In this instrument Timbrell investigated the dependence between projected r_{pr} (see pp. 2-3) and sedimentational r_S radius of particles of glass and carbon. Here, as was noted above, the majority of particles was oriented randomly. The r_S/r_{pr} of glass particles varied strongly — from 0.5 to 1.1. Mean value of r_S/r_{pr} equaled 0.67 for glass and 0.74 for carbon particles.

Timbrell also determined the r_S of doublets from glass beads. With an identical radius r of the particles making up the doublet, its r_S equals on the average 1.13 r (orientation of doublets was apparently horizontal). For the dynamic form factor of doublets κ (i.e., ratio of resistance of medium to motion of doublets and spherical particles having the same volume) from these data follows the clearly oversized value $\kappa = 1.24$. In model experiments Eveson and others [30] measured the sedimentation rates of the same doublets in a viscous liquid at Re < 0.2. With a horizontal position of doublets, $\kappa = 1.15$ is found, and with a vertical $\kappa = 1.04$. Based on the theoretical calculations of Faxen [31] in the last case $\kappa = 1.023$.

Gurel et al. [32] offered an empirical formula for calculating the sedimentation rate of particles with a more or less isometric form based on their volume and surface, however this formula is

8

clearly unsuitable even for the simplest case of spherical particles.

Chowdnury and Fritz [33] from their model experiments with beads, cubes, octahedrons, and tetrahedrons at $Re < 0.2$ obtained the formula

$$x = 1/(1 \div 0.862 \lg x_s). \qquad (2.6)$$

where κ_s — coefficient of sphericity, i.e., ratio of the surface of a sphere with a volume equal to the volume of the given body, to the surface of the latter. Values of κ calculated by this formula are close to those found by other authors.

In the work by Ludwig [34], who measured the sedimentation rate of cylinders in a viscous liquid at small Re, the orientation of the cylinders is not shown, and the results differ very strongly from those obtained by other authors.

Van der Leeden et al [35] measured rates, obtainable with drops of water, of solutions of surface-active substances and certain organic liquids with $r = 1.8-3.0$ mm when falling from different heights. Considering that air resistance does not depend on acceleration, but is determined only by the velocity of the drops, the authors determined the value of the coefficient of frontal resistance of the drop ψ in formula $F_\mu = -\psi \pi r^2 \gamma_\epsilon V^2/2$ in which r signifies in this case the radius of an undeformed drop. Since with a noticeable deformation of falling drops Re equals 1000-3000, and in this region of Re values ψ for a sphere has almost a constant value ~ 0.4, then here ψ is a function of only the form of drops. Using the well-known graph of distribution of pressures on a surface of a streamlined sphere, Hinze [36] calculated the change of form of falling drops. In the first approximation, mistaking deformed drops for oblate ellipsoids, Hinze found that relative decrease of drop radius in the direction of motion is equal to 0.069 We, where $We = \gamma_\epsilon r V^2/3$ — Weber number, σ — surface tension of liquid. Using ψ values for ellipsoids which were found from

9
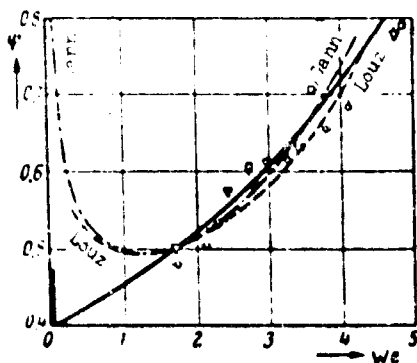
Fig. 1. Resistance of medium
to motion of liquid drops.
Solid curve — theoretical.

experiments in a wind tunnel [37] and the Hinze formula,
Van der Leeden et al. obtained a theoretical curve (ψ, We),
satisfactorily agreeing at We $=$ 1-5 with experimental data from
the author himself and other researchers (Fig. 1.).

Movement of Aerosol Particles in Limited Space

The question of sedimentation rate of a system of particles in
limited space (usually called "restricted settling"), which is of
great interest for technology, in recent years has been treated
in very many theoretical and experimental works. Here we will give
only those forms of equations found which are obtained at very
small volume concentrations of the dispersed phase ϕ.

Proceeding from the idea of Cunningham [38], but taking into
account the reverse movement of the medium, Happel [39] and
Kuwobara [40] obtained for the ratio of sedimentation rate of a
system of particles and an isolated particle at $\phi \to 0$ the formula
$V_s'/V_s = 1 - k\phi^{1/3}$ with k = 1.5 [39] and 1.62 [40]. Brinkman [41]
derived the formula $V_s'/V_s = 1-2.1\phi^{1/3}$, and Hauxley [42] the formula
$V_s'/V_s = 1-4.5\phi$.

In experiments conducted with more or less isodispersed
suspensions, only one author [43] obtained the formula $V_s'/V_s = 1-2.1\phi^{1/3}$.
Results of all the other works are expressed by the formula
$V_s'/V_s = 1 - k\phi \approx (1 - k\phi)^{-1}$ with k = 4.0 [44, 45]; 4 [46] and 5.4 [47].
Thus, our earlier conclusion [48] that in the expression for rate
of restricted settling at small concentrations ϕ should remain in

18

the first power is as if confirmed, however, further efforts are required for the theoretical foundation of this conclusion.

The basic difficulty in precis'on measurements of the ratio V_S'/V_S at small ϕ is convection. As Wilson points out [49], in very diluted aqueous suspensions of glass beads with $r = 1-5$ um at room temperature it is impossible to obtain strictly vertical trajectories of particles; this turned out to be possible only at $4°$, i.e., with the coefficient of thermal expansion of water equal to zero. Only in more concentrated suspensions and aerosols the downward gradient of concentration is sufficiently great to suppress convection. This circumstance is frequently ignored; furthermore, in aerosols which are not very coarsely dispersed it is difficult to combine two conditions — sufficiently high weight and sufficiently small computing concentrations (at which it is possible to disregard coagulation). Therefore, in the majority of works based on sedimentometric analysis of aerosols apparently large errors are committed.

Method of Vertical Electrical Field

Until recently the most exact method for investigation of aerosol particles, the method of vertical electrical field, was inapplicable to large particles: for suspending such particles in a Millikan capacitor it required such a great field strength that the phenomena of ionization, discharge, etc. began. According to the observations of Straubel [50], in the center of a horizontal metallic ring which is connected with a source of alternating current, with a voltage of several kilovolts it is possible to suspend and observe for a prolonged time drops up to 100 um in size. Here the small drops accomplish vertical fluctuations, but the large ones are practically stationary.

A similar but more improved and complex device for suspending large particles has been developed by Wuerker et al. [51]. The authors used a capacitor with convex plates, divided by an isolated convex ring. Between the plates, and also between them and the

11

ring adjustable potential differences were maintained. These consisted
of constant and variable components, creating a nonuniform field
in the capacitor. In the capacitor an adjustable vacuum was
maintained from 10^{-4} to 10^{-2} mm Hg column. From charged particles
of aluminum (r ≈ 10 μm) introduced into the capacitor at specific
values of potential particles were retained, which had a charge-to-
mass ratio of particles q/m lying in definite limits, and the
others were ejected by the field from the capacitor. By regulating
the value of potentials and frequency of fluctuations it was possible
to control the position and nature of particle fluctuations and to
accurately determine q/m. With an increase of pressure in the
capacitor amplitudes of particle fluctuations decreased due to an
increase of air resistance. The device is convenient for investigating
laws of resistance of a gaseous medium at small values of r/ℓ, with
particle fluctuations corresponding to large Re numbers, and for
studying a number of other problems in the mechanics of aerosols.

Thermophoresis and Diffusion-Phoresis

During the last few years much new data has been obtained on
thermophoresis of aerosols. On the basis of the modern theory of
phenomena of transfer in gases, Waldman [52] and B. Deryagin and
S. Bakanov [53] derived a more accurate equation for thermophoretic
force at r << ℓ. According to Waldman

$$F_T = -\frac{32 r^2 \varkappa_a \Gamma_a}{15 G_a} \cong -\frac{4 r^2 \Gamma_a / p}{\Gamma}.$$ (2.7)

where Γ_a — gradient of temperature in the gas, i.e., 8/π times
greater than the formula, derived by the elementary method, of
Einstein-Cawood[1] [54, 55]

$$F_T = -\frac{\varkappa r^2 \Gamma_a / p}{2 T}.$$ (2.8)

The accommodation coefficient for gas molecules on the surface of
particles is accepted as equal to 1. Thus, in this case the
radiometric force is proportional to the square of radius of
particles and does not depend on pressure, since pℓ = const. In

formula (2.7) κ_a signifies the relay segment of thermal conductivity of gas equal to $(15/4)$ $k\eta/m_g$, and for η the expression $\eta =$ $= 0.499$ $n_g m_g G_g \ell$ is taken.

The rate of thermophoresis at $r \ll \ell$ is equal to

$$V_T = -\frac{\varkappa_a \Gamma_a}{5\rho(1 + \pi a/8)} = -\frac{3G_g \Gamma_a}{8(1 + \pi a/8)T}. \qquad (2.9)$$

Here α is the fraction of diffusely-scattered particles of gas molecules.

In the formula of Bakanov and Deryagin $15\pi/128 (\approx 0.368)$ stands in place of $3/8 (\approx 0.375)$.

Thus V_T does not depend on particle size and weakly (through α) depends on their nature. F_T and V_T are connected together, as it is easy to ascertain, by the formula of Epstein [56] for mobility of particles at $\ell \gg r$.

In case $r \gg \ell$ the thermophoretic force is expressed [57] by the formulas

$$F_T = -\frac{9\pi \varkappa_a \eta^i r \Gamma_a}{(2\varkappa_a + \varkappa_i)\tau_g T} \qquad (2.9a)$$

(κ_1 - thermal conductivity of substance of particle). Since the thermal conductivity of gases is considerably less than the thermal conductivity of solid and liquid bodies, then for the rate of thermophoresis we obtain formula

$$V_T = -\frac{3\varkappa_a \eta \Gamma_a}{2(2\varkappa_a + \varkappa_i)\tau_g T} \approx -\frac{\varkappa_i \eta_a \Gamma_a}{\varkappa_i T}. \qquad (2.10)$$

Schmitt [12] used a Millikan capacitor with a heated upper plate to investigate thermophoresis of drops of silicone oil and paraffin

13

with $r = 0.7-1.2$ μm in various gases at pressures of 10-760 mm Hg column, i.e., in an interval of r/ℓ values approximately from 0.3 to 20. From the data obtained by the author it follows that approximately at $r/\ell \lesssim 0.4$ F_T practically no longer depends on pressure, i.e., according to the formula (2.7) here conditions of thermophoresis "at small r/ℓ" begin. Measurements showed further that at $r/\ell \lesssim 0.31$ F_T indeed is strictly proportional to r^2. Figure 2 shows the plot of lg F_T in function r/ℓ for drops of silicone oil of various size in argon. Since at $r/\ell < 5$ the plots are linear, then $F_T = F_{T0}$ exp $(-br/\ell)$, where F_{T0} corresponds to $r/\ell \to 0$. In all the gases, besides H_2, $b \approx 0.38$. The ratio of theoretical values of F_{T0} (formula 2.7) to experimental equals 1.05 in ar, 1.21 in N_2, 1.22 in CO_2 and 1.36 in H_2 (in H_2 the accuracy of measurements is doubtful due to the great rate of thermophoresis). A still better conformity with theory is obtained by the author for the rate of thermophoresis V_T (formula 2.9), in which he considers $\alpha = 1$. However, this contradicts data of the author about the mobility of particles (see p. 4).
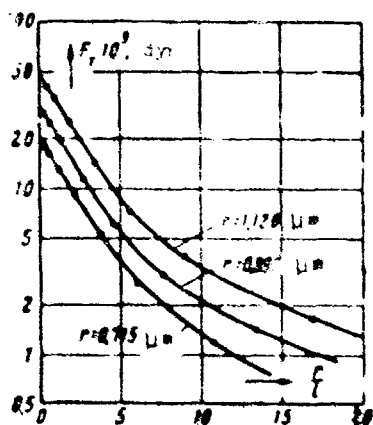
Fig. 2. Thermophoresis of drops of silicone oil in argon. Γ — 49.4 deg/cm.

Figure 3 gives the graph $V_T^* = pV_T/760$ (p — pressure in mm Hg column) in the function $r^* = pr/760 = 0.065 \cdot 10^{-4}$ r/ℓ (for drops of silicone oil), from which it is clear that, starting with $r/\ell \gtrsim 15$ the rate of thermophoresis ceases to depend on the size of particles, i.e., the area of "large r/ℓ begins. Thus, the
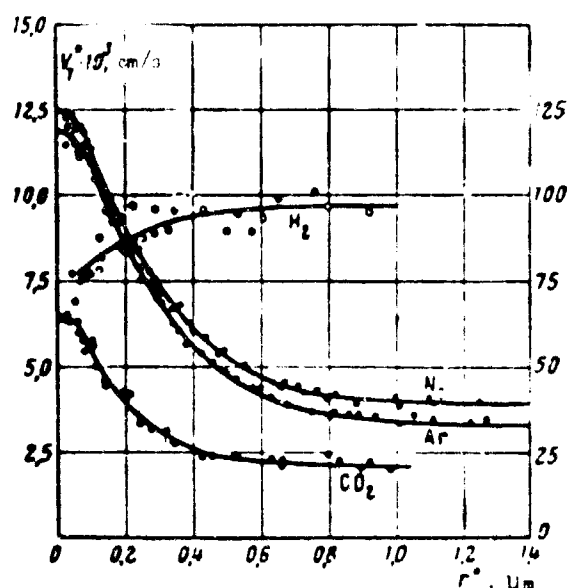
Fig. 3. Dependence of
rate of thermophoresis
on radius of droplets.
Γ — 49.4 deg/cm. On the
right — scale for H_2.

transition region spreads approximately from $r/\ell = 0.4$ to 15. The
influence of thermal conductivity of particles on F_T starts to
have an effect already at $r/\ell \approx 3$. The fact that in H_2 the rate
of thermophoresis of large particles is greater than of small is
explained by the exceedingly great thermal conductivity of H_2.

At large r/ℓ the ratio of theoretical and experimental values of
V_T equals 0.83 in ar, 1.09 in N_2, 0.71 in CO_2, and 1.07 in H_2.

From formulas (2.9) and (2.10) it follows that the ratio of
rates of thermophoresis of particles with $r \ll \ell$ and $r \gg \ell$ equals
approximately $0.4 \; \kappa_1/\kappa_a$. In air $\kappa_a \approx 6 \cdot 10^{-5}$ (cal·deg^{-1}·s^{-1}) this
ratio for particles of organic substances has the value 2-4, NaCl $\approx$
$\approx$ 100, for Fe $\approx$ 1000. Taking into account the work of Schadt and
Cadle (see below) the two last numbers, respectively, should be
decreased approximately to 4 and 20. As can be seen from the data
of Schmidt, the transition from formula (2.9) to (2.10) occurs in
air at an atmospheric pressure in an interval of r values of
approximately 0.025-1 um. In this same interval the rate of
thermophoresis should continuously decrease with the increase of r.
Therefore, in deposits obtained in a thermoprecipitator the average
size of particles should continuously increase from front (turned
toward the flow) to the trailing edge of the deposit. This has

15

—————• Direction of flow
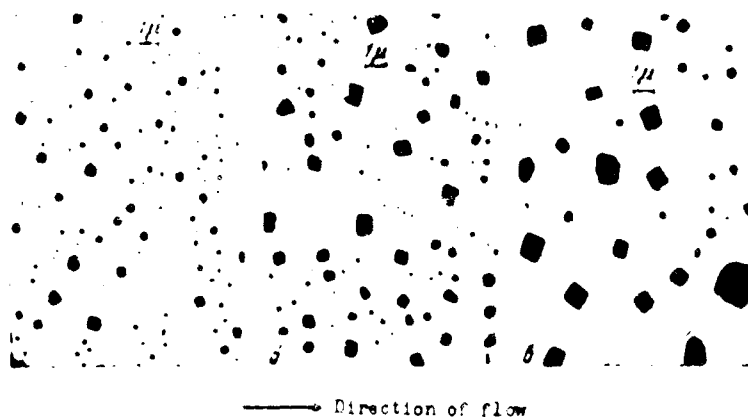
Fig. 4. Segregation of NaCl particles in
thermoprecipitator.

already been noted in the literature [58]. For an illustration we
present the photographs from different sections of a deposit of a
very polydispersed aerosol of NaCl in a thermoprecipitator
(Fig. 4, [59]). These were taken on an electron microscope.
Similar photographs were obtained recently by Thermer [60] with a
mist of MgO. It is necessary to note, however, that segregation
of particles by size continues in the thermoprecipitator also in the
region $r > 1$ μm, where it should have theoretically ceased. Besides
the data of Fig. 4 this is indicated by the well-known fact that
starting with $r = 2$ μm the effectiveness of precipitation in
thermoprecipitators begins to decrease noticeably with an increase of
r [61]. As calculations show [59], it is impossible to explain
this phenomenon by inertia of particles, their rotation in the flow,
and repulsion from the wall. It is possible that large particles are
torn down by the airstream. This question still remains
unanswered.

Schadt and Cadle [62] passed different aerosols — comparatively
monodispersed aerosols of stearic acid with $\bar{r}$ from 0.15 to 2.5 μm,
polydispersed aerosols of NaCl with $\bar{r} = 0.1$ and 0.2 μm, glycerine
with $\bar{r} = 0.25$ and 0.5 μm, and Fe with $\bar{r} = 0.7$ μm — through a
thermoprecipitator with heated tape 1.4 mm wide. Between the tape
and the plug of the precipitator a plane-parallel slot with a width
of 0.15 mm was obtained. Having measured the temperature of the

tape and width of the precipitation band and disregarding thermal convection in the precipitator the authors calculated the value of the ratio $\beta_e = F_T/r\Gamma_a$ and compared it with theoretical value of this ratio β_t, calculated by the formula of Epstein. There is a great deal of scattering in the values β_e, nevertheless it is clear from them that for particles with low thermal conductivity (stearic acid, $\kappa_1 = 3.0 \cdot 10^{-4}$, glycerine — $6.4 \cdot 10^{-4}$) β_e and β_t are values of one order, while for NaCl ($\kappa_1 = 1.5 \cdot 10^{-2}$) β_e on the average is 25 times, and for Fe ($\kappa_1 = 1.6 \cdot 10^{-1}$) — 50 times greater than β_t.

Thermophoretic force for particles of organic substances and NaCl is approximately identical, and for Fe it is approximately 5 times less. This divergence cannot be explained by electrical effects, since tape was connected with the precipitator housing. Let us note that all the measurements of thermophoresis in the Millikan capacitor were conducted with droplets of organic liquids which possess low thermal conductivity. This also explains the concurrence with theory obtained in these measurements. If the formula of Epstein was applicable in all cases, then metallic aerosols practically would not be precipitated in a thermoprecipitator.

In the application of a thermoprecipitator for investigation of aerosols under an electron microscope the temperature of the grid (or diaphragm) on which the film is deposited is considerably lower than the temperature of free sections of film, and therefore particles are precipitated chiefly on the wires of the grid and connot be photographed. Certain authors [63, 64] consider that due to the dependence of rate of thermophoresis on dimension of particles errors appear in the determination not only of concentration, but also distribution of dimensions of particles. This question still is not clarified; the stated difficulties can be eliminated if precipitation in the thermoprecipitator is done on free film, and then the grid is placed under it [64].

Based on the experiments of Watson [65], during lateral illumination the thickness of the "black" layer surrounding the

heated bodies, i.e., a layer not containing aerosol particles, is approximately constant over the entire height of the body and is expressed by the formula

$$h = K (T - T_0)^{\alpha} p^{-\beta}.$$

(2.11)

where K — constant, $T - T_0$ — difference of temperatures of body and medium, p — pressure of gas. Value of indices $\alpha \approx 0.5$, $\beta \approx 0.6$. Theoretical calculation of h was performed by Zernik [66]. In his opinion the thickness of the black layer is determined by the interaction of two factors — thermophoresis and a comparatively small, normal to surface (and directed toward it), component U_n of free convection of gas. U_n was calculated theoretically by Schmidt Beckmann [67] and determined experimentally by Kraus [68] for cases of a vertical plate and horizontal cylinder. Taking in the first expression for V_T (2.10) $\kappa_1 = 0$ (which of course cannot be done since $\kappa_1 > \kappa_a$), Zernik obtained for the middle of the plate and for a horizontal passing through the axis of the cylinder values for h which were close to those found by Watson [65]. It is necessary to note, however, that according to the theory of Zernik for the lower edge of a heated body $h = 0$ and is gradually expanded upwards, while according to the figures of Watson h is more or less constant. Furthermore, as the author himself points out, his calculations are applicable only at numbers $Gr = 10^4 - 10^9$, whereas in the experiments of Watson $Gr = 5 \cdot 10^2 - 5 \cdot 10^4$. Further, the following is still incomprehensible: in these experiments a very clear-cut limit of the black layer was observed, even in the case of a very polydispersed aerosol of MgO with $r = 0.05-1$ μm, and the thickness of the layer was identical for various aerosols. All these facts indicate that the concurrence of theory with experiment obtained by Zernik was apparently accidental.

It is necessary to note that for technology there is much greater importance in the reverse case of thermophoresis — solid aerosol particles settling on the cold walls of boilers and heat exchangers made of hot gases will form a layer with low thermal conductivity, considerably reducing heat transfer, the efficiency factor of boiler plants, etc.

18

Recently a series of experimental works [69, 70] has appeared in which detailed investigations have been made of different optical factors on which the sign of photophoresis (positive or negative) depends. In the article by Rohatschek [71] the theory of different types of complet photophoresis (magnetophotophoresis, gravitation photophoresis, etc.) is thoroughly expounded.

Aitken [72] already noted that in the vicinity of bodies moistened by volatile liquid a black layer will be formed even in the absence of temperature difference. This observation was then confirmed by Watson [65]. Facy [73] described the formation of a gradually thickening black layer at the surface of an evaporating water droplet. Conversely, during condensation of supersaturated steam on a droplet aerosol particles move to it and are absorbed. Facy gave an inaccurate explanation of these phenomena: he considered that a phenomenon of diffusion-phoresis which is analogous to thermophoresis takes place here, i.e., movement of particles caused by the gradient of concentration of components of the gas mixture. As we will see below, diffusion-phoresis indeed exists, however, in the experiments of Aitken, Watson, and Facy the basic role is played by another phenomenon, also induced by gas diffusion, the Stefan flow, i.e., hydrodynamic flow of a steam and gas mixture, directed normally to the surface of an evaporating liquid and compensating diffusion of the gas to this surface [74]. Attention was first turned to this by B. Deryagin and S. Dukhin [75]. Rate of this flow

$$U = - \frac{D_g \, \text{grad} \, c'}{c'}. \tag{2.12}$$

where c' — concentration of gas, D_g — coefficient of diffusion of gas (or vapor) in a mixture of one and the other. In case of a spherical droplet with radius R

$$U = \frac{D_g (c_S - c_\infty) R M'}{c' r^2 M} \tag{2.13}$$

where c_S — concentration of vapor at the surface of drop, c_∞ — far

from it, ρ — distance from center of drop, M and M' — molecular
weights of vapor and gas.

Movement of aerosol particles, induced by Stefan flow in a number
of cases has a significant value. Thus, during precipitation of
aerosols by atomized water, in particular in a Venturi scrubber,
with gas unsaturated by water vapor Stefan flow prevents, and with
supersaturation promotes the capture of particles by drops. Therefore
heating of water atomized in the neck of the scrubber and increasing
the evaporation rate of drops noticeably lowers the effectiveness of
the scrubber [76]. As Facy points out [73], during condensation of
vapor on drops of natural clouds and fogs an intensive destruction
of nuclei of condensation takes place. On the other hand, the
opinion expressed by Aitken [72] and others [75] that Stefan flow
prevents the settling of aerosols in the lungs is apparently
incorrect, since inhaled air is saturated by water vapor (and is
heated) already in the traceae [77].

A theory of diffusion-phoresis has been developed by B. Deryagin
and S. Bakanov [78] and Waldmar [52] for the case $r \ll \ell$. In a
binary gas mixture the velocity of an aerosol particle equals,
according to Waldman,

$$ V_D = \frac{(m_1' \delta_1 - m_2' \delta_2) D_g \, \text{grad} \, n_1}{n_1 m_1' \delta_1 + n_2 m_2' \delta_2}, \tag{2.14} $$

where m — mass, and n — concentration of molecules of components,
$\delta = 1 + \pi\alpha/8$. Here the velocity of a particle is attributed to the
system of coordinates in which the algebraic sum of all the gas
molecules, intersecting the area element normal to the gradient of
concentration, is equal to zero. If the gas is in a closed vessel
and the gradient of concentration is identical everywhere, such a
system will be a fixed system of coordinates. Here V_D is directed
to that side in which the heavier gas diffuses (with small
differences in the value of coefficient δ). The reason for
diffusion-phoresis in this case is the following: the percentage

of heavier molecules, i.e., those possessing a great deal of momentum bombarding the particle from one side is greater than from the other side.

In the equation derived by Bakanov and Deryagin, V_D is expressed not through D_g, but through masses and radii of gas molecules, therefore the equation is more complex.

Let us underline once again the distinction between diffusion-phoresis and movement of particles in Stefan flow. As can be seen from equation (2.14), at $m_1'' \delta_1 \quad m_2' \delta_2$ diffusion-phoresis vanishes, while Stefan flow is preserved.

In examining the rate Φ of precipitation of an aerosol with concentration n_0 on a spherical drop along with condensation of vapor on it, i.e., during the joint action of diffusion of particles themselves and Stefanov flow, B. Deryagin and S. Dukhin [67] arrived at the formula[2]

$$\phi \quad \frac{4\pi D_g R (c_\infty - c_s) n_\bullet}{c \left[\exp\left[D_g (c_\infty - c_s) / x\right] - 1\right]},$$ (2.15)

where D — coefficient of diffusion of aerosol particles. We see from here that Stefan flow does not affect precipitation of an aerosol on a drop only at small values of the ratio $D_g (c_\infty - c_s)/D c$. By formula (2.15) it is easy to calculate the effect of Stefan flow during absorption of condensation nuclei by clouds.

A direct measurement of repulsion forces which effect aerosol particles near an evaporating drop was undertaken by P. Prokhorov [79]. A measurement was made of the force effecting a silvered glass bead with $r \approx 1$ mm at various distances from a water drop with $r = 2$ mm. Basic difficulty in these experiments was presented by convection currents, caused by a lowering of temperature of the evaporating drop. For eliminating convection the drop was heated to air temperature with the help of a thin metallic filament. In

spite of these measures of precaution the measured forces turned out to be ~2 times greater than those calculated by the formula of Stokes and (2.13).

Till now we have examined diffusion-phoresis of "neutral" particles, i.e., those which do not interact with the gaseous environment. S. Dukhin and B. Deryagin [80, 81] investigated the behavior of a drop of volatile liquid in a medium with a gradient of concentration of vapor the same as that of the liquid. In this case the drop moves in the direction of the gradient with a speed equal in first approximation (at $c \ll c'$) $V_D = D_s$ grad c/c'. It is easy to understand the cause of this phenomenon which the authors call "diffusion polarization" of a drop: on that half of the surface of the drop which is turned in the direction of a decrease in concentration of vapor, the evaporation rate, and consequently also the Stefan flow and rebound force induced by it are greater than on the opposite half; therefore the particles will move in the direction of increase in concentration of vapor. If the gradient of concentration is created by evaporation of a liquid, then, as can be seen from formula (2.13), diffusion-phoresis is exactly compensated by Stefan flow and in first approximation the drop will be stationary. It is a different matter if the temperature of the drop and the surface from which evaporation occurs are different: if the drop, as this usually occurs, received a psychrometric temperature T_p, then with a surface temperature less than T_p the drop will be attracted to it, and in the opposite case be repulsed. This is easy to understand from the above-cited reasoning. Therefore freezing drops of natural clouds repulse and melting icicles attract water drops.

In the second approximation even at an identical temperature of evaporating drops between them there should appear a small force of interaction, the sign of which depends on the substance of the gas and liquid. For water drops in air this is a repulsive force.

V. Fedoseyev and A. Polyanskiy [82] measured the repulsive force between two evaporating water drops with r = 1 mm at 20° and

60% atmospheric humidity and found that with a distance of 0.1 mm
between drops this force is equal to $1.6 \cdot 10^{-4}$ dyn. Since the authors
took no measures to eliminate convection, then from these data it is
difficult to make any conclusions.

In work [83] an analysis is made of the thermophoretic effect
induced by cooling of evaporating drops for cases of nonevaporating
and evaporating aerosol particles. Here the authors disregarded
diffusion effects. Whereas calculation shows that depending on the
properties of the liquid, particles, and gas, and on the particle
size either force can predominate, i.e. either attraction or
repulsion develops. In the experiments described up to now
repulsion of particles from the surface of evaporation was always
observed, i.e., a predominance of diffusion effects.

Footnotes

[1]In the book "Mechanics of Aerosols" instead of formula (2.8)
the formula (16.1) is erroneously inserted. It expresses the
photophretic force acting on particles of aerosols at r << ℓ. Also
relative to photophoresis are formulas (16.3)-(16.6) in this book.

[2]The problem of the introduction of factor M'/M just as in
formula (2.13), is complex and will not be discussed here.

C H A P T E R 3

RECTILINEAR NONUNIFORM MOVEMENT OF AEROSOL PARTICLES

Nonuniform Movement of Particles at Small and Large Re Numbers

In the case of nonuniform movement of small spherical particles in a nonuniformly moving medium the complete fundamental equation of aerosol dynamics [84] takes the form

$$\frac{4}{3}\pi r^3(\gamma\dot{V} - \gamma_a\dot{U}) + \frac{2}{3}\pi r^3\gamma_a(\dot{V} - \dot{U}) + 6\pi\eta r\left[V - U - \frac{r}{\sqrt{\pi\nu}}\int_0^t \frac{\dot{V}(\theta) - \dot{U}(\theta)}{\sqrt{t - \theta}}d\theta\right] - \frac{4}{3}\pi r^3 g(\gamma - \gamma_a) = 0. \tag{3.1}$$

Gravity acts as an external force here, $\dot{U}$ and $\dot{V}$ signify time derivatives. Assuming

$$\alpha = 9\nu\gamma_a / r^2(2\gamma + \gamma_a) \approx 1/\tau; \quad \beta = 3\gamma_a / (2\gamma + \gamma_a) \approx 3\gamma_a/\gamma$$

we will reduce this equation to the form

$$\dot{V} - \beta\dot{U} = \alpha(U - V - V_s) + \sqrt{\frac{9\nu}{\pi}}\frac{r}{r}\int_0^t \frac{\dot{V}(\theta) - \dot{U}(\theta)}{\sqrt{t - \theta}}d\theta \tag{3.2}$$

Tchen [85] gave the following solution for this integro-differential equation

$$V(t) = \frac{1}{\theta}\int_0^\infty e^{-ku}\sin(\theta y)\, F(t-y)\, dy. \tag{3.3}$$

where

$$k = \alpha(1 - \tfrac{3}{4}\beta) \approx 1/\tau; \quad \theta^2 = \alpha^2 - k^2 = 3\alpha^2\beta\left(1 - \tfrac{3}{4}\beta\right) \approx \frac{9\gamma_g}{2\tau^2};$$

$$F(t) = \alpha^2[V_s - U(t)] = \alpha(1 - 2\beta)\dot{U} + \beta\dot{U} -$$

$$-\sqrt{\frac{3\alpha^3}{\pi}}(\beta - 1)\int_0^\infty \frac{\dot{U}(t-x)}{\sqrt{x}}\,dx \approx \frac{V_s - U}{\tau^2} + \frac{\dot{U}}{\tau} + \frac{3\gamma_g U}{\tau} +$$

$$- \sqrt{\frac{9\gamma_g}{2\gamma\tau\pi}}\int_0^\infty \frac{\ddot{U}(t-x)}{\sqrt{x}}\,dx. \tag{3.4}$$

Pearcey and Hill [86] calculated the effect of the integral
member in equation (3.1) on particle movement in a quiet medium
after cessation of action of external force. In the first
approximation the supplementary path, passable by a particle at
the expense of this effect, is proportional to the square root from
time, i.e., $\ell_1 = \infty$, however, in the second approximation ℓ_1 turned
out to be a finite quantity. An exact calculation of ℓ_1 is very
difficult; approximate calculation has been made by authors,
unfortunately, only for values of the ratio γ_g/γ, corresponding to
movement in the air of particles with a density <0.15.

Serafini [87] gave an analytic solution of the problem of
determination of particle movement in gaseous environment in the
absence of external forces at large Re numbers (solved by the
author of the survey by the graphic method [88]). Here he
originated from the following expression for coefficient of drag
of a sphere:

$$\psi = (24/R)(1 + \epsilon\, Re^{2/3}).$$

(ϵ — constant) and obtained for the velocity of a particle at
the time t the formula

$$V = \frac{V_0}{Re_0\varepsilon^{2/3}}[(Re_0^{2/3}\varepsilon^{-1} + 1)e^\theta - 1]^{-3/2}. \tag{3.5}$$

where $\theta = 3\eta t/\gamma r^2$, V_0 and Re_0 — initial values of these quantities.
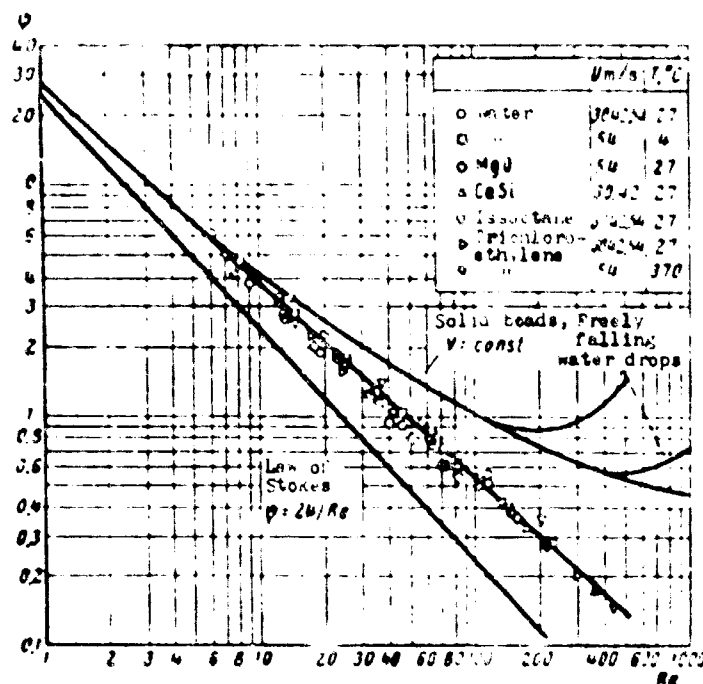
Fig. 5. Resistance of medium during
ncnuniform movement of particles.

For the path passed the following expression is obtained

$$x = \frac{r_s^{-1}}{\Im_t} \left\{ Re_0^{1} \, t^{1} + \text{arc tg}(Re_0^{-1} \, t^{-1}) - \right.$$
$$- \left[(Re_0^{-1} \, e^{-1} + 1) \, e^{-} - 1 \right]^{-1} - \text{arc tg} \left[(Re_0^{-1} \, e^{-1} - 1) \, e^{-} \quad 1 \right]^{1} \right\} \tag{3.6}$$

whence for maximum value x, i.e., for $\ell_1 (\theta \to \infty)$ it follows that

$$l_1 = \frac{r_s^{-1}}{\Im_t} \left[Re_0^{1} \, t^{1} + \text{arc tg}(Re_0^{-1} \, t^{-1}) - \frac{\pi}{2} \right]. \tag{3.7}$$

From the experimental works on this problem we will point out
the experiments by Ingebo [89], who introduced different aerosols
with spherical particles with r = 10-60 μm into a wind tunnel in
which the speed of airflow was 30-54 m/s, and determined by a
photographic method the dimensions and velocity of particles at
different distances from the place of entry of the aerosol. From
here accelerations and forces acting on the particles were calculated
in the function of relative velocity of particles and air. As can
be seen from Fig. 5, the value of coefficient ψ at small Re is the

26

same as during uniform movement, but is considerably lower at large
Re. As can be seen from the experiments of Schmidt and Lennon [90],
during accelerated movement of particles resistance is higher than
during uniform movement; by analogy one should expect lower
resistance in slowed-down (with respect to medium) movement, as
in the experiments of Ingebo. The author expressed the results of
his measurements by the empirical formula

$$\mathbf{\Psi} = 27 \, Re^{-0.84} \; (6 < Re < 400).$$ (3.8)

Aerosols in a Sound Field

Gucker and Doyle [91] undertook an experimental check of theory
of fluctuation of particles in a sound field. For this, in
sufficiently isodispersed dioctyl phthalate mists (obtained in
a Sinkler-Lamer oscillator) with $\bar{r}$ from 0.8 to 4 μm the sedimentation
rate of drops was determined ultramicroscopically. From here
the value $\bar{r}$ in a given fog was found.

Further by formula [92]

$$V_o/U_o \quad (1 \quad \omega^2\tau^2)^{-1} \cdots [1 + (2\pi\tau/t_p)^2]^{-1/2}$$ (3.9)

(ω — angular frequency, τ — relaxation time of drops, t_p — period
of oscillations) the theoretical value was calculated for the ratio
of the amplitude of fluctuations of drops and air. With the help of
very small drops U_0 was determined (at a frequency of 4850 Hz),
further the V_0 of a large number of drops was measured, and the mean
value V_0/U_0 was calculated. Although scattering of experimental
points, induced mainly by fluctuations in intensity of sound, is
quite great, nevertheless agreement between measured and calculated
values should be recognized as satisfactory.[1]

S. Dukhin [94] turned attention to the circumstance that in a
standing sound wave the fluctuations of aerosol particles, not fully

absorbed by fluctuations of the medium, are anharmonic and somewhat asymmetric. As a result the particles gradually shift to junctions of waves, where in certain cases this effect should considerably exceed the effect of radiation pressure.

For the coefficient of sound absorption due to viscous losses Epstein and Carhart [95] derived the expression

$$x_a^v \approx \frac{6\pi \nu r n}{c_s}\left(1 + \frac{1}{3}\right)\mu_v$$ (3.10)

where

$$\mu_v = \frac{V_m^2}{U_0^2} = \frac{\beta^4}{\beta^4 + 3\beta^3 + \frac{9}{2}\beta^2 + \frac{9}{2}\beta^3 + \frac{9}{4}\beta^4}$$ (3.11)

— exact expression for ratio of squares of amplitudes of relative velocity of particles and medium and speed of medium [96], c_S — speed of sound $\beta = (2\nu\omega)^{1/2} r$, $f = 2\pi \omega_{1k}$.

For the coefficient of sound absorption, caused by the periodic irreversible transition of heat from the particle to the medium and back and corresponding increase of entropy and decrease of free energy, the following expression is obtained

$$x_a^\chi = \frac{4\pi \chi_a r n}{c_s}\left(\frac{c_p}{c_v} - 1\right)\left(1 + \frac{1}{3}\right)\mu_\chi$$ (3.12)

$$\mu_\chi = \frac{\beta^4}{\beta^4 + 3\sqrt{0} : \frac{9}{2}\theta^2 + \frac{9}{2}\theta^3 + \frac{9}{4}\theta^4}$$ (3.13)

c_p/c_v — ratio of heat capacities of gas with constants p and v, χ_a — coefficient of temperature conductivity of medium, $\theta = (2\chi_a/\omega)^{1/2} r$. μ_χ expresses the degree of temperature balance of particle and medium. With large θ these temperatures almost coincide, decrease of free energy is insignificant, and $\mu_\chi \approx 0$. With very small θ particle temperature is hardly changed, temperature drop and loss of free energy practically attains the maximum possible value, and $\mu_\chi \approx 1$.

Additivity of values a_a^v and a_a^χ is observed only at moderate

particle density ($n < 10^6$) and with the condition $(c_p c_v - 1) \omega X_u c_s < 1$, i.e., for air with $\omega \ll 4 \cdot 10^5$.

In experiments by Zink and Delasso [97] a sound pulse was passed through an aerosol made up of spherical particles of Al_2O_3 with $r = 2.5$-7.5 μm and $n \approx 3 \cdot 10^4$. The sound pulse consisted of several tens of sinusoidal waves. Oscillograms from incident waves and those passing through the aerosol were obtained on the same screen. Based on amplitude ratio the coefficient of absorption was determined, and based on the distance between sinusoids — time for passage of sound through the aerosol, and from here the speed of sound in the aerosol. For calculations the particles of the aerosol were split into several fractions, α_a^{ν} and α_a^{X} were calc lated for each fraction according to the above-cited formulas and were summarized. As can be seen from Fig. 6, in air a very good coincidence of theoretical and experimental data is obtained. The same coincidence is obtained also in helium. In argon and oxygen the experimental points lie somewhat higher than the theoretical curves (by 5-10%).
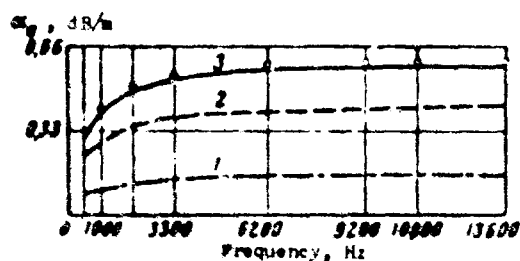
Fig. 6. Absorption of sound waves by an aerosol:
$1 \cdot \alpha_a^{X}$ (t oretically);
$2 \cdot \alpha_a^{\nu}$ (theoretically);
$3 \cdot \alpha_a^{\nu} + \alpha_a^{X}$ (theoretically);
o — experimental.

For decreasing the speed of sound Δc_S, induced by suspended particles, the authors deduced a formula which is applicable only at small Δc_S

$$\Delta c_S = \frac{1}{2} c_S \left[\frac{M_r (1 - \mu_r)}{M_g} + \frac{R_g c_r M_r (1 - \mu_r)}{c_r M_g C_p} \right].$$ (3.14)

where M_r/M_g — mass ratio of dispersed phase and medium, c_r/c_v — ratio of their specific heats, C_p — molar heat capacity of gas with a constant p, R_g — gas constant.

Here the right member of formula (3.14) should be summarized
for all fractions of the aerosol. The first member in (3.14)
determines the decrease in speed of sound due to an increase in
the density of the system, the second member — due to an increase
of its heat capacity. Both these phenomena are caused by the
presence of particles of the dispersed phase. So that these factors
have an effect on the speed of sound, it 's necessary that aerosol
particles participate to some degree in the oscillations of the
medium and absorb and give off heat. This circumstance is also
expressed by factors μ_ν and μ_χ. Thus, the effects of sound absorption
and the decrease in its speed are additional in respect to one
another. Formula (3.14) also agrees well with experimental data.

Hydrodynamic Interaction Between Particles

Switching to hydrodynamic forces of interaction between aerosol
particles,[2] we will dwell first on the simplest case — the theory
of interaction of two spherical particles in a Stokes approximation.
For this, at first they find the field of flow, satisfying simplified
equations of Stokes-Navier (without inertial members) and the
following conditions at an infinite distance from the particles the
speed of flow is equal to zero, and at the surface of the particles
coincides with the speed of the adjacent section of particle
surface. The problem is solved by method of successive
approximations: taken as zero approximation is the sum of fields of
flow, induced by each particle and expressed by the known formulas
for viscous flow past a sphere in a Stokes approximation.

In the case of parallel movement of two identical particles, zero
approximation leads to the formula

$$V = (F/6\pi\eta r)\left[1 + \tfrac{3}{4}(1 + \cos^2\theta \tfrac{r}{\rho})\right]. \qquad (3.15)$$

where V — particle velocity, F — force, acting on each particle,
θ — angle between the line of centers and direction of movement,
ρ — distance between centers of particles. Zero approximation

30

does not exactly satisfy conditions on the surface of particles,
but by means of successive addition of correction members to it
all the better observance of these conditions is attained. Solutions
are obtained in the function of ratio r/ρ, usually in the form of
power series, where the convergence of the series and the accuracy
of solutions drop sharply during approximation of r/ρ to 0.5, i.e.,
with the drawing together of particles at small distances.

Since the fields of flow are linear with respect to speeds of
both particles, then for determination of forces of hydrodynamic
interaction it is sufficient to calculate these forces for two
cases: for movement of particles along the line of their centers
(in this case the force $F_{||}$ is apparently directed along this same
line) and $F_\perp$ normal to it. In the most important case of movement of
particles in one plane $F_\perp$ lie in that same plane and, due to symmetry
of Stokes flow during flow past a sphere is also directed normal to
the line of centers. In this case the particles should also rotate
so that on the internal (turned to other particle) side of these
particles the speeds of forward and rotational movement are directed
to one side, but on the external side to various ones.

In general one should separate the velocities of particles into
components $V_{||}$ and $V_\perp$, determine the forces $F_{||}$ and $F_\perp$, and put
them together. In view of the symmetry of Stokes flow past a sphere,
with an equality of radii r_1, r_2 and particle velocities V_1 and V_2
the forces of interaction, having an effect on both particles, are
also equal both in value and in direction.

The problem of calculating the forces of hydrodynamic interaction
between two spherical particles has been dealt with by a number of
research workers. Hocking [98] and Faxen [99] deduced the formulas
(the first for $F_{||}$ and $F_\perp$, the second — only for $F_{||}$) for a general
case of $r_1 \neq r_2$, $V_1 \neq V_2$, Smoluchowski [100] — for $F_{||}$ and $F_\perp$ at
$r_1 \neq r_2$ and $V_1 = V_2$, Burgers [101] — the same for $r_1 = r_2$ and $V_1 =$
$= V_2$, and Stimson and Jeffery [102] for $F_{||}$, $r_1 = r_2$, $V_1 = V_2$.

According to Burgers

31

$$F_\parallel = 6\pi\eta r V'\left[\frac{3}{2}\frac{r}{\rho} - \left(\frac{r}{\rho}\right)^3 \frac{15}{4}\left(\frac{r}{\rho}\right)^4 \cdots\right], \tag{3.16}$$

$$F_\perp = 6\pi\eta r V\left[\frac{3}{4}\frac{r}{\rho} \cdot \frac{1}{2}\left(\frac{r}{\rho}\right)^3 + \cdots\right]. \tag{3.17}$$

From these formulas it follows that the ratio of speed of sedimentation of two identical interacting particles and an isolated particle equals

$$V_S'/V_S \quad 1 - \frac{3}{4}(1 - \cos^2\theta)\frac{r}{\rho} + \frac{1}{2}(1 - 3\cos^2\theta)\left(\frac{r}{\rho}\right)^3 -$$
$$- \frac{15}{4}\cos^2\theta\left(\frac{r}{\rho}\right)^4 + \dots, \tag{3.18}$$

where θ — angle between line of centers and vertical. Furthermore, it is easy to see that particles settle vertically only with $\theta = 0$ or $\pi/2$, otherwise their trajectories are inclined vertically in the direction of line of centers on an angle ϕ, expressed by the formula

$$\sin\phi \quad \frac{3}{4}\frac{r}{\rho}\left[1 - \frac{2}{3}\left(\frac{r}{\rho}\right)^2 \quad \frac{1}{3}\left(\frac{r}{\rho}\right)^4 + \dots\right]\sin\theta\cos\theta. \tag{3.19}$$

For Smoluchowski the expression $[1 - 3r/2\rho]$ is in the brackets.

Table 1 gives the calculations by different formulas for values V_S/V_S' for the settling of identical spherical particles along the line of their centers, and also the experimental data of Eveson et al. (see below). Not included in the table is the formula of Faxen, since the power series contained in it converge very slowly during approximation of r/ρ to 0.5.

As can be seen from the table, only the very complex formula of Stimson and Jeffery gives satisfactory coincidence with experimental data down to contact of particles, and therefore should be recognized as the most exact. Next in accuracy is the comparatively simple formula of Burgers, which therefore is given here.

Experimental investigation of the hydrodynamic interaction of two particles at small Re (~ 0.01) was conducted by Eveson et al. [30],

Table 1. Theoretical and experimental values V_S/V_S' during settling of two identical spherical particles along the line of centers in a Stokes approximation.

Author	r/ρ					
	∞	0.1	0.2	0.3	0.4	0.5
Stimson and Jeffery	1.0	0.870	0.776	0.712	0.677	0.645 *
Smoluchowski (complete formula)	1.0	0.872	0.730	0.752	0.760	0.813
Smoluchowski (simplified formula [103])	1.0	0.870	0.770	0.690	0.625	0.571
Burgers	1.0	0.870	0.778	0.718	0.695	0.718
Hocking	1.0	0.871	0.777	0.710	0.637	0.220
Experimental data	1.0	0.900	0.800	0.730	0.686	0.655

*This value was obtained by Faxen [31] from the formula of Stimson and Jeffery by means of a simple mathematical procedure.

who measured the sedimentation rate of plastic beads with r =
= 1.4-2.4 mm in castor oil at angles θ from 0 to 90° in a vessel
25 cm in diameter, so that boundary effect was insignificant. In
all cases the results of the experiments were analogous to those
given in Table 1 and relative to a case of θ = 0: at small r/ρ the
relationship V_S/V_S' was somewhat higher than theoretical, and with
convergence of the beads this divergence decreased. From the fact
that both beads moved with an absolutely identical speed, it follows
that the regimen of flow was indeed Stokes. Angle of inclination
of trajectories to vertical agreed well with the calculations of
Smoluchowski (see above). Surprisingly the authors did not reveal
rotation of particles. The cause of small divergences between
theory and experiment at small r/ρ, where theoretical calculations
are quite exact, is unknown.

In an analogous work Happel and Pfeffer [104] investigated only
the case of θ = 0 at Re = 0.008-0.03. Very good agreement was
obtained with the formula of Stimson and Jeffery in the entire
studied interval of values r/ρ from 0.09 to 0.5.

V. Pshenay-Severin [105] analyzed the problem of the hydrodynamic
interaction between particles of various size settling along the same
straight line (θ = 0). In this case in the Stokes approximation

$$V_{S1}' \approx V_{S_1} + \frac{3r_2}{2\rho} V_{S_2}; \quad V_{S_2}' \approx V_{S_2} + \frac{r_1}{2\rho} V_{S_1}. \qquad (3.20)$$

If index 1 pertains to a particle moving ahead and $r_2 > r_1$, i.e., the second particle overtakes the first, then, as can be seen from formulas (3.20), hydrodynamic interaction decreases the closure rate of the particles. The effect is still stronger at small distances between particles, when formulas (3.20) are already inapplicable.

The same author [106] investigated this problem by the method of Stimson and Jeffery. As an example, it can be seen from the table presented by him that in air the settling rates of water drops with $r_1 = 4$ μm and $r_2 = 6$ μm (for which $V_{S1} = 0.20$ and $V_{S2} = 0.46$ cm/s) during their convergence at a distance $\rho = 16$ μm are equal to 0.49 and 0.53 cm/s.

It is necessary to stress that calculation of hydrodynamic interaction in a Stokes approximation is permissible only under the condition $\beta = V\rho/\nu \ll 1$. Noticeable deflections can start already when the condition $Vr/\nu = Re \ll 1$ is observed, i.e., the formula of Stokes is still applicable for movement of one particle. Based on calculations of V. Pshenay-Severin, 9% at $\beta = 0.2$ and 21% at $\beta = 0.5$.

In switching to the theory of hydrodynamic interaction in an Oseen approximation, we will first give the formulas brought out by Oseen himself [107] for forces acting on two spherical particles with radii r_1 and r_2, moving in the same direction (along the axis x) with an identical speed V_S, where the first particle is moving in front. Besides the usual Stokes force $- 6\pi r_1 V_S$, in the direction of movement it is being acted on by the force[']

$$F_x^{(1)} = \frac{6\pi r_1 r_2 V_S}{4\rho} \exp\left[- \frac{V_S (\rho + x_1 - x_2)}{2\nu} \right].$$

(3.21)

where x_1 and x_2 — coordinates of particles, and along the line of centers the force

$$F_\rho^{(1)} = \frac{6\pi r_1 r_2 V_S \nu}{\rho^2} \left\{ 1 - \left(1 + \frac{V_S \rho}{2\nu} \right) \exp\left[- \frac{V_S}{2\nu} (\rho + x_1 - x_2) \right] \right\}.$$

(3.22)

34

Forces acting on the second particle thus obtain a transposition of indices. Forces $F_x^{(1)}$ and $F_x^{(2)}$ are directed to the side of movement just as in the Stokes approximation. Force $F_{(\rho)}^{(1)}$ is directed aside from the second particle, i.e., is a repulsive force. Force $F_\rho^{(2)}$ at small angles of θ, for example, when moving on the same straight line, is directed toward the first particle, and at large θ, for example, when moving on the same front — in the opposite direction (repulsion).

At $r_1 = r_2$ and movement on one straight line ($x_1 - x_2 = \rho$)

$$F^{(1)} = F_x^{(1)} + F_\rho^{(1)} = \frac{9\pi\eta v r^3}{\rho^3}\left[1 - \exp\left(-\frac{V_s\rho}{v}\right)\right] = \frac{9\pi\eta^2 V_s}{\rho}\frac{1-e^{-\beta}}{\beta} \qquad (3.23)$$

$$F^{(2)} = F_x^2 + F_\rho^2 = \frac{9\pi\eta r^3 V_s}{\rho}. \qquad (3.24)$$

where $\beta = \rho V_s/v$. Since $(1 - e^{-\beta})/\beta < 1$, then the first particle moves slower than the second. Ratio of speed of their convergence to V_S equals

$$\theta = \frac{3}{2}\frac{r}{\rho}\left[1 - \frac{1-\exp(-\beta)}{\beta}\right]$$

(here we assume that the movement of particles is quasi-stationary, i.e., is completely determined by forces acting on them at that moment). In the case of water drops with $r = 30$ μm $\theta = 0.05$ at $r/\rho = 0.05$; 0.086 at $r/\rho = 0.1$ and 0.112 at $r/\rho = 0.2$.

Thus, in the Oseen approximation sedimenting particles of the same size converge quite rapidly. The reason for this is the asymmetry of Oseen field of flow past a sphere: the speed of flow, induced by a moving particle, from behind the particle decreases with distance much slower than in front of particle (Fig 45, see p. 130). During sedimentation of particles of various size along one straight line, at $r_2 > r_1$, i.e., when the second particle overtakes the first, Oseen hydrodynamic forces (in contrast to Stokes) also noticeably increase, based on calculations of

35

V. Pshenay-Severin, the closure rate of particles. This question
is examined in more detail in connection with the theory of
gravitational coagulation in Chapter 7.

V. Pshenay-Severin [108] also investigated the influence of
viscosity on the hydrodynamic interaction of particles of the
same size in a sound field. The author calculated the closure rate of
particles in Oseen approximation by the same method as for uniform
movement of particles, but taking into account the specific nature
of oscillatory movements: thus it was accepted that hydrodynamic
convergence of particles occurs only at a relative velocity of
particles and medium, corresponding to $Re > 1$. It was shown that
with an amplitude of rate of oscillations of a gaseous environment
$U_0 = 4-10$ m/s, i.e., with a density of sound energy 50-200 erg/cm^3,
the convergence time for particles with $r = 1-15$ μm from $\rho = 100r$
to 10r during favorable relationships between the period of
oscillations t_p and relaxation time of particles τ makes up a
fraction of a second. This means that this effect can play a
large role during sound coagulation of aerosols. Maximum effect
is attained at t_p from 4 to 8τ. It is necessary to note that
obviously these calculations are applicable only under the
condition that the period of oscillations considerably exceeds
the time necessary for the flow disturbed by one particle to reach
the other particle, or that the amplitude of oscillations is
considerably larger than the distance between particles. On the
other hand, a noticeable effect is possible only at $\tau/t_p > 0.1$, i.e.,
during incomplete entrainment of particles by sound waves. From
the table of τ values [109] it is clear that at $U_0 = 4-10$ m/s, the
interval of values t_p, for which both inequalities are observed
(considering $\rho = 100r$), is quite narrow at $r = 1$ μm, but is expanded
considerably by transition to $r = 1$ μm.

Of the experimental works in this area we will point out the
experiments by Dorr [110], in which the force of interaction was
determined between two hollow glass beads with $r = 2.8-4.4$ mm,
suspended in the antinode of a standing sound wave with a frequency

of 525 Hz on glass filaments. Natural frequency of oscillations of
suspended beads was 1 Hz and they practically did not accomplish
the forced oscillations. With a change of amplitude of rate of
oscillations from 0 to 35 cm/s the force was strictly proportional
to U_0^2, in agreement with theory. With the angle θ between direction
of oscillations and line of centers equal to $\pi/2$, the absolute
magnitude of force was expressed at $\rho/r \gtrsim 3$ by the theoretical
formula

$$F = \frac{3\pi \tau_0 r_1^3 r_2^3 V_{r0}^2}{2 r^4}\left(\frac{3}{2} \cos 2\theta - \frac{1}{2}\right). \qquad (3.25)$$

where V_{r0} — amplitude of relative oscillation of particle and medium,
but with the convergence of beads force increased considerably
faster than by this formula. In the case $\theta = 0$ coincidence was
apparently more complete but clear data on this question are
not available in the article by Dorr.

Electrostatic Scattering of Aerosols

We will switch to electrostatic scattering of aerosols. In a
polydispersed aerosol with unequal charges of particles for each
fraction it is possible to write

$$-\frac{dn_i}{dt} = 4\pi B_i q_i n_i \sum_i n_i q_i \quad 4\pi B_i q_i n_i n\bar{q}. \qquad (3.26)$$

where $\bar{q}$ — average charge of particles. The solution of the system
of nonlinear differential equations (3.26) is very difficult and
no one has undertaken it yet. For a change of total particle
density $n \quad \sum_i n_i$ we have

$$-\frac{dn}{dt} = 4\pi n q \sum B_i q_i n_i = 4\pi n^2 \bar{q} B q. \qquad (3.27)$$

Integration of this equation is impossible, since $\bar{q}$ and $\overline{Bq}$ are
functions of time, for the determination of which it is necessary
to integrate the entire system (3.26). Only in the case when

electrical mobilities $B_1 q_1$ of all particles are more or less identical and, consequently, $\overline{q}$ and $\overline{Bq}$ do not change during scattering, then for an aerosol it is possible to use the equation

$$\frac{1}{n} - \frac{1}{n_0} = 4\pi \overline{q}\,\overline{Bq}\,t \approx 4\pi\overline{q^2}\,\overline{B}t, \tag{3.28}$$

which we will present in the form

$$n = \frac{n_0}{1 + \beta t}, \tag{3.29}$$

where $\beta = 4\pi\overline{q^2}\overline{B}n_0$.

During transmission of an isodispersed unipolar charged aerosol with identical charges on the particles through grounded tube with a radius R and length x with average speed $\overline{U}$ the concentration of aerosol coming out of the tube, both during laminar and during turbulent flow, is equal, according to equation (3.29), to

$$\frac{n_0}{1 + \beta x/U}. \tag{3.30}$$

Thus, the total mass of particles, settled in 1 s on the walls of the tube due to electrostatic scattering, equals

$$\Phi_s \quad \pi R^2 \overline{U} \; (n_0 - n)\, m \quad \frac{\pi R^2 \beta x n_0 m}{\left(1 + \beta x U\right)} \quad \frac{\pi R^2 \beta x c_0}{1 - \beta x \overline{U}}. \tag{3.31}$$

where m — mass of particle, c_0 — initial concentration by weight of aerosol.

Passing through the tube here is an electrical current with the force

$$I_s = q\Phi_s/m \tag{3.32}$$

Formula (3.31) can be presented in the form

$$x = \pi R^2 c_0 \overline{U} x \; \Phi_s - \overline{U}\beta \tag{3.33}$$

Through a tube made up of a series of isolated sections Foster [111] passed a fog obtained by thermal decomposition of wood and charged with help of a corona discharge. The mass of deposit in each section and force of current passing through it was determined. From here were calculated ϕ_x and I_x in function x. In coordinates $(x, x/\phi_x)$ linear graphs were obtained in agreement with the formula (3.33), and based on these c_0 and β were determined. The density of drops in the fog was also measured. Since c_0, β and I_x are known functions of three unknown values n_0, m, and q, then they could be calculated from these experiments. For r values are obtained within the limits 0.075-0.144 µm, for q depending on the intensity of the charge 6-32ϵ (ϵ — elementary charge), where the value q was reflected little on the value r. From this satisfactory coincidence of experimental data with theoretical, it follows that the fog was comparatively isodispersed and charges of particles differed little.

In the work by Drozin and LaMer [112] fairly monodispersed aerosols of stearic acid with $\bar{r}$ = 0.3-1.0 um were charged unipolarly with a corona discharge and the average charge of particles in a function of their radius was determined. Here, in agreement with source material, electrical mobility of particles increased with an increase of $\bar{r}$. A charged aerosol was introduced in a wide flat horizontal capacitor and was precipitated under the impact of a field on the lower capacitor plate. The charge imparted to the plate in a unit of time was measured continously up until complete precipitation of the aerosol, and based on the curve obtained the distribution of particle size was calculated. Values of $\bar{r}$ determined in this way coincided with spectra of a higher order measured tyndallometrically.

In the opinion of the authors of the work, the mobility of particles of the above-indicated size should be calculated according to the simple Stokes formula without any corrections. In justification of this surprising opinion, which contradicts both theory and extensive experimental data, Drozin and LaMer refer to a survey of experimental results obtained in their laboratory. These

are inaccessible to the author. On the other hand, they did not
consider electrostatic scattering. From Fig. 4 of their article it
is possible to estimate the value of the initial space charge of
the aerosol in one of the experiments $\sim 2.10^{-3}$ esu/cm^3. It follows
from this that at the time of setting the aerosol in motion in the
capacitor the electrical field induced by space charged for the
upper and lower border of the aerosol had an intensity ~ 0.03 esu,
i.e., was of the same order with the external field (0.055 esu).
Therefore the charge, imparted to the plate in a unit of time,
in the beginning of the experiment was noticeably greater than in
the absence of a space charge, but the time for complete precipitation
of aerosol had to increase (this is pointed out in the article). It
is possible that for compensation of the error appearing thus, the
authors had to reject corrections to the Stokes formula. Furthermore,
it is doubtful whether or not in the comparatively bulky condenser
in which these experiments were conducted it was possible to
completely remove convection.

Unipolarly charged aerosols, apart from medicine, will probably
find application during the treatment of closed locations, gardens,
etc., with insecticide preparations, since in contrast to uncharged
aerosols they settle in considerable quantities on the walls and
ceiling of locations (A. Kitayev [113]) and on lower surface of
leaves (Gohlich [114]), and they are deposited much more completely
when blown through the foliage of trees [114]. Furthermore,
according to Gohlich unipolar charged aerosols (dusts) give a more
uniform, less aggregated deposit, apparently due to mutual repulsion
of particles, and they cling to leaves (see p. 145) more strongly.

Electrostatic scattering is effectively demonstrated on free
jets of aerosols: during unipolar charging the streams are
noticeably expanded [114].

[1]In the account of the problem of entrainment of particles by fluctuations of the medium, in "Mechanics of Aerosols," p. 91, an inaccuracy is committed. At very large values for the ratio of relaxation time of particle to period of fluctuations τ/t_p the ratio V_0/U_0 does not aspire to zero, as stated in the book. In this case for calculation of V_0/U_0 one should use, instead of approximate formula (3.9), the exact formula [92].

$$\frac{V_0}{U_0} = \left(\frac{1 - 3\beta + \frac{9}{2}\beta^2 + \frac{9}{2}\beta^3 + \frac{9}{4}\beta^4}{f^2 + 3f^3 + \frac{9}{2}\beta^2 + \frac{9}{2}\beta^3 + \frac{9}{4}\beta^4} \right)^{\frac{1}{2}}$$

(values f and β see below), from which it follows that at $\tau/t_p \to$ $\to$ ∞, $V_0/U_0 = 3\gamma_g/2\gamma$. The same expression is obtained for fluctuations of particles in an ideal liquid [93].

[2]In Fig. 23 in "Mechanics of Aerosols" (p. 101) the direction of arrows should be reverse.

[3]In the author's book "Mechanics of Aerosols," p. 100, only formula (3.22) is given and the forces expressed by formula (3.21) are omitted.

C H A P T E R   4

CURVILINEAR MOVEMENT OF AEROSOL PARTICLES

Hydrodynamics of an Aerosol Liquid

Important conclusions for the mechanics of aerosols can be obtained by examining the movement of an isodispersed system of particles, taking into account their inertia, as a flow of a hypothetically compressible liquid, the density of which is equal to particle density (Robinson [115]). The author was limited to a case of potential flow of a medium and proportionality of resistance of the medium relative to the velocity of a particle and the medium and proved the following theorem: if the flow of an aerosol liquid at a certain moment is potential (for example, at a very great distance from a streamlined body, where the velocity of particles and medium coincide), then it will remain potential. It follows from this, in particular, that the trajectories of particles cannot cross. This theorem is true only in the case when external forces acting on the particles also possess potential.

Using the div operator to the fundamental equation of movement of particles

$$\frac{DV}{Dt} = -\frac{1}{\tau}(V - U) + F. \qquad (4.1)$$

where V and U — velocity vectors of particle and medium, F — vector of the external force and DV the total differential of speed of an element of aerosol liquid, Robinson proved that div $V \le 0$, i.e., that

the concentration of aerosol can increase only with its motion. The correctness of this conclusion can be ascertained by examining a stream tube with a constant cross section and bent in one place. In the zone of the bend for the internal contour of the tube the radius of curvature is less, and the speed of flow, and, consequently, centrifugal force, based on properties of potential flow, are greater than for the external contour. Therefore the stream tube of an aerosol liquid will shift with respect to the stream tube of the medium and simultaneously will narrow, i.e., the concentration in it increases. Let us note that during rotation of an aerosol as one whole, i.e., during vortex flow the concentration of the aerosol will, on the contrary, decrease.

L. Levin [116] proved that during solenoidalness of external forces (div $F = 0$), for example, in the case of gravity and in the absence of inertia ($\tau = 0$) the concentration of aerosol along the trajector of particles is constant. At $\tau \neq 0$ and constant F the concentration of a flowing aerosol can remain constant only under the condition $U = $ const, i.e., in a uniform field of flow. In the opposite case the concentration should change, i.e., as we saw above, increase. Since in the absence of inertia and with $F = $ const concentration does not change (we consider the medium incompressible), then it follows from this that the growth of concentration should increase with the growth of τ (at least, at not very large τ)[1] and thus the dispersed composition of a flowing polydispersed aerosol should be changed, in other words, segregation of particles with various τ should occur.

Movement of Particles in a Transverse Electrical Field

The oscillation method for determining the size and charge of particles [117] in its original form is inapplicable to the determination of size of particles with $r < 0.5$ μm, since speed of their sedimentation is small and Brownian movement is intensive, however, by using a strong electrical field it is possible to quite accurately determine amplitude of oscillations of particles with r up to 0.15 μm, and by recharging to measure their charge, and

consequently, also size (Ye. Gladkova, G. Natanson, [118]). This method is especially convenient when working with comparatively isodispersed aerosols, since in this case it is possible to dispense with recharging.

Passing to the settling of aerosols from a laminar flow, we note first of all that the rectilinearity of laminar flow in straight tubes is disturbed considerably earlier than the critical value Re_f. In smooth round tubes a colored stream, according to the observations of Prengle and Rotful [119], starts to bend at the axis of the tube already at $Re_f = 1220$; with an increase of Re_f this disturbance of rectilinearity spreads to the walls and reaches them at $Re_f = 2000$.

A differential method for the determination of electrical mobility of particles [120] was carried out by Gillespie and Langstroth [121]. A laminar flow of air was passed downward through a parallel plane capacitor. In the middle of the airflow moved an isokinetically injected thin stream of aerosol. Hinkle et al. [122] passed the same type of stream between cylindrical electrodes and photographed it with lateral illumination. Here a stream of uncharged aerosol preserved its width; in the case of charged particles a small stream was expanded (Fig. 7), and based on the distribution of optical density in a cross section of the stream it was possible to roughly determine the distribution of electrical mobility of particles.
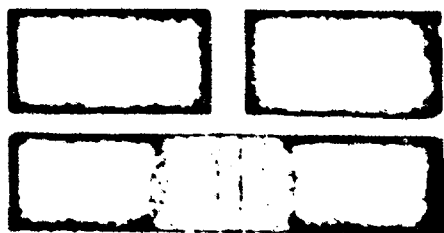

Fig. 7. Expansion of stream of charged aerosol in an electrical field. Above — uncharged aerosol

In the work by Yoshikawa et al. [123] an aerosol with r = = 0.5-10 µm was introduced in a wide metallic tube through a layer of parallel narrow plastic wires, creating flow with a constant speed over the entire section of tube, along the axis of which was

stretched a corona conductor. Behind the conductor along the axis
of tube was located a narrow metallic cylinder, serving as the
internal electrode of the cylindrical capacitor. Since particles
which had moved near a corona conductor received a higher charge,
but their path up to the external electrode was longer, then, by
selecting the voltage and all the dimensions of the instrument, it
was possible to focus particles of identical size in one section of
the external electrode. Due to the fact that charges, obtained by
particles in a corona discharge, are proportional to r in a power
>1, the particles were disposed in the deposit in order of decreasing
size.

For finding the relationship between average charge and mobility
of particles in amicroscopic aerosols Nolan and O'Connor [124],
parallel with volt-ampere characteristics (I, Π) obtained during
passage of aerosols through a capacitor, used a condensation nuclei
counter to determine curves (n, Π), where n — number of particles
settled in a capacitor at voltage Π from each cubic centimeter of
aerosol, and from here calculated the number of particles with
mobilities from u to ∞. All the particles then split into several
fractions based on their mobility and for each fraction the total
charge and number of particles were calculated, and from here the
average charge of particles. We will refer to this work again
on p. 88.

Aerosol Centrifuges and Cyclones

In the investigation of aerosols centrifuges have an important
advantage over instruments of the cyclone type: low rate of flow
of the aerosol in the rotor and, as result, absence of turbulence
and blowoff of the deposit by airflow.

The Goetz centrifuge [125] is similar to the conifuge [26], but
the aerosol flows along a spiral channel with a rectangular cross
section, located on the periphery of the cylindrical rotor of
the centrifuge. Thus, in this centrifuge, in contrast to the

45

conifuge, aerosol particles are immediately subjected to the
action of maximum centrifugal force and the entrance effects induced
by this circumstance noticeably distort the distribution of larger
particles in length of the deposit. Furthermore, as can be seen
from the articel by Goetz, upon entrance into the channel the
aerosol fills all of its cross section, and the site of precipitation
of the particles depends not only on their size, but also on the
initial position during entrance into the channel, i.e., separation
of particles of various size takes place imperfectly.

In the cyclone theory they usually disregard speed of gas flow
in the cyclone which is directed toward the axis of the component
U_ρ. According to Feifel [126] and Barth [127], only those particles
are precipitated whose radial speed under the impact of centrifugal
force is greater than U_ρ on their entire path to the wall, and this
determines the maximum size of particles precipitated in the
cyclone. Thus, in the opinion of these authors the cyclone should
work as a separator. In reality, as experiments show, the
separating action of the cyclone is very imperfect.

Solbach [128] measured U_ρ in various points of a direct-flow
cyclone and calc lated trajectories and effectiveness of settling
of particles of various size, taking into account radial drain.
Measurements by the author of clay dusts with $\bar{r}$ = 1-6 μm gave
satisfactory agreement with calculations.

V. Maslov and Yu. Marshak [129] investigated the settling of
fractions of $K_2Cr_2O_7$ powder with r = 3.5-12.5 μm in a vertical
direct-flow cycline, the walls of which were lubricated with vaseline.
Radius of the cyclone R varied from 2.5 to 20 cm, entrance
(tangential) speed was from 2 to 21 m/s, width of feeder tube h =
= 0.4 R. Flow in these experiments was self-simulating. Experimental
values of ϑ in the function Stk number fall on the same curve
(Fig. 8), the form of which depends only on the ratio of length L
and radius R of the cycline.
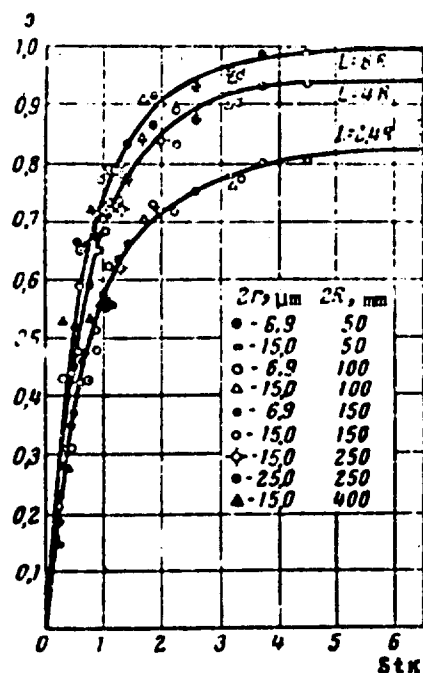
Fig. 8. Settling of bichromate dust in a direct-flow cyclone.

Walter [130] worked with very narrow (R = 0.75-1.4 cm) and long (L = 16-20 cm) cyclones with a very short exit pipe. ϑ initially increased with speed of flow, attained a maximum, and then no longer changed. Growth of ϑ with an increase of size and particle density and with a decrease of R was much stronger than that for other authors. Thus, in one experiment at R = 0.75 cm and dust concentrations of 10, 100, and 500 mg/m^3 ϑ equaled 0.8; 0.99, and 0.998. With R = 0.95 cm and at r = 0.25, 0.30, and 0.35 μm ε equaled 0.6, 0.987, and 0.999. No one has yet obtained such high efficiencies in a cyclone. It is also difficult to understand the high separating action of cyclones in these experiments, contradicting both theory and data of other authors (see Fig. 9 [131]). The situation is apparently different with apparatuses specially designed for separation of dust (Micropleks) [Editor's NOTE: Mikropleks, Russian word not confirmed]. They represent a very low cyclone with flat upper and lower floors, the height of which is equal to the height of the feeder tube (Rumpf [130]). Gas moves in the apparatus along a flat spiral and emerges through an opening in the center of one of the floors. For elimination of wall disturbances the floors rotate at approximately the same speed as the gas. Through the apparatus only those particles can pass which under the impact of centrifugal force have a speed less than U at the axis of the

apparatus. The separating effect of such apparatuses is considerab..y higher than separating effect of cyclones (Fig. 9).
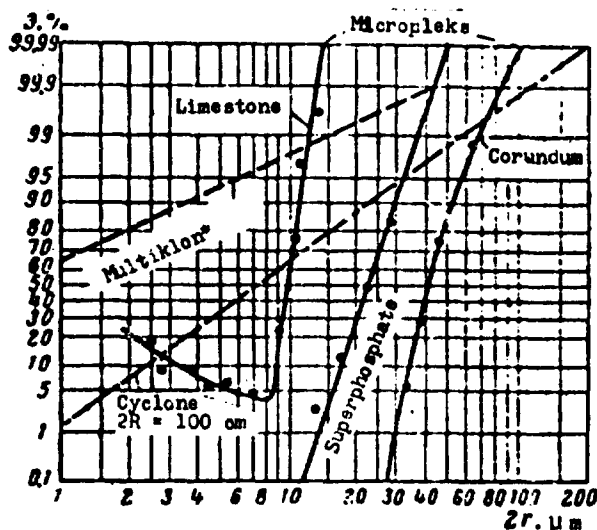
Fig. 9. Effectiveness of cyclones and "Micropleks" apparatuses in function of particle dimensions. *[Editor's NOTE: Russian word not confirmed].

Daniels [132] investigated the effectiveness of direct-flow cyclones with R = 2.5 cm and L = 25 cm on fractionated quartz dust and found that ϑ very slowly increases with an increase of r: with a flow rate cf 20 ℓ/s from 0.72 at r = 10 μm to 0.83 at r = 60 μm, but at higher speeds ϑ starts to decrease even at r > > 25 μm. By special experiments the author showed that large particles of quartz rebound from the walls (see p. 145) and by this disrupt the smaller particles. Therefore, with moistening of the walls with water ϑ reaches 1 already at r $\bar{>}$ 12 μm. According to the experiments of Stairmand [133], wetting the walls of the cyclone considerably increases ϑ for particles of all dimensions investigated by him (r = 1-25 μm).

Vaffe et al. [134] proposed for the dispersion analysis of aerosols an instrument of the cyclone type, consisting of spiral-like channel with a rectangular cross section. The height of section

48

gradually decreases, rate of flow and centrifugal force increase toward the axis of the spiral, at which there is a lateral opening for the escape of gas. Basic deficiency of instruments of this type is the blowoff of the precipitate induced by the high rate of flow and the breaking up of aggregates in the boundary layer. Aerosol centrifuges, as already was said, are free from this deficiency.

Louvered Dust Separators

The mechanisms of operation of louvered dust separators has been investigated by Smith and Goglia [135], working with very hard alundum dust. By passing a very thin fraction of dust through a dust separator and observing it under lateral illumination, the authors determined the field of flow in the apparatus (Fig. 10), and then converted to large particles. As can be seen from Fig. 11, particles which rebound like elastic bodies (A) do not pass through the louvers, but slowly rebounding particles (B) or those moving at a great angle to the line of louvers (C) are attracted by air current through the louvers. The effectiveness of a dust separator is very low at $r = 10$ μm, but grows rapidly with an increase of r and reaches 0.95-0.97 at $r = 20$ μm. For less elastic particles, aggregates, etc., effectiveness of the apparatus should nevertheless be considerably lower (see p.143).

Deposit of thin dust

Fig. 10. Field of flow in a louvered dust separator.
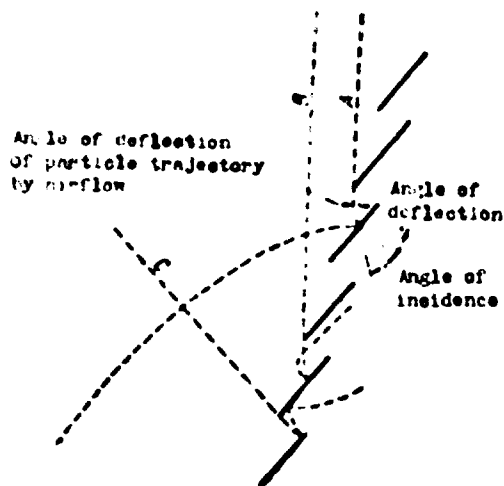
Fig. 11. Trajectories of alundum particles in a louvered dust separator.

Intake of Aerosol Samples

We will switch to the problem of intake of aerosol samples. L. Levin [116] calculated the effectiveness of intake of a sample from a uniform flow of aerosol in a point drain (i.e., a very narrow opening), taking into account inertia and sedimentation of particles, and obtained the formula

$$\vartheta = n/n_0 = 1 - 0.8k \div + 0.08\,k^2 + \cdots \tag{4.2}$$

$$k = \left(\tfrac{4\pi}{\Phi}\right)^{\!\prime\prime}\tau\,(|U_0 \div V_s|)^{\!\prime\prime}. \tag{4.3}$$

where n_0 and n — concentration of initial aerosol and sample taken, τ — relaxation time of particles, Φ — volume of aerosol drawn in 1 s U_0 — speed of undisturbed flow, V_s — speed of particle settling. Accuracy of formula (4.2) decreases with an increase of k; it equals $\sim1\%$ at k = 0.25 and $\sim2.5\%$ at k = 0.5. This formula is applicable also at a finite dimension of the opening under the condition that the average rate of flow in the opening $U \geq U_0$.

A case of increase in concentration in the sample cannot be encountered in this theory, since the rate of flow in an infinitely narrow opening in any case is greater than U_0. As formula (4.2) and (4.3) show, for a decrease in concentration in the sample it is necessary to have, in addition to inertia of particles, the presence of particle motion in an undisturbed aerosol, i.e., either flow of

. . . . . U . . r settling of particles under the influence of
an external force (V_3). Further from these formulas it follows that
for the extraction of proper samples at high speeds of flow of
aerosol and with large particles it is necessary to use high speeds
of suction, and that the average dimension of particles in the sample
is less than in the initial aerosol.

In the case of intake of a sample in an infinitely narrow flat
aperature a formula is obtained which is applicable at $\bar{U} > \pi U_\bullet$

$$\vartheta \sim 1 - 0.451\, k + 0.148\, k^3 + \dots . \tag{4.4}$$

where

$$k = \frac{2\pi\tau}{\Phi'}(|U_\bullet + V_s|)^2. \tag{4.5}$$

and Φ' — rate of suction per unit of length of aperture.
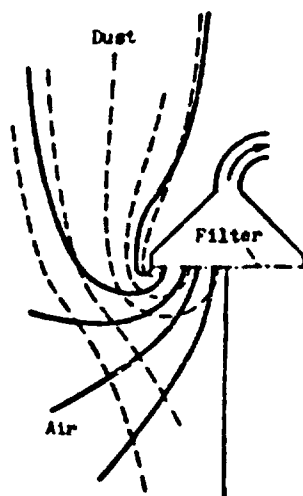
Fig. 12. Intake of aerosol
sample through overturned
funnel with a filter.

Walton [136] investigated the intake of a sample from an aerosol,
moving slowly in a horizontal direction, through an overturned
funnel with radius R (Fig. 12) with a filter which creates a
uniform rate of flow U at the entrance into the funnel. The
author disregarded inertia of particles. According to rules
established by him earlier [137], the number of particles drawn

51

..t. a filter in 1 s equals $\pi R^2 n (U - V_s)$, and effectiveness of intake
$\vartheta = 1 - V_s / U$. Here the deposit on the filter should be absolutely
uniform, which has been confirmed experimentally. All of this is
true only at a very small funnel height, otherwise this simple
picture is complicated due to the precipitation of particles on
the walls of the funnel, entrance effects, etc.
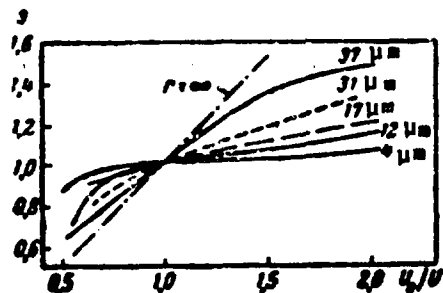
Fig. 13.   Fig. 14.

Fig. 13. Dependence of sample intake efficiency on
ratio of rate of flow outside (U_0) and inside (U) a
tube.
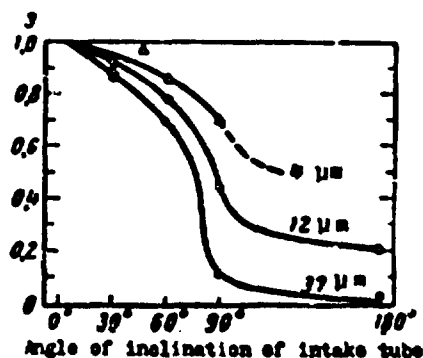
Fig. 14. Dependence of sample intake efficiency on
slant of tube toward direction of flow ($U_0/U = 1$).

Figures 13 and 14, taken from the article by Watson [138], give
the results of experiments by a number of authors on selection of
samples: in Fig. 13 — dependence of efficiency of intake of sample
through a tube, located parallel to the flow, on the ratio flow
rates outside and inside the tube, in Fig. 14 — dependence of ϑ on
the slant of the tube toward the direction of flow. Diameters of
particles are shown on the curve.

If an aerosol with concentration n_0, flowing with a speed U_0, is
aspired at the rate U into an intake tube with radius R and with
infinitely thin walls located parallel to the flow, then the flow
lines of gas entering the tube at a sufficiently great distance from

it are limited by a cylindrical surface with radius R_0 so that $\pi R^2 U = \pi R_0^2 U_0$. If $U < U_0$, $R > R_0$, i.e., flow lines diverge upon approaching the tube, then the particle flux inside the stated surface which is equal to $\pi R_0^2 n_0 U_0$, will completely enter the intake tube. From the ring-shaped space, limited by cylinders with radii R_0 and R, all the flow lines pass outside the intake tube. Of the particles located in this space a certain part α will enter the tube due to inertia. The flux of these particles equals $\alpha \pi (R^2 - R_0^2) n_0 U_0$. The sum of these two fluxes is equal to the flux inside the tube $\pi R^2 n U$, where n — concentration of aerosol inside tube. From this it follows that

$$\frac{n}{n_0} = 1 - \alpha + \alpha \frac{U_0}{U}. \qquad (4.6)$$

In the case of $U > U_0$ in this equation the sign of α should be reversed. The value of α is changed from ~ 0 for very fine up to ~ 1 for very large particles and depends, naturally, on the type of field of flow at the entrance into the tube. With the help of rather rough calculations Badzioch [139] arrived at the formula

$$\alpha = (1 - e^{-L/l_1}) \frac{l_1}{L}, \qquad (4.7)$$

in which l_1 — inertia path of particle, L — distance from tube, at which noticeable expansion (or narrowing) of flow lines (i.e., not a very definite value) starts. The author calculates l_1 not by the formula (3.7) but by the formula of Stokes, which in this case (Re = 6-17) leads to noticeable errors.

Figure 15 gives the results of experiments by Badzioch in a wind tunnel with spherical particles of zinc and round ones of a silicate catalyst ($\gamma = 1.4$) with average sedimentation radii $r_s = 10$-15 μm. As can be seen from the graph, experimental points are contained between two curves (4.7) with values L 2 and 5 cm. The great extent of scattering of experimental points is not surprising at such considerable intervals of values U_0 (8-24 m/s) and U_0/U (0.25-4.1)

53
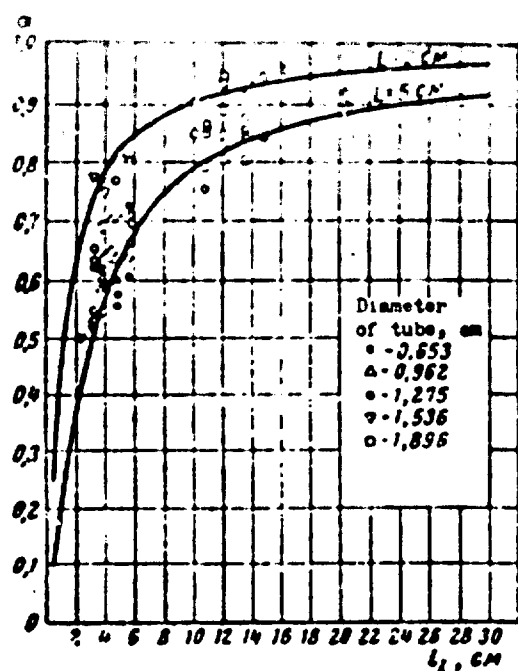
Fig. 15. Dependence of parameter α during intake of sample on the inertia path of the particles.

In which the experiments were conducted. The considerations of the author on the dependence of L on R are weakly founded, are not confirmed by experiment, and therefore are not presented here. A semiempirical method for determination of the relationship between α and $\ell_1 R$ = Stk is proposed by Watson [137].

Walter [140] measured the flow field during intake of a sample through a tube with thick walls (Fig. 16). We see that even during isokinetic intake a dead zone with lowered speed will be formed in front of the entrance to the tube. Current lines here are strongly distorted; with an increase in the aspiration rate the current lines are noticeably rectified. In agreement with these data during the isokinetic intake of dust according to Walter very unstable and understated (up to 50%) concentration values are obtained. With an increase of aspiration rate (even a few times) constant and more or less regular results are obtained in complete contradiction with the data in Fig. 13.

Dennis et al. [141] investigated the work of intake tubes of the neutral type. In these the isokinetic state is controlled by
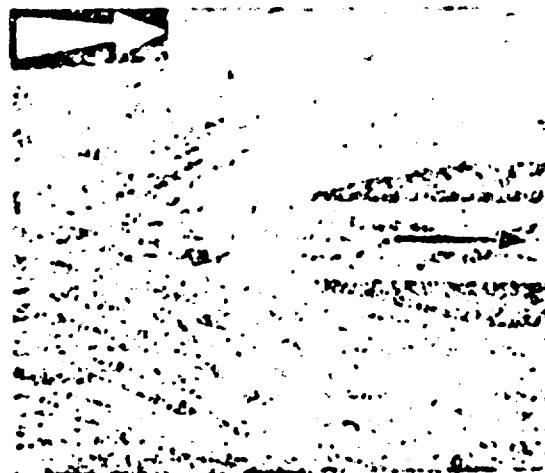
GRAPHIC NOT
REPRODUCIBLE
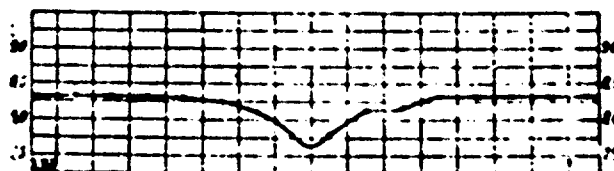
Fig. 16. Field of flow during iso-
kinetic intake of sample through tube
with thick walls. Below, the rate of
flow along the axis of tube, m/3.

the equality of static pressures inside and outside the intake tube.
It turned out that with observance of this condition the concentration
of dust in the tube is too low and for obtaining correct results it
is necessary that the external pressure is greater than internal, i.e.,
it is necessary to increase the aspiration rate. The more it is
increased then the greater the flow rate outside the tube. However,
according to Dennis this is explained not by the incorrectness of
principle of isokinetic intake, but by a loss of pressure in tube
due to friction and eddies.

Thus, the problem of intake of aerosol samples from a flow has
still not been definitely solved. The main difficulty in the
solution of this problem is apparently the exact determination of
true concentration in the flow of a coursely dispersed aerosol.

Slot Instruments

A very thorough investigation of the work of konimeters, i.e.,
slot instruments with round openings, was conducted by Rober [142].

. . . . attention was given to three types of nozzles - cylindrical, conical and a nozzle with a curvilinear profile, in which the speed of flow increases linearly with the distance covered. In the two last cases the ratio of diameters of entrance and exit openings equaled 10. From the experiments of Rober it follows that, although the Re_f numbers reached 4000-5000, the flow was laminar — a circumstance which was not considered in proper light in previous works. Here a parabolic profile of flow velocities could not be established in the nozzles. Having measured these profiles, the author calculated the speeds obtained by aerosol particles with different τ in nozzles of various form. Least relative velocity of particles and air (least splitting up of aggregates in the opinion of the author) is attained with a form of nozzles, intermediate between cylindrical and curvilinear.

There are several factors promoting the displacement of particles toward the axis of the nozzle: displacement of current lines connected with a change in flow profile, the effect described on pp. 5-6, and, finally, in nozzles with cirvilinear profile — inertial displacement. The last effect has the greatest significance: in experiments with polydispersed coal dust at $\overline{U}$ = 50-100 m/s and radius of outlet R = 0.2 mm, a noticeable (by ∿15%) narrowing of the dust stream was established in comparison with the width of the outlet in curvilinear nozzles; in nozzles of other types the presence of narrowing was not reliably established. Since particles moving near the walls of a nozzle emerge from it at a low speed, then it is clear that narrowing of the aerosol stream very much promotes an increase in the efficiency of the konimeter, and this in its turn demonstrates the advantage of curvilinear nozzles.

Theoretical calculation of the field of flow in a stream emerging from a konimeter (in contrast to calculation in a stream coming out of a flat slot) is very difficult. Rober's model experiments with tobacco smoke emerging from a cylindrical tube with 2R = 10 mm at a distance of d = 10 mm from tube to plate (the equality 2R and d was also observed in the experiments described below) with
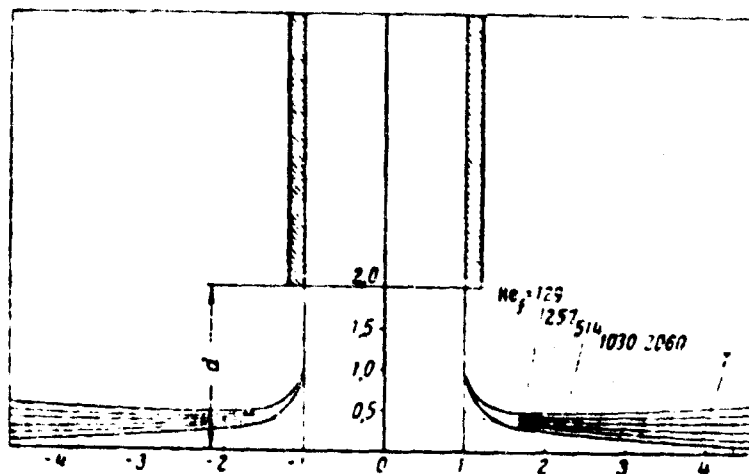
Fig. 17. Contours of streams coming out of
a konimeter at various Re_r numbers.

a parabolic profile of flow velocity gave the results shown in
Fig. 17 for the contour of the stream. Curve T corresponds to an
ideal case – preservation by the stream of its average velocity
during spreading. Hence Rober made the conclusion that in the region
adjoining the tip of the nozzle, in which practically the
precipitation of all the particles occurs, the flow can be considered
self-simulating.

The results of Rober's primitive calculation of trajectories of
particles conform poorly with data from the model experiments by the
author with lycopodium powder. In these experiments we used
cylindrical tubes with a diameter of 9 mm and such a length that
in them it was possible to form parabolic velocity profile, and
the spores practically obtained the speed of air. The Re_r number
varied within limits of 280-9500. Trajectories of particles between
the tube and the plate were photographed. Results of the experiments
are shown in Fig. 18, in which $x_1 = \rho_1/R$, $x_2 = \rho_2/R$, ρ_1 and ρ_2 – distances
of particle from the axis at the beginning and end of trajectory,
$\theta = R/\tau\bar{U}$. For lycopodium powder $\tau = 0.0028$ s. The straight line in
Fig. 18 corresponds to $\tau = \infty$.

The data obtained by Rober about the mechanism of formation of
a ring-shaped deposit in konimeters are interesting. With sufficiently
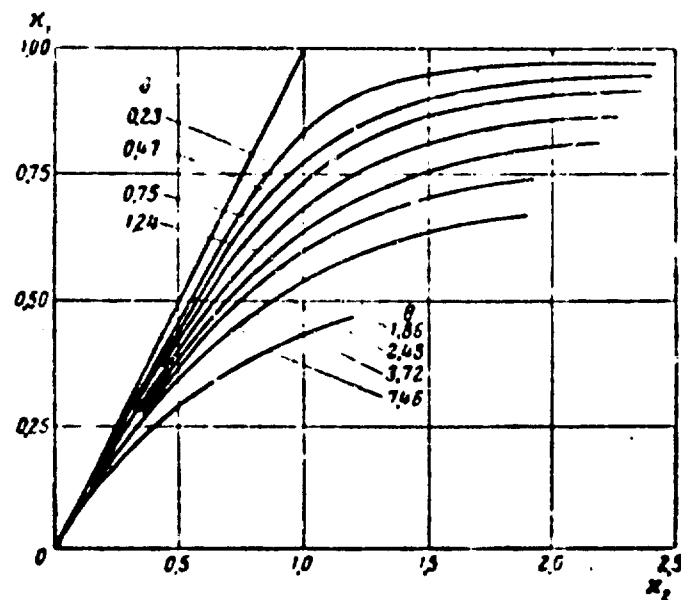
Fig. 18. Trajectories of particles
in a konimeter.

effective lubrication of plates the ring-shaped deposits will not
be formed, i.e., it indeed is caused by blowoff or, more correctly.,
the rebound of particles initially reaching the plate. However,
the formation of a deposit is caused not by deceleration of flow
near the plate, as this was usually assumed, but by vortices forming
behind the point of separation of the laminar boundary layer from the
plate. This is indicated by the following facts: a deposit will be
formed only at a rate of flow exceeding a certain critical value;
diameter of the deposit increases with an increase of the rate of
flow; the inner edge of the deposit is very sharp. During the
formation of deposits, due to deceleration in rate of flow everything
would occur differently.

The results of the last part of the work by Rober, which deals
with the effectiveness of adhesion of particles of dust to a plate,
are expounded on p.145. As a result of his investigations,
Rober considers as optimum a nozzle with a curvilinear profile:
diameters of inlets and outlets 3.0 and 0.3 mm, respectively,
length 15 mm, average speed of flow at outlet 200 m/s. However,
the conclusion of the author that in such a konimeter complete
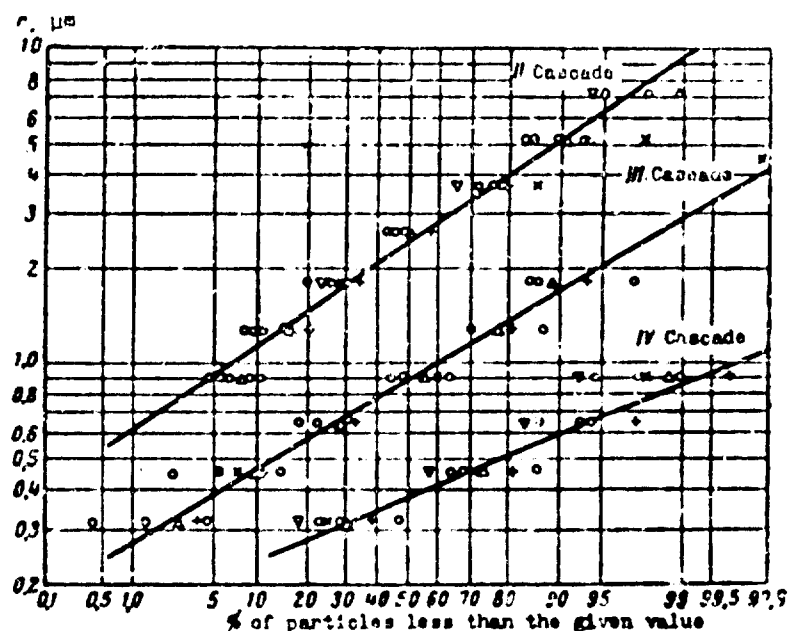
Fig. 19. Settling of particles of U_3O_8 in a cascade impactor.

precipitation of particles with $r > 0.25$ um (with $\gamma = 1$) should take place (founded on a series of rather rough calculations), is not fully convincing.

Cascade impactors have found wide application for dispersion analysis of dusts recently (especially in the United States). The following method turned out to be very convenient. First the impactor is calibrated, i.e., with the help of a microscope a determination is made of the average size of particles of a given dust deposited in each cascade. Then either by weighing on microbalances or by an analytical method the mass of deposit in each cascade is determined, and in such a way the fractional composition of dust is found. Very significant here is the question of how completely different fractions are separated in the impactor. Figure 19 gives the results of a series of measurements of U_3O_8 dust which were made by Lippman [143]. Here in all the measurements the concentration of dust was different. As can be seen from the graphs, in the deposits obtained in all three cascades, a logarithmically normal distribution of sizes of particles was

observed. Here the sizes of the smallest particles in the deposit
of fourth cascade are equal, i.e., separation is very incomplete.
However, the value of the median radius and mass of deposit in each
cascade is usually sufficient in practice to characterize the degree
of dispersion of the dust.

Inertial Precipitation of Aerosols on Bodies of Different Form

During the last few years a rather large number of works have
appeared on the inertial precipitation of aerosols on bodies of
different form. Extensive calculations of the coefficient of
inertial precipitation of particles from potential flow were carried
out in the Lewis Flight Propulsion Laboratory with the help of a
mechanical integrator specially designed for this purpose. The
authors originated from equations of motion of particles at large Re,
which in the absence of external forces for spherical particles
take the form

$$\tau \frac{dV_x}{dt} = \frac{Re\,\zeta}{24}(U_x - V_x) \text{ etc.} \tag{4.8}$$

or, passing to dimensionless variables x' = x/R,

$$t' = tU_0/R, \quad U_x' = U_x/U_0, \quad V_x' = V_x/U_0 \text{ etc.,}$$

$$\frac{dV_x'}{dt'} = \frac{Re\,\zeta}{24\,Stk}(U_x' - V_x') \text{ etc.} \tag{4.9}$$

Here $Re = 2r\,[(U_x - V_x)^2 + (U_y - V_y)^2]^{1/2}\nu$ and only at small Re the
equations (4.9) take a simple form

$$\frac{dV_x'}{dt'} = \frac{1}{Stk}(U_x' - V_x'); \quad \frac{dV_y'}{dt'} = \frac{1}{Stk}(U_y' - V_y') \tag{4.10}$$

and it is possible to calculate separately the movement of particles
along axes x and y. In general it is necessary in each point to
know the Re value and to simultaneously calculate movement along both
axes.
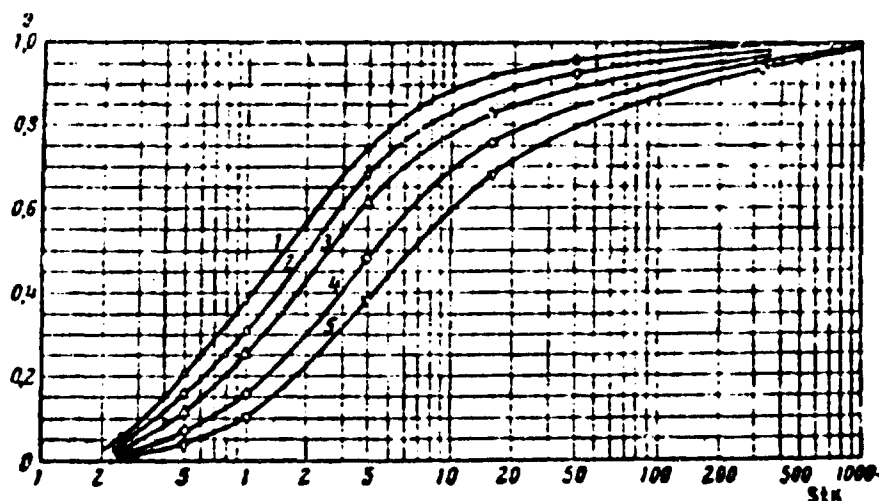
Fig. 20. Inertial precipitation of particles during potential flow past a cylinder; 1 — $\phi = 0$; 2 — $\phi = 100$; 3 — $\phi = 1000$; 4 — $\phi = 10,000$; 5 — $\phi = 50,000$.

Figure 20 presents the graphs for (ϑ, Stk), calculated by Brun et al. [144, 145], for precipitation on a cylinder with different values of the parameter $\phi = Re^2/Stk = 18\gamma_k RU_w/v\gamma - 9 Re_f \gamma_k/\gamma$, not depending on the size of particles, but jointly with the Stk number characterizing the degree of deviation of their movement from movement according to the Stokes formula, which corresponds to very small values of ϕ. A comparison of these evidently very exactly calculated graphs with those obtained by Langmuir and Blodzhett[2] shows that the values of ϑ in the latter are very low (in places up to 10%).

Figure 21 shows the curves for local coefficients of precipitation ϑ_{loc}. Such is called the ratio of number of particles, precipitated from uniform particle flux on a given element of surface, to their number, which would be precipitated at rectilinear trajectories of particles on an equidimensional element of surface perpendicular to these trajectories. Maximum value of ϑ_{loc} (with Stk $\to \infty$) is obviously equal to sin θ. These graphs also give the width, expressed in radians, of the deposit on a cylinder, determined by the points of intersection of the curves with the axis of abscissas. Furthermore, in the work they also calculated the

61
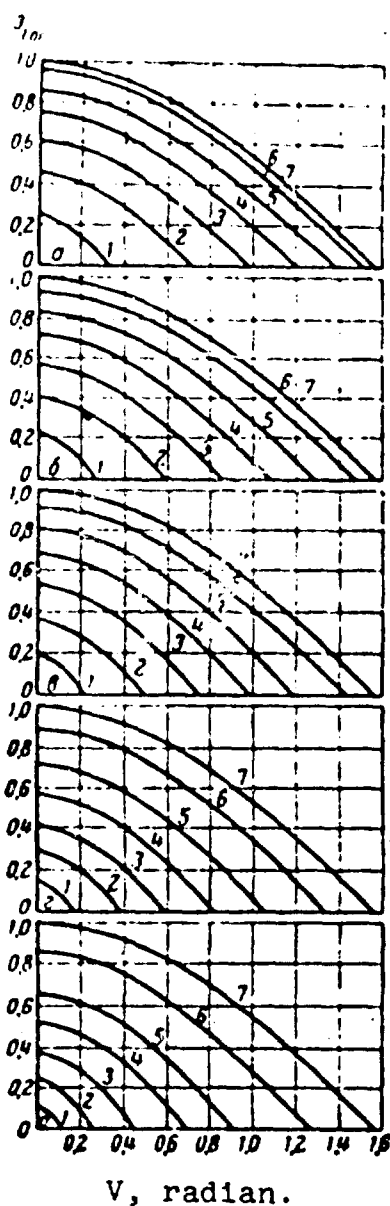
Fig. 21. Local coefficient of precipitation during potential flow past a cylinder: a) $\phi = 0$; b) $\phi = 100$; c) $\phi = 1000$; d) $\phi = 10,000$; e) $\phi = 50,000$. 1 — Stk = 0.25; 2 — Stk = 0.50; 3 — Stk = 1; 4 — Stk = 2; 5 — Stk = 4; 6 — Stk = 16; 7 — Stk = ∞.

V, radian.

velocities of particles along both axes at the time of their collision with cylinde·.

Analogous calculations have been made for precipitation on spheroids [147], wings of aircraft [148, 149],[3] in two-dimensional channels with a turn at 90° [151], etc. The effect of compressibility of air on value of coefficient of precipitation has also been calculated. This effect is important at speeds of flow which are comparable with the speed of sound, and leads to a small lowering of ә [152]. This effect is insignificantly small at very large and very small Stk numbers, and for a cylinder at $U_0 = 130$ m/s attains a maximum at Stk ≈ 5, where it leads to a lowering of ә by 0.5% at $\phi = 0$ and by 3% at $\phi = 50,000$.

Fonda and Herne [153] conducted an exact calculation of precipitation on a sphere during potential and viscous flow (Fig. 22).

Knowledge of theoretical curves (ә, Stk) for cylinders makes it possible to determine the content of liquid water and average dimension of drops in supercooled clouds — the most imporant factors in the formation of ice on aircraft [144]. For this they use somewhat slowed down revolving cylinders of different diameter set on the airplane fuselage. Drops of water hitting against the surface of cylinders freeze and cover the cylinders with a thin uniform layer
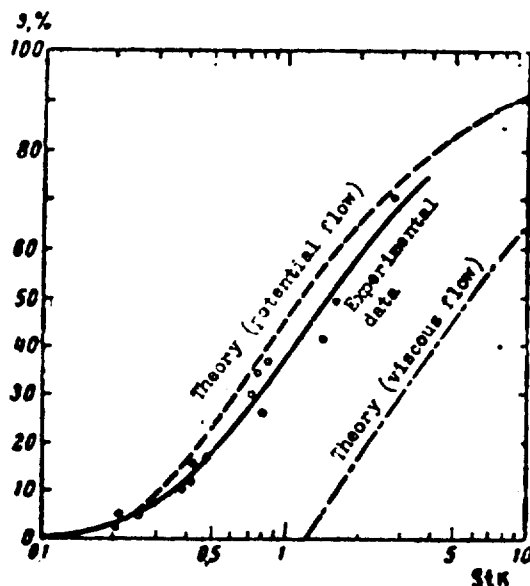
Fig. 22. Inertial precip-
itation of particles on a
sphere.

of ice. They determine the mass of ice ϕ', settled on an unit of
length of each cylinder in an unit of time, equal to $2RU_0c$, where
c — concentration by weight (water content) of the cloud, U_0 - speed
of aircraft. Data obtained are plotted in coordinates [lg(x), lg (1/R)]
and a curve is drawn through the points.

For simplicity let us take the situation that a cloud is
isodispersed. Since under the conditions of the experiment lg x =
= lg ϑ + const and lg Stk = lg (1/R) + const, then the experimental
[lg (x), lg (1/R)] and theoretical (lg ϑ, lg Stk) curves have to conform during
parallel shifting and based on the extent of displacements on both
axes one can determine the values of c and Stk, and from here r.
In view of the fact that together with R the parameter ϕ is changed,
it is necessary to use curves (lg ϑ, lg Stk), plotted not with ϕ = const,
but with ϕ Stk = Re^2 = const, since specifically this value remains
constant in these experiments. It is also necessary to select
that value of constant at which it is possible to join the
theoretical and experimental curves. In actual polydispersed
clouds the calculation is complicated, and accuracy of determination
of concentration by weight and weight median radius of drops in
this case is not great.

Tribus et al. [154] and, in more detail, Serafini [87] examined

63
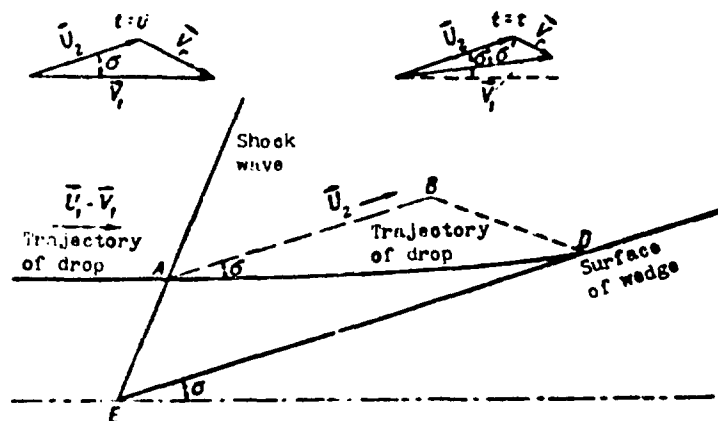
Fig. 23. Trajectories of drops during
supersonic flow past wedge-shaped profile.

the precipitation of water drops on two-dimensional wedge-shaped
profiles at supersonic speeds of flow (Fig. 23). In this case the
field of flow differs sharply from those examined earlier. The flow
(with speed U_1) in front of the shock wave formed before the profile,
remains undisturbed. Behind the wave the flow U_2 is also uniform,
but is directed parallel to the surface of wedge. The drop, initially
having the velocity $V_1 = U_1$, after crossing the wave possesses
relative velocity $V_r = V_1 - U_2$ and its absolute velocity is composed
of constant velocity U_2 and gradually decreasing velocity V_r. The
particle reaches the surface of wedge in the case when its inertia
range ℓ_1 in the direction V_r is greater than the distance BD.
Trajectories of all drops up to crossing with the surface of the
wedge obviously have an identical form. Using formula (3.7), it is
possible with the help of simple trigonometric calculations to
determine the critical value of segment AE, through which will pass
all the drops attaining the surface of the wedge, the corresponding
value ED, i.e., the width of deposit on the wedge, and also local
coefficients of precipitation. It is obviously not necessary to
speak in this case of the general coefficient of precipitation.

Due to simplicity, the favorite method for investigation of
aerosols — the precipitation of particles on a glass plate set
perpendicular to the flow — could give good results if the values of

the local coefficient of precipitation in the function of Stk
number in the middle of plate were exactly known; during constiuction
of the distribution curve of particle dimensions one should on.y have
to divide the number of particles of a given size, counted in the
precipitate, into the ϑ_{lo} number corresponding to this size.

At fairly large Re_f numbers flow past a plate occurs with
detachment of flow from the edges of the plate. For this case
L. Levin [155] calculated ϑ_{lo} in the middle of a plate (see Table 2).
It is very significant that the value ϑ_{lo} here turned out to be
practically constant for the entire inner part of the plate, m:king
up more than half of its width. It is necessary, however, to
consider that in Table 2 no consideration is given to the boun ary
layer effect or the effect of contact, i.e., it can bc used on.y at
high values of Re_f and small values of r/h, where h — half-wid h of
the plate $(Stk = 2r^2\gamma U_a/9\psi_i)$.

Table 2. Local coefficients of precipitation
on flat plate from a potential flow with
detachment.

Stk	$\frac{1}{4}(\pi \div 4) = 0.5...$	1	2	3	4	5	7,5	10	15	20	30
ϑ_{lo}		0	0,15	0,35	0,44	0,49	0,56	0,63	0,67	0,72	0,77	0,81

Proceeding from the theory of flow of an "aerosol liquid"
(see p. 43), Robinson [115] obtained an approximate formula for the
coefficient of precipitation during potential flow past a cylindrical
surface of arbitrary profile and small Re numbers. During der:vation
of this formula it was accepted that the value U — V is small
everywhere, which is clearly incorrect near the surface of bod;,
and, indeed, the formula gives values of ∋ which are strongly too
high at all values of Stk besides Stk = ∞.

Further Robinson proved that if speed of sedimentation of
particles is considerably less than the speed of flow, the effects
of precipitation at the expense of gravity and inertia are addltive.

G. Natanson [156] calculated, using the numerical method (disregarding the coupling effect, i.e., considering R >> r), Stk_{kr} for Stokes particles during viscous flow past a sphere based on Stokes: Stk_{kr} = 1.21 ± 0.01 in very good agreement with the value found earlier by langmuir [157]. During flow past a sphere according to Oseen at Re_f = 0.1 Stk_{kr} = 1.15 ± 0.01 and during flow past a cylinder according to Oseen at Re_f = 0.1 Stk_{kr} = 4.3 ± 0.1.

The problem of calculating Stk_{kr} at small Re_f is examined in a general form by L. Levin [157]. The value of Stk_{kr} is closely connected with the nature of flow near the front stagnation point. The speed of flow along axis x in all cases can be expressed by the approximate formula $U_x = -ax^n$, if the beginning of the coordinates is placed at the stagnation point. Taking $Stk_{kr} = Aa^m$, where A and m are constants, it is possible to show that m = -1/n. Thus, during potential flowing around, when n = 1, Stk_{kr} = 1/4a [159]. During viscous flowing around a sphere and cylinder, as can be ascertained from the corresponding equations of field of flow, n = 2 and Stk_{kr} = $A/a^{\prime\prime}$. From the expression derived by Levin for a in the case of Oseen flow past a sphere, a = (24 + 12 Re_f)/(16 - 3 re_f), it is easy to see that in the area of applicability of Oseen equations Stk_{kr} slowly decreases with an increase of Re_f.

L. Levin also estimated the boundary layer effect on the value of Stk_{kr} during potential flowing around: he showed that Stk_{kr} does not exceed the value z, determined by equation

$$z = \frac{1}{4a} + \left(\frac{0.65}{\pi \beta a^{\prime\prime} Re_f^{\prime}} \right)^{\prime\prime}. \tag{4.11}$$

where constant β equals 3.8 when flowing around a cylinder and 1.8 when flowing around a plate. For a cylinder z = 0.17 at Re_f = 10^5 and 0.25 at Re_f = 10^3, i.e., noticeably exceeds the value of Stk_{kr} in the absence of a boundary layer (0.125).

Davies and Peetz [160] calculated coefficient of precipitation of Stokes particles on cylinder taking into account coupling for

three cases: potential flowing around without a boundary layer and viscous flowing around at $Re_f = 10$ and 0.2. Besides this calculations were made of velocities of particles at the time of collision and for case r/R << 1, the width of the deposit, and local coefficients of precipitation. Results of calculations of ə are shown in Figs. 24-26. For $Re_f = 10$ the field of flow calculated by Thom [161] is taken; here the value $Stk_{kr} = 0.42$ is obtained. Thus, the authors obtained considerably lower values for ə than Landahl, who originated from the same field of flow [162]. The Landahl curve is undoubtedly incorrect, since already at Stk = 6 it reaches the curve for potential flow.

For $Re_f = 0.2$ the authors used the field of flow calculated by Davies [163] during flowing around a cylinder with this Re_f. As already indicated in the literature [156], these calculations are inaccurate near the stagnation point; it emanates from them that the speed of flow along the axis x here equals $U_x = -ax$ which, as we saw above, takes place only during potential flowing around. Therefore the value $Stk_{kr} = 0.899$, calculated from the value of coefficient a, is undoubtedly minimized. The stated circumstance was apparently reflected also on the accuracy of initial sections of curves in Fig. 26. This remark pertains also to the case $Re_f = = 10$.
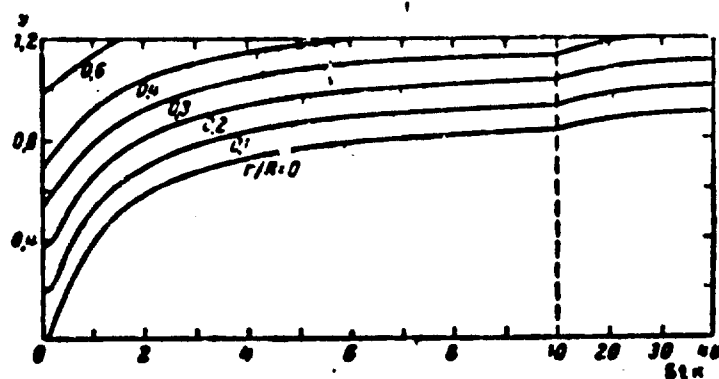
Fig. 24. Inertial precipitation on a cylinder during potential flowing around taking into account the coupling effect.
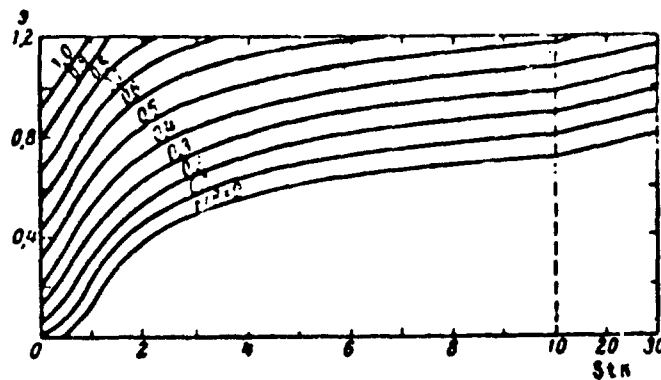
Fig. 25. Inertial precipitation on cylinder at $Re_r = 10$.
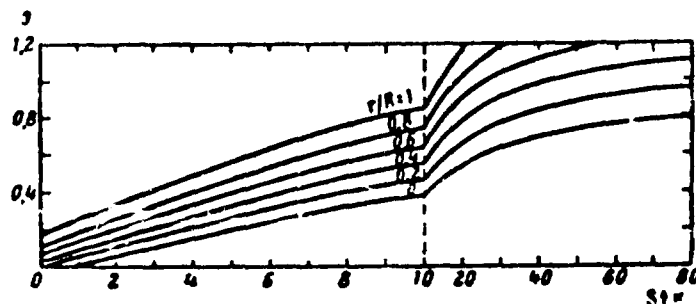
Fig. 26. Inertial precipitation on a cylinder at $Re_r = 0.2$.

We will switch to experimental investigations of the settling of aerosols from a flow onto various bodies. Gregory [164] worked with lycopodium power ($\bar{r} = 16$ μm), precipitated on cylinders which were lubricated with a sticky composition with r = 0.1-10 mm at an airspeed of 1-10 m/s in dynamic tube. His results are close to the data of Rantz and Uong [162].

Lewis and Ruggieri [165] sprayed colored water in a wind tunnel with a 2 × 3 m cross section at U = 76 m/s and determined by the colorimetric method the amount of fog precipitated on bodies located in the tunnel (bodies were covered with strips of filter paper); these were spheres with R = 7.5 and 22.5 cm, ellipsoids, and a cone. Since the fogs ($\bar{r} = 5.5-9.5$ μm) were quite polydispersed, then the theoretical calculation of precipitation was performed taking into account dispersed composition of the fog. Figure 27 gives the

68
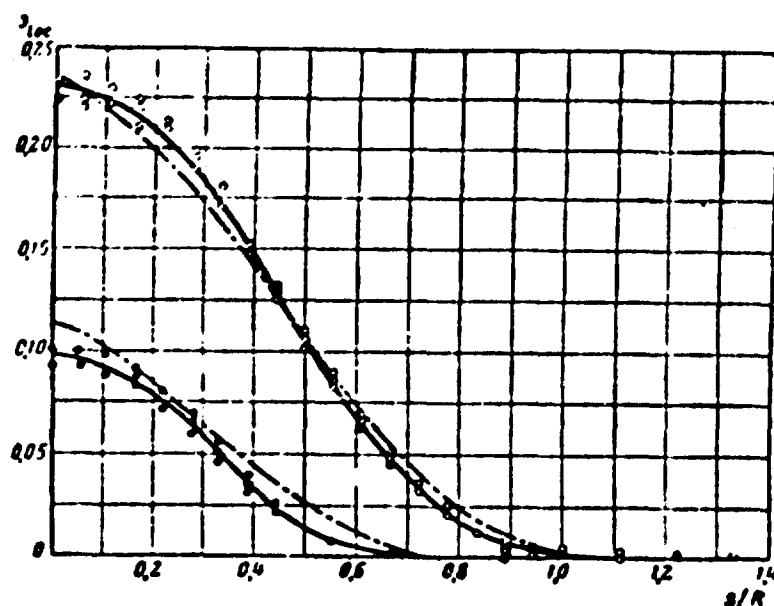
Fig. 27. Inertial precipitation of water
drops on a sphere. Solid curves — experi-
mental, intermittent — theoretical. Lower
curves: $r_m = 5.75$ µm; $Stk_m^! = 0.06$; upper
curves. $r_m = 8.35$ µm, $Stk_m^! = 0.11$.

theoretical and experimental curves of local coefficient of
precipitation in function of dimensionless distance from the
stagnation point s/R for two values of weight median radius of drops
and the respective corrected Stokes number, expressed through the
true value of length of inertial path [see formula (3.7)]. As
can be seen from the figure, agreement of theory with experiment
is fully satisfactory here.

V. Ignat'yev [166] measured the coefficients of precipitation of
coal and iron dust, separated by air elutriation into fractions
with $\bar{r}$ from 6 to 100 µm, onto cylinders with R = 0.6-2.5 cm in a
descending vertical flow with U = 2-16 m/s, i.e., at Re_f =
= 1600-54,000. On the cylinder was placed a vaseline lubricated
celluloid tape and the precipitated particles were calculated under
a microscope. The relation r/R was always <0.02, i.e., the coupling
effect could be disregarded. In every series of experiments the
dependence of a on r at constant U and R was determined. The curve
(η, Stk), obtained at U = 2 m/s and R = 2.5 cm is very close to the
theoretical curve for large Re_f, but along with the increase of the

relation U/R the curve is shifted all the more to the right and at
U = 16 m/s and R = 0.6 cm approximately coincides with the curve
of Davies for Re_f = 0.2 (Fig. 26). The reasons for this phenomenon
are vague. Since the factor ϕ in these experiments <100, then,
according to Fig. 20, we are not dealing with deviations from the
Stokes formula.

The curves obtained by V. Ignat'yev for the dependence of local
coefficient of precipitation on angle θ are close to the theoretical
curve in Fig. 21, but near the axis of abscissas are bent and approach
the axis asymptotically, i.e., a certain quantity of precipitation
will be formed there, where according to calculation it should not be.
This is possibly caused by a shift of the layer of vaseline with
particles under the impact of airflow or transverse turbulent
pulsations.

The dependence of coefficients of precipitation on the direction
of flow found by V. Ignat'yev is interesting. In Fig. 28 are
given curves (ϑ_{lok}, θ) at U = 2 m/s, R = 2.5 cm and at various values
of $\bar{r}$ for descending (1) and ascending (2) flows. As can be seen
from the graphs, curves 1 and 2 differ strongly at small and large
values of $\bar{r}$ and almost coincide at average values. This is explained
by the fact that speed of sedimentation precipitation, determined by
the value V_S, is proportional to Stk, and the dependence (ϑ, Stk) is
expressed by a curve with a bend. It is easy to ascertain that under
the conditions of the experiments the straight line (V_S, Stk)
intersects curve (ϑU, Stk) in two points and between them $V_S < \vartheta U$, and
outside them — just the opposite. At Stk = 0.09, i.e., lower than
Stk_{kr}, sedimentation precipitation completely dominates. The small
deposit on the lower side of the cylinder in an ascending current is
caused only by a certain polydispersionality of the dust fraction,
and on the upper side of the cylinder the deposits obtained in
ascending and descending flows are quite close. At $\bar{r}$ = 108 μm V^S
reaches 110 cm/s, i.e., is equal to half the speed of flow and
therefore here sedimentation again essentially affects the value
of ϑ.

70
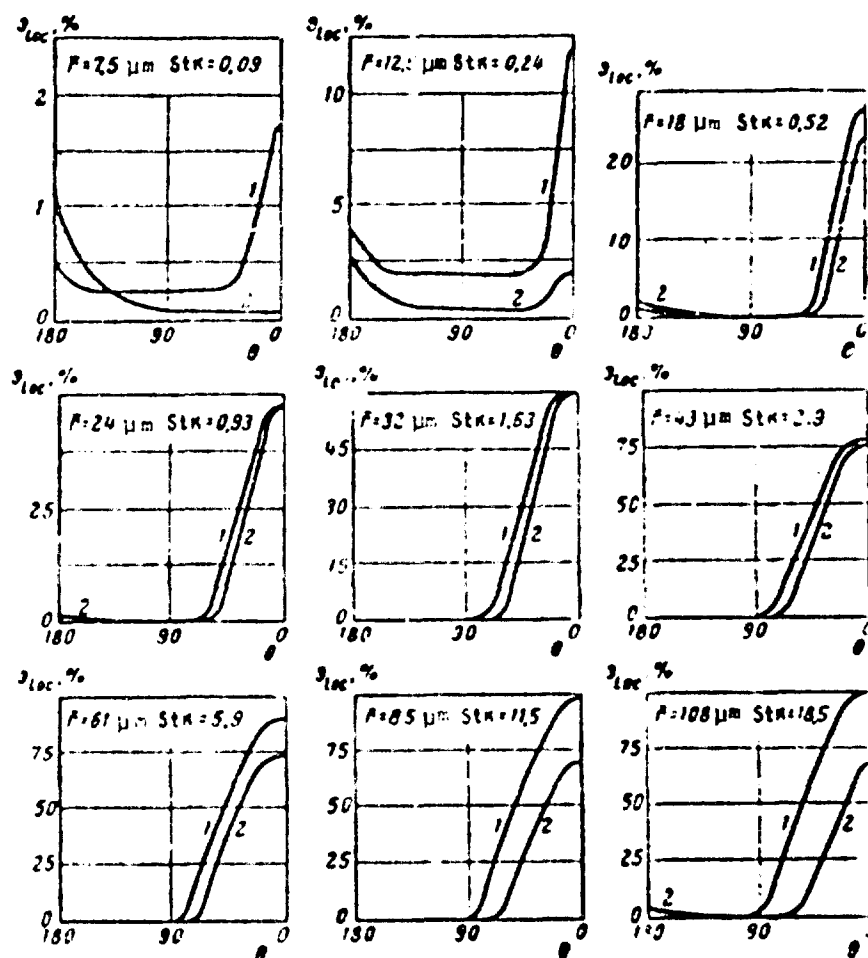
Fig. 28. Inertial precipitation of coal dust
on a cylinder descending (1) and ascending (2)
flows.

The experiments by A. Amelin and . Bey kov [167] were corducted
in horizontal tubes at $\bar{U} = 1\text{-}16$ m/s and R = 0.5-1.25 cm with a
polydispersed (r = 1-30 μm) oil mist (in the precipitate particles
of various size were counted separately) and with porcelain dust
$\bar{r} = 4.4$ and 18 μm. The graph obtained (ə, Stk) is characterized by
exceedingly low values of ə at small Stk (ə = 0.01 at Stk = 1) and
a very steep climb; the curve reaches a line ə = 1 at Stk = 1ϵ,
not asymptotically, but under a finite angle. These strange results
are apparently caused in principle by the erroneous method of
measuring the concentration of aerosol in a flow [168].

Jarman [169] passed a monodispersed kerosene fog with r = 8-24 um

through a wide wind tunnel with a speed of $\bar{U}_0 = 1$ m/s and determined the amount of fog precipitated on small metallic grids placed in the tunnel. Speed of flow through the grids was not measured, but was calculated by the formula $U = \bar{U}_0/[1 + (1 - \beta)/4\beta^2]$ [170], where β — specific area of openings in the grid (cm^2/cm^2). Since in these experiments $Re_f = 6\text{-}18$, then for comparison with theoretical the curve in Fig. 25 was selected. Experimental values of $\Im$ were on the average 0-25% higher than theoretical, as it should have been expected, since in a system of cylinders the current lines pass nearer to their surface than in single cylinders. For the precipitation of aerosols on series of consectuvely located grids see pp. 94-95.

Electrostatic Precipitation of Aerosols from a Flow on Bodies of Various Form

In a number of works the precipitation of aerosols from a flow under the action of electrical forces has been investigated. With the help of a computer Kraemer and Johnstone [171] calculated coefficients of precipitation of aerosols from potential and viscous flows on a conducting spherical collector under the action of electrostatic forces, taking into account the coupling effect, but neglecting inertia of particles. Corresponding to various electrostatic forces are the dimensionless parameters K, expressing the relation of the electrical force acting on a particle found c the surface of the collector, and the values of $6\pi\eta r U_0$, characterizing the resistance of the medium to the movement of the particle (applicability of the Stokes formula is assumed):

$$K_E = \frac{qQ}{6\pi R^2 r \eta U_0}; \quad K_N = \frac{q^2}{6\pi \eta U_0 R i}; \quad K_S = \frac{2Rnq^2}{\psi U_0}$$

$$K_T = \frac{(\varepsilon_h - 1) r^2 Q^2}{(\varepsilon_h + 2) 3\pi R^4 \eta U_0}; \qquad K_0 = \frac{q^2 n R^{-1}}{3\pi U_0 R}; \qquad (4.12)$$

where q and Q — charge of particle and collector, R — its radius, n — number of particles in 1 cm^3, U_0 — speed of flow far from the collector, R' — radius of aerosol cloud. K_E corresponds to the Coulomb force between the charged collector and the charged particles.

K_T — induction force between charged collector and uncharged particles, K_M — the same between charged particles and isolated uncharged collector. K_G and K_S pertain to a case of an unipolar charged aerosol. K_G corresponds to the force between particles and the charge inducted by them in the grounded collector, K_S — force, having effect on particles from the side of other particles. Here the observance of inequalities $\frac{4}{3}\pi r^3 n = \phi \ll 1$ and $\phi R'^2/R^2 \ll 1$ is assumed.
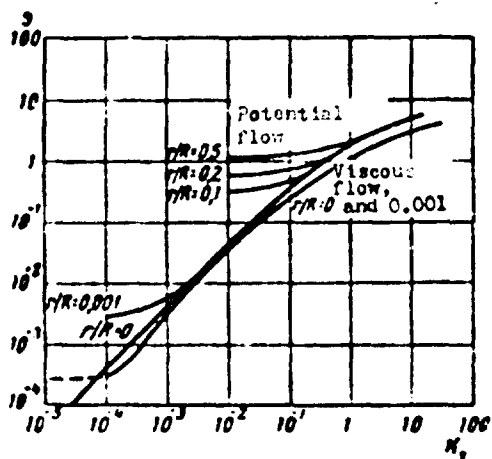
Fig. 29.

Fig. 30.

Fig. 29. Precipitation of uncharged aerosol on charged isolated sphericial collector.

Fig. 30. Precipitation of bipolar charged aerosol on uncharged isolated spherical collector.

Figure 29 gives the results of calculations for a case of a charged collector and uncharged particles, in Fig. 30, for a case of uncharged isolated collector and bipolar charged aerosol, in Fig 31, for a case of charged collector and aerosol with unipolar charges of the opposite sign (where the authors disregarded induction in particles). The relationship r/R characterizes the coupling effect. The authors showed that a simple summation of coefficients of precipitation, induced by different electrical forces, sometimes gives strongly overstated values of э in comparison with accurately calculated values. In Fig. 32 are given the results of experiments

73
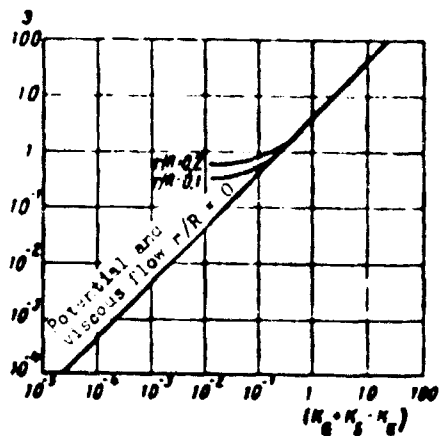
Fig. 31.   Precipitation of
unipolar charged aerosol on
spherical collector charged
with the opposite sign.
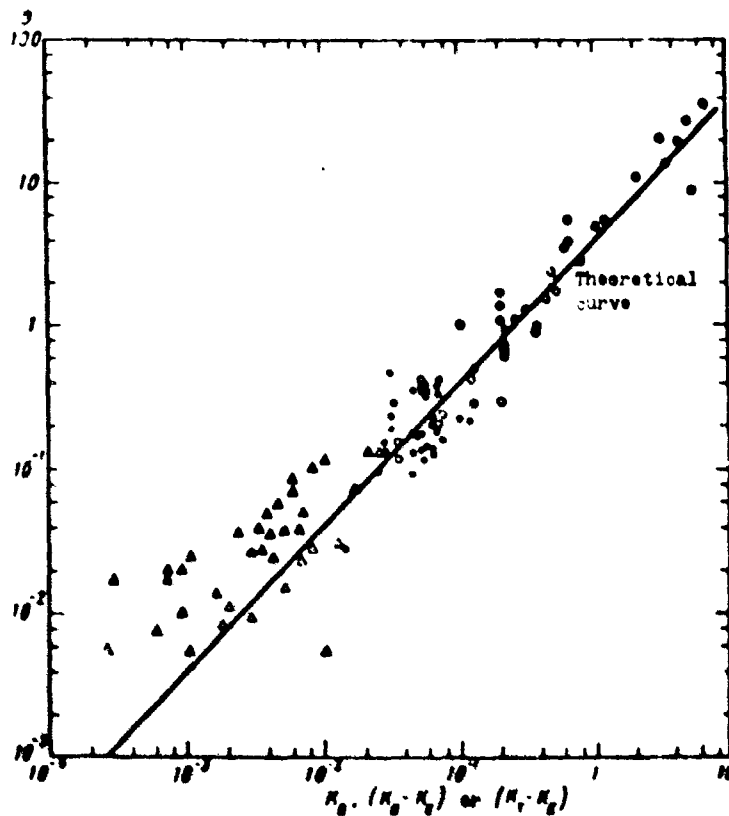
Fig. 32.   Precipitation of charged mist
of dioctyl phthalate on a spherical
collector.   o – charged collector,
unipolar charged aerosol $(K_G - K_E)$; Δ –
charged collector, bipolar charged
aerosol $(K_T - K_E)$; ● – grounded collector,
unipolar charged aerosol (K_G).

74

by the authors with aerosols of dioctyl phtholate, with $\bar{r} =$ = 0.27-0.59 μm, charged unipolarly or bipolarly, at R = 0.3-0 55 cm, U_0 = 1.5-6.9 cm/s, and $\bar{q}$ = 0.15-137 elementary charges. In a 1 three series of experiments one of the parameters K clearly dominated the others and they could be disregarded.

G. Natanson [172] investigated the precipitation of aerosols on cylinder from a flux under the action of electrostatic forces taking into account the coupling effect, but neglecting inertia of particles. Here one should distinguish two basic cases: when limiting trajectories of precipitated particles 1) touch on the cylindrical surface, and 2) envelope it and intersect in the near stagnation point. In the first case precipitation occurs basically on front side of cylinder, in second, — over its entire surface. The second case takes place when the radial component of velocity of a particle coming in contact with the surface of cylinder, i.e., the algebraic sum of radial speed of flow and velocity of a particle under the action of electrical force, everywhere is directed into the cylinder, as for example, very small values of r/R. Subsequently we will limit ourselve. to an account of this case. For precipitation of charged particles on a cylinder charged by another sign G. Natanson found, disregarding induction forces,

$$\vartheta = \frac{2\pi BQ'q}{U_0 R}.$$
(4.13)

where B — mobility of particles Q' — charge of unit of length of cylinder. For a charged cylinder and uncharged particles, at large Q' and small U_0, i.e., at $\vartheta \gg 1$

$$\vartheta = \left(\frac{6(\varepsilon_k - 1)BQ'^2 r^3}{(\varepsilon_k + 2)U_0 R^3} - 1\right)^{1/2}.$$
(4.14)

Substituting U_0 in this formula for speed of sedimentation of particles V_S, it is possible to obtain the Cochet formula for precipitation of sedimentation particles on a charged cylinder [173]. At $\vartheta \ll 1$

$$\vartheta = \frac{4\pi(\varepsilon_k - 1)BQ'^2 r^3}{(\varepsilon_k + 2)U_0 R^3}.$$
(4.15)

In the examined cases э does not depend on the nature of flow.

During precipitation of charged particles on an uncharged cylinder and э << 1 there usually takes place in this case

$$э = \left(\frac{3\pi(e_k - 1)q^2B}{2(e_k + 2)U_e R^3}\right)^{1/3}$$

(4.16)

during potential flowing around and

$$э = \left[\frac{(e_k - 1)q^2B}{(e_k + 2)U_e R^3(2.00 - \ln \text{Re}_f)}\right]^{1/3}$$

(4.17)

during viscous flowing around (based on Lamb).

G. Natanson also derived formulas for the first of the above-examined cases, when э depends on the position of point of contact of limiting trajectories with the surface of the cylinder. In this case э always depends on the nature of flow.

Roughly approximated formulas for precipitation from a potential flow on a cylinder under the action of electrostatic forces have been derived also Gillespie [174].

Since the field around charged bodies is solenoidal, then in the absence of inertia the concentration n_0 in the flow of an aerosol is not changed (see pp. 44-45), and, if far off from the body it is constant, then this is preserved also at the surface of the body. Therefore total flux of the aerosol to the surface, as noted by S. Dukhin and B. Deryagin [175], is equal to

$$\Phi = n_0 \oint (U_n + BF_n)\, dS.$$

(4.18)

where U_n and F_n — radial components of speed of flow and electrostatic or some other central force, and the integral is taken over the entire surface of the body. In this case it is not necessary to calculate the limiting trajectories of particles.

Since in the case of an electrostatic field $F_n = E_n q$, where E — field strength, and $\int E_n dS = -4\pi Q$, then for very small particles, when it is possible to compute $U_n = 0$

$$\vartheta = -\frac{4\pi q Q B}{U_\theta S_M},$$

(4.19)

where S_M — middle section of body. Formula (4.19), obtained by L. Levin [176], is accurate for a body of arbitrary form. For a cylinder it is modified into formula (4.13), for a sphere into formula

$$\vartheta = -\frac{4 q Q B}{U_\theta R^2}.$$

CHAPTER 5

BROWNIAN MOVEMENT AND DIFFUSION IN AEROSOLS

Diffusion Precipitation of Aerosols in a Fixed Medium

Usually in problems of diffusion precipitation of aerosols it is accepted that at a wall the concentration is equal to zero. This condition is not completely accurate. Similar to the known phenomenon of jump in concentration of vapor at the surface of an evaporating drop [177], an analogous jump in particle density at an absorbing wall should also exist in aerosols. It is easy to see that this jump has practical value only at an apparent average length of free path of aerosol particles, comparable with the dimensions of the body to which diffuses aerosol [178].

I. Todorov and A. Sheludko [179] investigated diffusion precipitation of an aerosol on the walls of a spherical vessel, taking into account sedimentation of particles for two types of boundary conditions on the walls of the vessel: with and without consideration for jump in concentration. Since the speed of sedimentation of Stokes particles is proportional to r^2, and diffusion rate to r^{-1}, then, as it is easy to see, the total speed of precipitation should have a minimum at a specific value of r, namely at $r_m \approx (3kT/-R\gamma_s)^{1/3}$. In pulmonary alveoli R ≈ 0.015 cm and at $\gamma = 1$ $r_m = 0.14$ μm in agreement with the calculations of Davies [180].

78

In an aerosol found in an infinitely long vertical cylindrical vessel with radius R, the average concentration at the moment t is equal [181] to

$$n = 4n_0 \sum_{\nu=1}^{\infty} \frac{1}{\beta_\nu^2} \exp\left(-D\beta_\nu^2 t / R^2\right).$$

(5.1)

Based on this formula "static diffusion" method is then proposed by Pollak and O'Connor [182, 183] and by Furth [184] for determining the degree of dispersion of aerosols (in contrast to the "dynamic diffusion method" described below). Portions of an aerosol were aspirated from a large gas tank into the cylindrical tube of a photoelectric counter of condensation nuclei and immediately the number Z of particles contained in the tube was determined. Tier new portions were introduced and Z was determined after different intervals of time. From the data obtained coefficient of diffusion D was calculated according to formula (5.1) and, further, the average radius of particles. Here systematically considerably lower values for D were obtained than during the application of the dynamic method. Since in these experiments the tubes for some reason were not ventilated with a surplus of aerosol, and the volume of aerosol aspirated was equal to the volume of the tube, then due to the parabolic profile of flow at the walls of the tube there remained a layer of variable thickness which did not contain particles. This led to a decrease of diffusion precipitation of particles on the walls. Thickness of layer was not determined by hydrodynamic calculations. Instead of this the authors took the thickness of the constant and selected it such a way as to remove the above-mentioned divergence. Furthermore, in the pipes used, which had a diameter ~2 cm, convection inevitably had to appear and the application of formula (5.1), strictly speaking, was not permissible. Let us note, however, that for polydispersed aerosols both diffusion methods give understated mean values of diffusion coefficient (see pp. 86-87).

Richardson and Wooding [185] investigated experimentally the
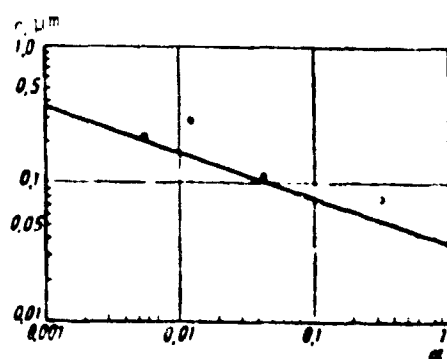
Fig. 33.   Diffusion precipitation of an aerosol in a horizontal plane-parallel slot.
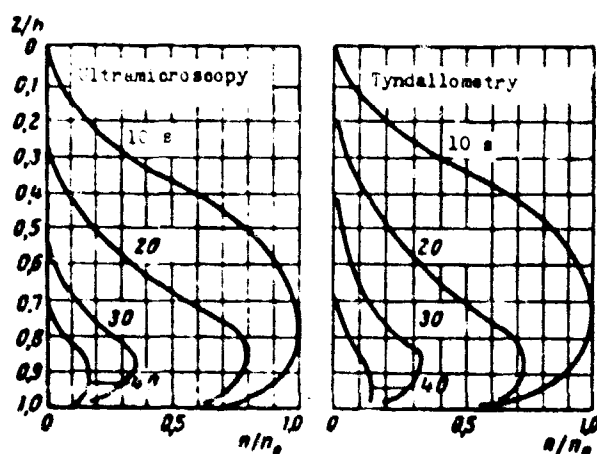
Fig. 34.   Distribution of particle density in a horizontal plane-parallel slot.

diffusion of an aerosol found between parallel horizontal walls. The work was conducted with rather isodipsersed aerosols with $\bar{r}$ = = 0.05-2 um with a distance of h = 0.2 cm between walls and the thorough thorough removal of convection. Concentration of aerosol in function of time t and height z was determined by two methods — tyndallometric and ultramicroscopic. The resulting calculated values of ratios $\Delta n/\Delta t$, $\Delta n/\Delta z$, and $\Delta (\Delta n/\Delta z) \Delta z$ were placed in equation $\partial n/\partial t = -V_s \partial n/\partial z +$ $+ D\partial^2 n/\partial z^2$ [186] and from here the value $a = D/hV_s$ was found. In Fig. 33 the theoretical curve $a = 3kT/4\pi r^2 \gamma gh$ is drawn in coordinates (lg r, lg a) and the experimental points obtained by the authors are plotted. Considering the nature of these measurements, coincidence should be considered completely satisfactory. Figure 34 gives

the curves n/n_0 in function z/h obtained by both methods. For some reason the authors did not make a comparison with theoretical curves [187].

Diffusion Precipitation of Aerosols from a Laminar Flow

The theory of diffusion of aerosols to walls from a laminar flow has a great deal of importance during the investigation of highly dispersed aerosols, since it is the basis of one of the most important methods for determination of particle size in such aerosols and, furthermore, makes it possible to estimate loss of particles induced by diffusion in connecting tubes, channels, etc. Therefore we will give more detailed data on this problem.

For a steady state of diffusion in a round tube with length x, i.e., with not very small values of the parameter $\mu = Dx/R^2\overline{U}$, Gormley and Kennedy [188] obtained the formula

$$n/n_0 = 0.819 \exp(-3.657\,\mu) + 0.097 \exp(-22.3\mu) + 0.032 \exp(-5.7\mu). \tag{5.2}$$

For unsteady conditions of diffusion, i.e., for small μ these same authors derived the formula

$$\overline{n}/n_0 = 1 - 2.56\,\mu^{\prime\prime} + 1.2\,\mu + 0.177\,\mu^{\prime\prime}. \tag{5.3}$$

Presented below are the values $\overline{n}/n_0$ calculated by these formulas for a number of values μ.

As can be seen from the data cited, at $0.01 < \mu < 0.1$ the values $\overline{n}/n_0$, calculated by formulas (5.2) and (5.3), differ by less than 1%. With $\mu < 0.01$ it follows naturally to use formula (5.3), with $\mu > 0.1$ — formula (5.2).

81

Table 3. Diffusion of aerosols
to walls during laminar flow in
a round tube.

μ	$\bar{n}/n_0$ by (5.2)	$\bar{n}/n_0$ by (5.3)
0	0,948	1,000
0,0002	—	0,991
0,0004	—	0,986
0,001	—	0,975
0,002	—	0,962
0,004	—	0,940
0,006	0,918	0,931
0,01	0,885	0,803
0,02	0,833	0,836
0,03	0,789	0,790
0,04	0,750	0,750
0,05	0,716	0,715
0,10	0,578	0,570
0,20	0,394	0,383
0,30	0,274	0,245
0,50	0,131	0,055
1,0	0,021	—0,19
2,0	0,0005	—0,25

For diffusion precipitation in a plane-parallel channel with a
distance 2h between walls the following formulas are derived:

by Gormley [189] for large $\mu = Dx/h^2 \bar{U}$

$$\bar{n}/n_0 = 0,9099 \exp(-1,885\,\mu) + 0,0531 \exp(-21,43\mu) \tag{5.4}$$

by Kennedy [190] for small μ

$$\bar{n}/n_0 = 1 - 1,175\,\mu^{\frac{2}{3}} + 0,1\mu + 0,0175\,\mu^{\frac{4}{3}} \tag{5.5}$$

by De Marcus [191] for any μ

$$\bar{n}/n_0 = 0,9149 \exp(-1,885\mu) + 0,0592 \exp(-22,33\,\mu) + \\ + 0,0258 \exp(-151,8\mu) \tag{5.6}$$

Presented below are the values $\bar{n}/n_0$, calculated by these formulas.

As can be seen from the data cited, formula (5.6) is indeed
univer al.

82

Table 4. Diffusion of aerosols to
walls during laminar flow in a plane-
parallel channel.

p	n/n_0 by (5.4)	n/n_0 by (5.5)	n/n_0 by (5.6)
0	0,963	1,00	1,00
0,001	0,960	0,988	0,993
0,002	0,957	0,982	0,987
0,005	0,949	0,966	0,971
0,01	0,936	0,946	0,951
0,02	0,911	0,915	0,920
0,05	0,846	0,846	0,852
0,1	0,760	0,758	0,764
0,15	0,688	0,685	0,692
0,20	0,625	0,620	0,629
0,30	0,518	0,507	0,520
0,40	0,428	0,407	0,430
0,60	0,294	0,233	0,295
0,80	0,201	0,08	0,202
1,0	0,138	—	0,139
1,5	0,054	—	0,054
2,0	0,021	—	0,021
4,0	0,0005	—	0,0005

Thomas [192] worked with a "diffusion battery" consisting of
20 plane-parallel channels with h = 0.05 mm and a length of 4' cm.
Aerosols of dioctyl phthalate with $\bar{r}$ = 0.16-0.5 μm were passed through
the battery with speeds o. -20 cm/s. For elimination of entrance
effects in parallel experiments an aerosol was passed through the
same battery with a length of 5 cm and as the basis of calculations
the tyndallometrically measured ratio of concentrations of aerosols
coming out of both batteries was used. Average dimensions of
particles were determined based on light scattering under two
different angles and on the Tyndall spectra of higher orders.

It was revealed that diffusion coefficients of aerosols
determined in such a way increased strongly (by two times) with an
increase in the speed of flow. The same observation was made by
Pollak et al. [182]. Preceeding from the clearly incorrect
assumption that this phenomenon is caused by turbulence, Thomas
extrapolated the resulting values of D to $\bar{U}$ = 0. After this the
values $\bar{r}$ calculated from D coincided with those found by the optical
method at $\bar{r}$ = 0.16-0.30 μm, but were nevertheless noticeably

83

understated at $\bar{r} > 0.3$ μm. In regard to the application of short battery for eliminating entrance effects, then in one article [193] Thomas reported that with such a method they obtained more exact results, but in another article [194] asserted the opposite.

Pollak and Metnieks [195] turned attention to the circumstance that in the case of a polydispersed aerosol the experimentally determined coefficient of diffusion should increase with an increase in the speed of flow. For simplification, in a formula of the type (5.2, the authors take only the first exponential member and accept that the aerosol consists of several isodispersed fractions. Let us assume that n_{10} and $\bar{n}_1$ are particle densities of the i-th fraction at the entrance to and exit from the channel, $n_* = \sum_i n_{i*}$ and $\bar{n} = \sum_i \bar{n}_i$ are corresponding total concentrations, and $p_{i*} = n_{i*}/n_*$ is the share of particles of each fraction. For the i-th fraction we have

$$\bar{n}_i = A n_{i*} \exp\left(-KD_i/\bar{U}\right) = A n_* p_{i*} \exp\left(-KD_i/\bar{U}\right). \tag{5.7}$$

The experimentally determined coefficient of diffusion D' satisfies equation

$$A n_* \exp\left(-KD'/\bar{U}\right) = \bar{n} = \sum_i \bar{n}_i = \sum_i A n_* p_{i*} \exp\left(-KD_i/\bar{U}\right). \tag{5.8}$$

Thus,

$$\exp\left(-KD'/\bar{U}\right) = \sum_i p_{i*} \exp\left(-KD_i/\bar{U}\right). \tag{5.9}$$

Further the authors differentiate this equation based on $\bar{U}$, considering D' a constant value, which is incorrect since D' is a function of $\bar{U}$. Therefore subsequently we will digress from the original conclusion.

Designating $\exp\left(-KD_i/\bar{U}\right) = z_i$ and, further, $z = 1 - x(0 < x < 1)$, we will obtain from (5.9)

$$D' = -\frac{U}{K}\ln\sum_i p_{i0}z_i; \quad \frac{dD'}{dU} = \frac{1}{U}\left(D' - \frac{\sum_i D_i p_{i0}z_i}{\sum_i p_{i0}z_i}\right) =$$

$$= \frac{1}{K}\left(-\ln\sum_i p_{i0}z_i + \frac{\sum_i p_{i0}z_i\ln z_i}{\sum_i p_{i0}z_i}\right) = \frac{1}{K}\left(\frac{\overline{z\ln z}}{\overline{z}} - \ln\overline{z}\right) =$$

$$= \frac{1}{K(1-\overline{z})}\left[\left(\frac{\overline{z^2}}{2} + \frac{\overline{z^3}}{6} + \cdots\right) - \left(\frac{\overline{z}^2}{2} + \frac{\overline{z}^3}{6} + \cdots\right)\right] > 0 \tag{5.10}$$

since $\overline{x^n} > \overline{x}^n$. Thus, the experimentally enumerable value D' increases with an increase in the speed of flow.

At $\overline{U} \to \beta$, by expanding the exponential functions in (5.9) we obtain

$$1 - \frac{KD'}{U} = \sum_i p_{i0}\left(1 - \frac{KD_i}{U}\right) \tag{5.11}$$

or

$$D' = \sum_i p_{i0}D_{i} \tag{5.12}$$

i.e., in this case we determine the average suspended value of D. It is easy to see that this conclusion can also be obtained from the complete formula (5.2)

At $\overline{U} \to 0$ it is possible, in any case, to be limited to one member of this formula, and in the sum $\sum_i p_{i0}\exp(-KD_i/\overline{U})$ to leave one member, corresponding to the fraction with the least D. Let us assume that this will be first fraction. In this case (5.9) takes the form

$$\exp(-KD'/\overline{U}) = p_{i0}\exp(-KD_1/\overline{U}). \tag{5.13}$$

At $\overline{U} \to 0$, obviously, $D' \to D_1$, i.e., we obtain from the experiment the least coefficient of diffusion in the mixture. The question of whether or not this conclusion holds good during continuous distribution of coefficients of diffusion requires special consideration, however in practice it is all the same very difficult to determine D both at very small and very high rates of flow. The

experimentally found values D always will lie somewhere between the minimum and average suspended value, and the closer to the later than the larger is $\bar{U}$.

In the light of these conclusions it is obvious that in his experiments Thomas artificially understated D in order to obtain better coincidence with true dimensions of particles. To explain the results of Thomas is quite difficult, since the larger particles which pass through channels easily scatter light more strongly and therefore the tyndallometric method should have given somewhat decreased values of D. Regarding the affirmation by Thomas that his aerosols were isodispersed, since they produced Tyndall spectra of higher orders, then here it is possible to refer to the work of Joyer and Pidgeon [196], who observed these spectra in a fog in which the radii of 80% of all the drops lay within the limits of 0.37-0.63 µm, and the remainder beyond these limits.

On the other hand it is possible that in time they will manage to use the dependence of measured values of D on the speed of flow in order to determine the distribution of particle dimensions in polydispersed aerosols. For aerosols consisting of several isodispersed fractions, a method for such a calculation is already given in the specified work of Pollak and Metnieks.

Chamberlain et al. [197] passed atmospheric aerosols, activated by thoron, through plane-parallel channels and determined the concentration at the exit from the channels 1) by counting the particles and 2) by filtration of the aerosol with subsequent determination of radioactivity of the filter. The first (more exact) method gave 2-3 times higher values for D than the second. This is not surprising since the radioactivity of activated particles increases with an increase of their dimensions.

A significant, but frequently disregarded factor during the diffusion method of investigating aerosols, are the charges of particles, causing an acceleration in the settling of particles on

the walls of channel at the expense of specular forces. Calculation of precipitation taking into account both diffusion and specular forces is very complex, but to estimate the influence of the latter is nevertheless possible. In a plane-parallel channel with conducting walls the following relationship exists between initial (at the entrance to the channel) distance of the particle from the nearest wall y and the abscissa of the point of its settling on the wall x.

$$\frac{Bq^2x}{6\bar{U}h^4} = \frac{1}{2}\left(\frac{y}{h}\right)^4 - \frac{1}{5}\left(\frac{y}{h}\right)^5.$$ (5.14)

where q — charge, and B — mobility of particles. For the ratio of number of particles, coming out of the channel and entering into it, we obtain, considering the parabolic profile of flow,

$$\frac{\dot{n}}{n_0} = 1 - \frac{3y_0^2}{2h^2}\left(1 - \frac{y_0}{3h}\right),$$ (5.15)

where y_0 — value of y at x, equal to length of channel.

Since $Bq^2x/6\bar{U}h^4 = Pq^2/6hkT$, then the ratio of rate of electrostatic and diffusion precipitation depends only on the width of the channel and charge of particles. For h = 0.5 μm and in the area of values ∟ = 0.05-0.8, in which measurements are usually conducted, this ratio equals ∿0.01 at 1, ∿0.1 at 10, and ∿1 at 100 elementary charges on the particles. At h = 0.125 mm the same values are attained for this ratio with half the charges. Thus it is possible to disregard the influence of electrical forces only with q on an order of one elementary charge. In this conclusion we did not consider the specular force from the other wall, but, as calculation shows, this force can be disregarded.

Using the method indicated on p. 46, Nolan and O'connor [124] determined the average charge and mobility in separate fractions of an aerosol, obtained by bubbling of air through a diluted solution of NaCl. Parallel in cylind⁻¹ ⁻ ρillaries coefficients of

87

diffusion were determined, and from them — mobility of the fractions. It turned out that the mobility determined by the second method was 7-11 times greater than the mobility determined by the first method. This ratio increased with an increase in the average charge of particles which changed from fraction to fraction from 9 to 106 elementary charges. The average radii of particles in fractions, determined by the diffusion method, decreased here from $2.7 \cdot 10^{-6}$ to $1.1 \cdot 10^{-6}$ cm, i.e., the charge decreased with an increase of r, which contradicts both theory and experiment. From the above-cited calculations it is obvious that the cause of these contradictions were specular forces unaccounted for by the authors.

The theory of diffusion to a sphere from a flux at small Re_f and large Pe (Peclet diffusion number) was developed by several authors, who obtained for the number of particles precipitated on a sphere in 1 s the expression brought out earlier by V. Levich [198],

$$\Phi = 7.9 \, n_* D^{*_*} U^{/_*} R^{*_*}$$ (5.16)

with several other values for the coefficient, namely 7.06 (Friedlander [199]) and 8.5 (G. Aksel'rud [200]). In dimensionless parameters for Sh (Sherwood numbers, i.e., Nusselt diffusions number) and Pé the formula (5.16) takes the simple form

$$Sh = \beta \, Pe^{*_*}$$ (5.17)

where β = 1.0 according to Levich, 0.89 according to Friedlander, and 1.07 according to Aksel'rud.

In connection with the great popularity among colloid chemists in using the Muller [201] theory of "orthokinetic" coagulation, i.e., the theory of diffusion to sphere from a flux, one should note that Muller originated from an incorrect boundary condition. He assumed that at the surface of a sphere the concentration gradient is directed everywhere normal to the surface, and disregarded tangential

transfer of particles in a flux. As a result Muller obtained an expression for normal gradient of concentration at the surface, from which it follows that the value of this gradient is a function of vectorial angle, which contradicts the initial assumption by the author.

There is no experimental data on diffusion precipitation of aerosols from a flux on spherical bodies, however, for checking formula (5.17) it is possible to use the data of G. Aksel'rud on the rate of dissolution of beads of benzoic acid in oil at $Re_f = 0.1$-2.5 and $Sc = \nu/D = 2.3 \cdot 10^6$, from which it follows that $Sh = 1.10\, Pe^{1/3}$ in excellent agreement with theory.

For large Re_f (600-2600) and the same values for Sc, G. Aksel'rud obtained theoretically and experimentally the dependence

$$Sh = 0.8\, Re_f^{1/2} Sc^{1/3} = 0.8\, Pe^{1/3} Re_f^{1/6}. \qquad (5.18)$$

In analogous experiments, but with water as solvent at $Re_f = 100$-700, $Sc \approx 10^3$, Garner et al. [202, 203] obtained the same dependence, but with a coefficient of 0.95.

An analogous problem for diffusion precipitation of aerosols on a cylinder at small Re_f and large Pe was solved by G. Natanson [204] on the basis of Lamb equations for flowing around a cylinder by a viscous flux. For the number of particles, precipitated in 1 s per unit of length of cylinder, the following expression is obtained

$$\Phi = \frac{4.64\, n_0 D^{2/3} U^{1/3} R^{2/3}}{[R(2.002 - \ln Re_p)]^{1/3}}. \qquad (5.19)$$

Friedlander [199], using a somewhat less accurate method, obtained the same expression with a coefficient of 3.52. In dimensionless parameters formula (5.19) takes the form

$$Sh = \frac{9\, Pe^{1/3}}{[2(2.002 - \ln Re_p)]^{1/3}}. \qquad (5.20)$$

where β = 1.17 according to Natanson and 1.035 according to Friedlander.

Friedlander considered that his formula is applicable only at Re_f < 0.001; for Re_f = 0.1 he obtained by numerical integration the formula $Sh = 0.557 Pe^{'}$, which agrees well with results of measurements of diffusion current from a cylindrical electrode at Re_f = 0.1 and Pe = 1000 [205].

Calculation of diffusion precipitation of particles taking into account the coupling effect is apparently impossible by analytic method. Friedlander proposed for this the following method of approximation. Proceeding from the expression for coefficient of precipitation on a cylinder due to coupling [206], he adds to the radius of a given particle its "diffusion radius," i.e., the radius of hypothetical particle, for which the coefficient of precipitation due to coupling is equal to the coefficient of precipitation of the given particle due to diffusion, calculated by the formula (5.19). It is doubtful that this method of calculation could give even approximately true results.

Prior to the appearance of the above-mentioned works they usually used the simplified method proposed by Langmuir [207] for the calculation of diffusion precipitation in a flux: it was assumed that on a collector particles will be precipitated which are moving along current lines, on the average distant from the surface of collector by distance x, equal to average Brownian displacement $(Dt/a)^{1/2}$, where t - time for flowing around the collector. For the Langmuir cylinder they took for x the mean quadratic distance of current lines from the surface in an interval of values for the vectorial angle θ from 30 to 150°, and for t — time for passage of this interval by particles of the medium. Thus was obtained formula (5.19) with coefficient 2.72.

L. Radushkevich [208] in his conclusion (taking into account the coupling effect) committed the same error as Muller (see p. 89).

He assumed that the tangential component of gradient of particle density at the surface of a cylinder is equal to zero, and obtained for the rate of diffusion to a cylinder at small Re_f the formula, which in the absence of a coupling effect takes the form $\phi' = kn_0 D$ (k — constant), i.e., velocity of precipitation does not depend either on the diameter of the cylinder or on the speed of flow, which is physically improbable.

In the case of potential flow past a cylinder at large Pe numbers

$$\phi' = \frac{8}{\sqrt{\pi}} n_0 D^{'\cdot 1} U^{'h} R^{'h} \tag{5.21}$$

(formula of Bussinek).

Fibrous and Tissue Filters

The theory of fibrous filters is being developed very slowly. One of the main reasons for its lag is the circumstance that the majority of authors in their calculations originate from precipitation of aerosols on isolated fibers, i.e., on the basis of Lamb field of flowing around a cylinder. Therefore the Re_f number enters into the result of calculations. Meanwhile, as already noted repeatedly, at small values of Re_f the flow in filters is self-simulating. As Tamada and Fujikawa [209] showed, the same holds true during flow in one series of parallel cylinders. In this case the force F', acting on 1 cm of cylinder length, at small Re_f is proportional to the speed of flow, i.e., the latter is self-simulating. This proportionality is observed to all the higher values of Re_f, the lesser the ratio of the distance between axes of cylinders h to their diameter (Fig. 35). Obviously, for the creation of a theory of filtration one should take as a basis the viscous flow in a system of cylinders at small Re_f, having determined it in model experiments or calculated it theoretically. Based on an alternate path the first steps have already been made by Japanese hydrodynamics [210].

The difficulty in calculating the effectiveness of filters is

Fig. 35. Hydrodynamic forces in a
system of parallel cylinders.
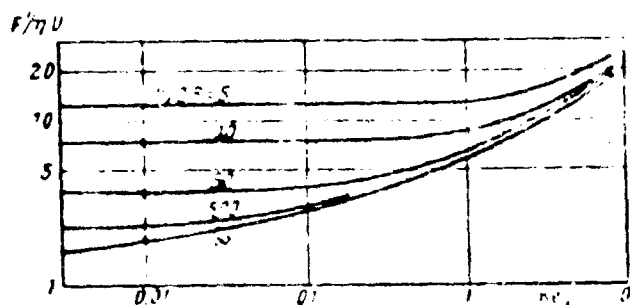
conditioned further by the simultaneous action of several mechanisms
of precipitation. The simple summation of separate effects,
practiced by certain authors [211, 212], cannot lead even to
approximately correct results. This problem is insolvable by
analytic methods. The application of numerical methods will
naturally require a huge amount of labor, but this is the only path
to the solution of the given problem.

Out of the very small number of works on the theory of filtration
which have appeared recently, we will dwell only on the work of
Friedlander [213]. From formula (5.20) it follows that the
coefficient of diffusion precipitation η_D on an individual
cylindrical fiber is proportional to $Pe^{-\prime}(2.002 - \ln Re_f)^{-\prime}$. In the
equation of flow Friedlander takes (without sufficient bases)
instead of $(2.002 - \ln Re_f)^{-1}$ (k - constant), from which it follows
that a_D is proportional to $Re_f^{\prime} Pe^{-\prime}$ and

$$a_D \, Pe \, r/R = k' \, Pe^{\prime\prime} \, Re_f^{\prime\prime} r/R. \tag{5.22}$$

Coefficient of precipitation due to coupling equals [214]

$$a_h = [(1 + r/R) \ln (1 + r/R) -$$
$$- \frac{(r/R)(2 + r/R)}{2(1 + r/R)}] \Big/ (2.002 - \ln Re_f) \approx \frac{(r/R)^2}{2.002 - \ln Re_f},$$

from which

$$a_h \, Pe \, r/R = k' \, Re \, (r/R)^3 \, Re_f^{\prime\prime} = k^{\bullet} [Pe^{\prime\prime} \, Re_f^{\prime} \, R]^2. \tag{5.23}$$

At small Pe and r/R, when the effect of diffusion predominates, one should use formula (5.22), at large values — formula (5.23).

By plotting in coordinates $\lg(\text{or Pe } R)$, $\lg(\text{Pe}^{\cdot}\text{Re}_f^{\cdot} r R)$ the experimental data of a number of authors on filtration of aerosols through fibrous filters, pertaining to values Stk < 1, Friedlander obtained a curve, the tangent of slope of which at small values of $\text{Pe}^{\cdot} \text{Re}_f^{\cdot} r R$ has the value ~ 1.2, at large values — the value ~ 3, and arrived at the conclusion that the inertial effect in fibrous filters at Stk < 1 and Re_f < 1 can be disregarded. In these calculations the following errors are committed. 1) As already pointed out, flow in filters does not depend on Re_f number. 2) In the wide interval of values for Re_f (0.01-2), to which the experimental data used by Friedlander pertain, it is impossible to substitute $(2.002 - \ln \text{Re}_f)^{-1}$ for $k \text{Re}_f^{\frac{1}{2}}$. 3) The upper part of the Friedlander curve is plotted according to Wong et al. (Fig. 38, p. 97), from which it is clear that, starting already with Stk $\gtrsim$ 0.7, ϑ increases sharply with an increase in the Stk number. Therefore the conclusions of this work are unconvincing.

For characteristics of filter quality during specific standard conditions of filtration, i.e., at given values r and U, it is expedient to use the ratio of the logarithm of breakthrough to the resistance of the filter

$$ \mathfrak{z} = \frac{\lg(1 - \vartheta)}{\Delta p}, \tag{5.24} $$

since this value does not change during the joining of several filters into one multilayer filter [215]. For the characteristics of quality of the filter material it is possible to use the same formula, inasmuch as the thickness of the filter does not enter into it.

Of the experimental works we will dwell first on experiments of Gallili [216] with a "model" filter. Fairly isodispersed fogs of

dioctyl phthalate with $\bar{r}$ = 0.55-0.70 µm, and which did not contain charged particles, were passed with a speed of 12-18 cm/s through a tube with a diameter of 5 cm. In it was mounted a large number of lattices made from wires with a radius R = 0.025 mm stretched out in parallel. Distance between wires h varied from 0.13 to 0.27 mm; the distance between lattices equaled 5.5 mm. The Re_f number changed within limits of 0.36-0.54, Stk — within limits of 0.018-0.043, r/R — within limits of 0.022-0.028. Based on the breakthrough of the aerosol the coefficient of precipitation was calculated for individual wires ә. It increased with an increase of U and r. A change in U affected value ә more strongly than a change in r^2; furthermore, the stated Stk values were considerably lower than critical during viscous flow plast isolated cylinders. It follows from this that either the coupling effect (despite the opinion of Gallili) played a significant role in these experiments, or the presence of neighboring cylinders at the above-indicated distances so strongly changes field of flow that the calculations made for isolated cylinders do not give even a correct order of magnitude of ә in a system of cylinders. Values of ә obtained in these experiments are shown in Fig. 36. From the formula of Davies [217] for these values of Stk and r/R it follows that ә = $4.5-5.1 \cdot 10^{-3}$, i.e., a value of the same order. With decrease of distance h between wires ә at first started it increase strongly as one should have been led to expect, since with this the current lines approached the wires. It is surprising that with a further decrease of h ә ceased to change or only decreased slightly. Gallili explains this by the rebounding of drops from the surface of wires, however, with the comparatively small U in these experiments such an explanation does not seem convincing. In general, experiments with model filters are of great interest for the theory of filtration of aerosols through fibrous filters.

In the experiments of Thomas and Yoder [218] a fairly iosdispersed fog of dioctyl phthalate was passed through filter with a thickness of 1.2 cm made from resin covered glass fibers with R = 0.75 µm. The results of these experiments (Fig. 37) clearly show the existence
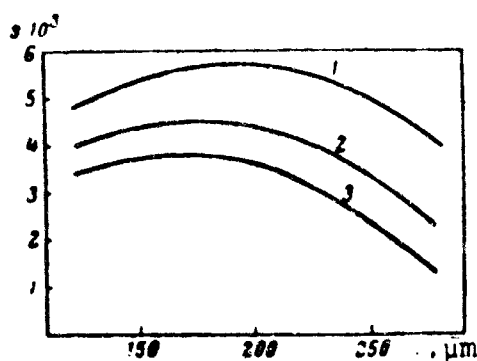
Fig. 36. Coefficient of precipitation on wires depending on the distance between them: 1 — 18.7 cm/s; 2 — 15.0 cm/s; 3 — 12.5 cm/s, r = = 0.60 µm.
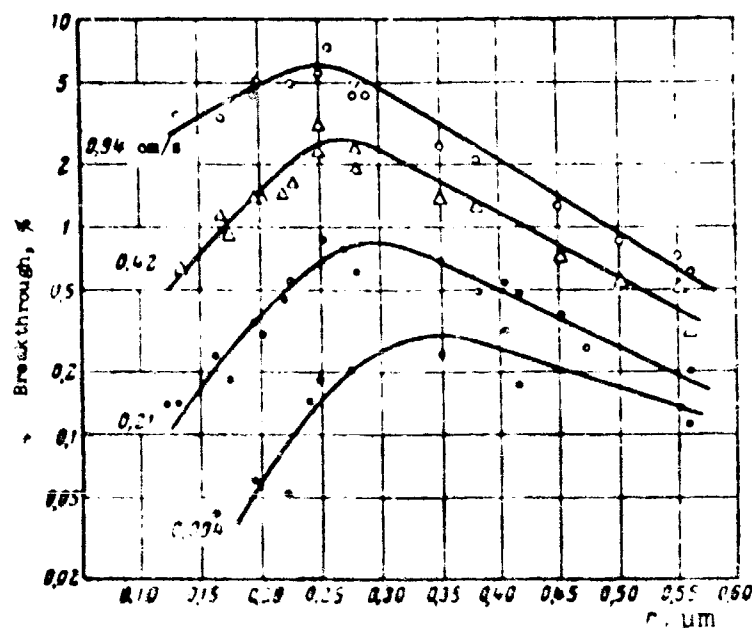
Fig. 37. Dependence of effectiveness of filters made of glass fibers on the dimension of particles and speed of flow.

of a particle radius r_{min}, at which the effectiveness of the filter is minimum. Here, in agreement with theory, r_{min} decreases with an increase in the rate of flow. Therefore certain authors, working at high rates of flow, also did not detect the existence of r_{min}. In a comparison of the results of Thomas and Yoder with data of other authors (see, for example, Fig. 38), it is necessary to consider that the first were obtained at considerably lesser speeds of flow and on very thin fibers, and the basic role here was played by the effects of diffusion (this is indicated by the decrease of ℮ with an increase in the speed of flow) and coupling. In the left part of the
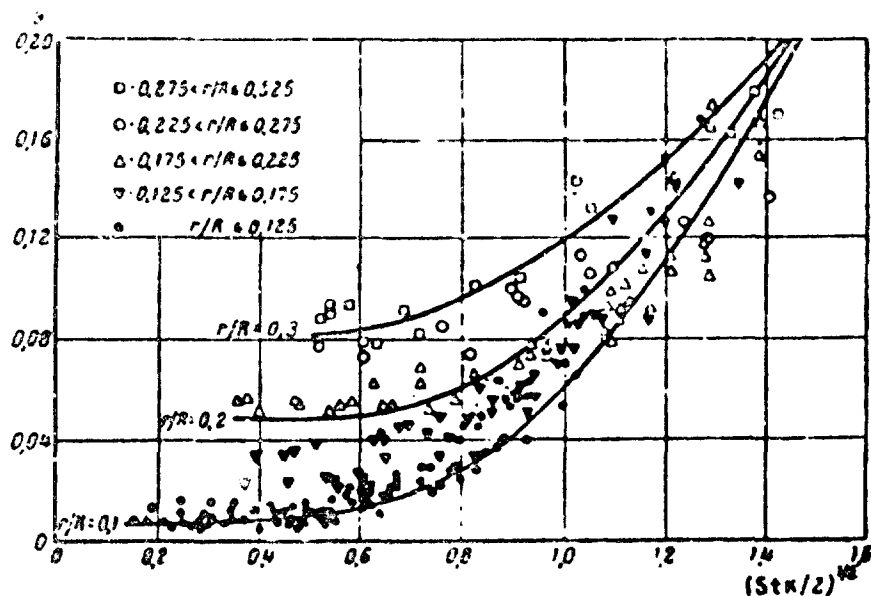
Fig. 38. Dependence of effectiveness of filters
made of glass fibers on Stk and r/R.

curves in Fig. 37 diffusion dominates over all remaining mechanisms
and Ɵ decreases with the increase of r. The right side of the curves
corresponds to the left part of the curves of Ramskill and
Anderson [219]: here Ɵ increases with an increase of r and decreases
with an increase of U. Examination of these curves shows that this
area is clearly expressed only in filters with very thin fibers.
Therefore, although the diffusion effect in this area still prevails
over inertial, the total effect of inertia and coupling is already
greater than the diffusion effect.

In the experiments by Wong et al. [220] fairly monodispersed
fogs of H_2SO_4 with $\bar{r}$ = 0.2-0.65 μm were passed through filters made
of glass fibers with R = 3.5-9.6 μm and a space factor ϕ =
= 0.045-0.10 at U = 17-260 cm/s, i.e., at Re_f = 0.04-1.4. From the
experiments coefficients of precipitation were calculated for
separate fibers Ɵ in the Stk function at various values of r/R,
shown in Fig. 38. From this it is clear that at Stk < 0.5 inertial
effects hardly play any role.

Humphrey and Gaden [221] passed spores of Bac. subtilis with
r ≈ 0.575 μm through a filter made of glass fibers glued with

resin and detected a very sloping maximum of effectiveness at
$U = 30$ cm/s. In experiments with multilayer filters there was
strict observance of the proportionality of the logarithm of
breakthrough and the number of layers. This indicates the high
degree of isodispersion of these spores.

A great influence is apparently exerted on the effectiveness of
filters by the uniformity of their structure. Loose places in the
filters possess simultaneously lesser filterable effectiveness and
lessen resistance to flow, and in the case of highly-dispersed
aerosols these two effects accumulate. Unfortunately, experimental
data concerning this problem are lacking in the literature.

A reverse action produces partial stopping up of filters. Here
there is great importance in the structure of the deposit. Coal
dust, which on filter fibers forms aggregates in the form of
upright branching chains, very considerably increases ∂, while
spherical particles of methylene blue (obtained by atomization of
solution of dye and drying of drops) lie on the very surface of
the fibers, do not produce aggregates, and exert a quite weak
influence on ∂ [222].

Leers [223] passed aerosols of NaCl ($\bar{r} = 0.2$ μm) through very
thin (0.1 μm) filters, on which it was convenient to examine the
structure of the deposit. Particles were precipitated chiefly on
earlier precipitated particles. Branching chains gradually appeared
and inside the filter they formed a secondary filter made of very
thin dust fibers. Here the effectiveness of the filter increased
considerably faster than its resistance. The author explained the
increase of aggregates by mechanical capture, but apparently the
main role here is played by electrical forces [224]. Drops of fogs
produce an opposite effect — they spread over the surface of fibers,
increase their diameter, and thereby lower the ∂ of the filter.

An analogous phenomenon was observed during passage of a fog
made up of an aqueous solution of H_2SO_4 through filters made of glass
fiber in the experiments by Fairs [225]. Fairs worked with molded

filters (preformed filter-mats), obtained by annealing of pressed glass wool with R = 2.5-7.5 μm. During prolonged testing of such filters they gave θ = 0.95-0.97. After treatment of fibers with silicone θ was increased up to 0.996-0.998. Here the drops of fog, merging on water-repellant fibers, formed large spherical drops which easily dripped off the fibers.

La Mer and Drozin [226] during filtration of mondispersed aerosols with $\bar{r}$ = 0.1-0.6 μm through different fibrous filters found that θ decreases linearly with an increase of r (in these experiments θ varied from 0.70 to 0.93). It is obvious that the complex real relationship between θ and r here was accidentally approximated by such a simple dependence. During filtration of aerosols with solid particles (synthetic wax) the lg $(1 - \theta)$ decreased linearly with an increase in the quantity of deposit on the filter. It is also very difficult to give a theoretical explanation to such dependence.

Precipitation of solid particles does not always increase θ. According to the observations by Hasenclever [227] during transmission of quartz polydispersed dust with $\bar{r}$ < 2.5 μm through a paper filter at a speed of 6 m/s, θ initially increases somewhat (from 0.85 to 0.95), then gradually drops (at θ = 0.3 the experiment was discontinued). Apparently under these conditions such a great pressure drop is created that the particles are pressed through the filter.

In a number of works the influence of charges of particles and fibers on effectiveness of filters has been investigated. According to the experiments of Rossano and Silverman [220] during transmission on an aerosol of methylene blue with $\bar{r}$ = 1 μm through a filter made of glass fibers with R = 25 μm at a speed of 16 cm/s, for uncharged aerosols θ = 0.65, for unipolar charged aerosols with an average charge of 1000 elementary charges per particles θ = 0.72. The authors explain this effect by the fact that precipitated particles repulse particles which are just entering the filter and delay

their motion in frontal layer of the filter. Of course, in reality
reality the effect is caused by specular forces.

A noticeable increase in the effectiveness of filters made from
glass fibers when they are covered by a layer of substance with a
high insulating capacity — polyethylene or polystyrene — was
observed by Winkel [229]. The finest layer of glycerine, applied
to fibers treated thusly, rendered a reverse action.

So that wool-resinous electrostatic filters preserve their
effectiveness for a sufficiently long time, it is necessary to
apply resins with a resistivity on an order of 10^{21} $\Omega \cdot$cm [230].
Such filters can be kept more than 10 years, however they lose
effectiveness rapidly following passage through them of certain
fogs (for example, tricresyl phosphate) and radioactive aerosols,
during irradiation by X-rays, etc.

In a comparison of electrostatic filters with asbestus-cellulose
(aerosol of methylene blue) it turned out that at small speed of
flow (up to 30 cm/s) greater effectiveness is possessed by the
first, at high speed — by the second [228]. This is not surprising,
since the influence of electrical forces drops with an increase in
the speed of flow.

Gillespie [231] passed through wool-resinous filters neutral
aerosols of stearic acid and charged aerosols, obtained by
atomization of solutions of polystyrene. As it should have been
expected, in this case the effect of charging particles was expressed
very strongly. It increased with a decrease in the dimension of
particles.

Billings et al. [232] describe electrostatic filter with an
external field; a filter with a thickness of 12 mm made of glass
fibers, with R = 0.5-1.5 µm, covered by phenol resin was placed
between metallic grids. During passage of an aerosols of $CuSO_4$ with
$\bar{r}$ = 0.9 µm the effectiveness of the filter equaled 0.92. When

99

potential differences of 10-15 kV were superimposed on the grids θ was increased to 0.98. Since charge of particles was not measured, then it is difficult to say what is the mechanism of this phenomenon — is this the direct action of the field on charged particles or the influence of induction forces, caused by heterogeneity of the field between fibers.

Recently for the investigation of aerosols wide use has been made of membrane filters with very narrow capillary channels with a width on an order of 0.1-1 μm. During filtration through these filters, in addition to the earlier examined mechanisms of precipitation, a well-known role is played by the mechanical confinement of particles, the size of which are larger than the width of the channels.

Fitzgerald and Detweiler [233] revealed, during passage of an aerosol of $KMnO_4$ through AA and HA Millipor filters of this type, that at r > 0.05 um the aerosol is held back completely, at r = 0.01-0.013 μm θ attains minimum value — 0.78 at H = 10 cm/s, 0.62 at 20 cm/s, and 0.20 at 40 cm/s. With a further decrease of r θ again increases. However, Walkenhorst [234], working at U = = 32 cm/s with an aerosol of WO_3, found that the θ of thin German membrane filters continuously decreases with a decrease of r from 0.994 at r = 0.05 μm to 0.972 at r = 0.005-0.01 μm. It is difficult to say what the cause of this difference is. Apparently it is the different width of channels in the tested filters.

Membrane filters are used both during the determination of concentration by weight, and also during investigation of aerosols under a microscope and during determination of countable concentration. The particles are practically completely precipitated on the frontal surface of the filter and turn out to be in one optical plane, which is understandably very important during microscopy. Methods have also been found for electron microscopy of particles precipitated on these filters.

Snyder and Pring [235] investigated the problem of clogging of tissue (bag) filters by solid particles. Increase in the resistance of filters when they are clogged up by course aerosols can be expressed by the formula $\Delta p = kG$, where G — mass of deposit on 1 cm^2 of filter. In the case of finely-dispersed aerosols the coefficient k is increased somewhat with an increase of G, obviously due to the thickening of the deposit along with the growth of G. The larger the specific surface of fibers in the tissue, the less k. Therefore in tissues with nap k is less than in smooth tissues. Thus, for one and the same aerosol in glass tissue k is 10 times, and in orlon tissue with weak nap 4 times, greater than in the same tissue with a strong nap, and in general in different tissues and for various aerosols k can vary by more than a 1000 times.
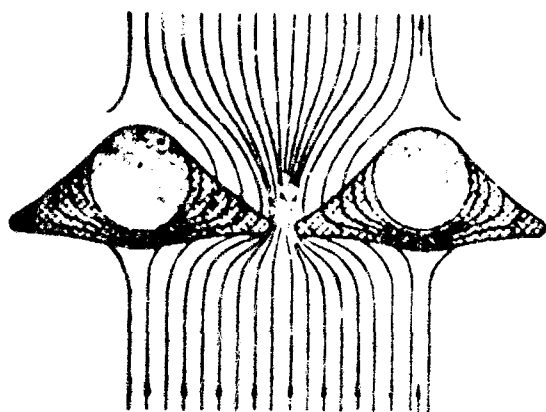
Fig. 39. Formation of dust deposit on a metallic grid.

N. Yeliseyev [236] studied the mechanism of formation of aerosol deposits on tissues in model experiments on filtration PbO and ZnO smokes through metallic grids with a radius of wires of 25 µm and an opening of 80 µm (Fig. 39). As can be seen from figure, the deposits forming on the frontal side of the filaments grow in width more than in thickness, and finally cover the intervals between filaments, forming a solid filterable layer, impenetrable for particles out of which it was formed. The degree of filling up space in such a layer is $\phi = 0.06$, i.e., it is very porous; this explains its comparatively small resistance to the flow of gas.

During the first dusting of a clean tissue for the formation of

a filterable layer very little deposit is required — on an order of 10 g/m^2. As it is known, filter tissues (bags) are periodically blown through with air in the opposite direction and shaken for the removal of deposit. Here less deposit is removed than was held back, and during prolonged work the density of the deposit reaches 1000 g/m^2. Apparently, along with the "active" deposit which forms the filterable layer, a large quantity of passive deposit accumulates on the tissue. After every blowing out channels will be formed in the filterable layer. The aerosol skips through these, however, they are very rapidly clogged up; this requires only 0.2-0.3 g/m^2 of deposit. It is interesting that resistance of an intact filterable layer is the same in both directions, in a destroyed layer resistance during reverse blowthrough is 2-3 times less than during direct — the aggregates sitting in the upper part of the channels act as ball valves. Further N. Eliseyev showed that reverse blowing without deformation of the tissue is not very effective. It lowers resistance by only 6-15%, whereas deformation of tissue so strongly destroys the deposit that resistance is reduced by 70-94%. In practice reverse blowing is always accompanied by strong deformation of bag filters.

Thomas and Yoder [237] investigated filtration of highly dispersed aerosols through columns with a granular filling. Figure 40 shows the filtration curves of aerosols of dibutyl phthalate through a column with shot; all the data is in the caption to the figure. Under these conditions (small speeds of flow, very large R) effects of coupling and inertia should be insignificant and overall effectiveness is very small. The main roles are played by diffusion (predominant in the ascending side of curves) and sedimentation (predominant in the descending branch) mechanisms. Therefore ϶ decreases very strongly with an increase in speed of flow. The great role of sedimentation is clearly expressed in the dependence of ϶ on the direction of flow. A probable mechanisms of this phenomenon is shown in Fig. 41, in which is depicted the total speed of a sedimenting particle in ascending and descending flow. The authors obtained analogous curves with columns made of sand [218], where ϶
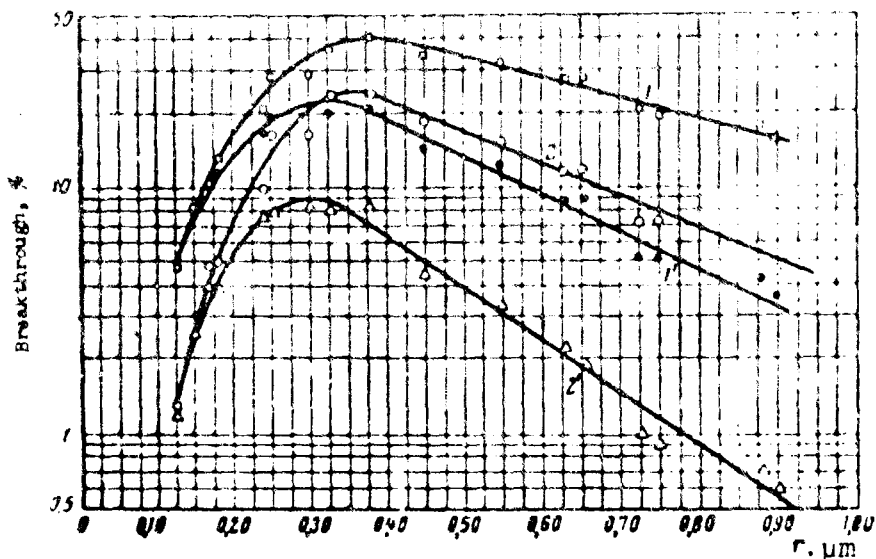
Fig. 40. Filtration of aerosols through a column with shot. 1 — ascending flow; 1' — descending flow, U = 1.49 cm/s; 2 — ascending flow; 2' — descending flow, U = 0.745 cm/s. Radius of shots R = 0.75 mm, height of column 80 cm, area of section 11.2 cm^2.

Fig. 41. Precipitation of particles on a granular filling in ascending and descending flows.

noticeably decreases with an increase of both speed of flow and size of grains. Here grain with an irregular shape gives a better effect than round ones.

Experiments with filtration of a polystyrene aerosol with large charges on particles through a column with shot are interesting. During treatment of column with a radioactive preparation discharging the aerosol, breakthrough is increased by 7-15 times. Such a high effect of induction forces in a column is explained by the low

103

effectiveness of other mechanisms c. precipitation under the given
conditions.

Settling of Aerosols in the Respiratory System
and During Bubbling

We will switch to the settling of aerosols in the respiratory
system.[*] Experiments by Morrow et al. [238] were conducted with
aerosols of NaCl from $r = 0.02-0.35$ µm. Here, depending upon
respiratory rate, the effectiveness of settling ϑ in the entire
respiratory system fluctuated from 50 to 80 . It is necessary to
consider that the particles should be noticeably enlarged in the
respiratory system, which is saturated with water vapor.

In experiments by Altshuler et al. [239] breathing was carried
out through the mouth; fairly monodispersed fogs of triphenyl
phosphate ($\gamma = 1.3$) were used and total deposition in the entire
respiratory system was determined. Results of the experiments are
shown in Fig. 42; respiratory rate is given in the figure caption.
Minimum ϑ was observed at $r = 0.2$ µm. Attention is drawn to the
large difference in the value of ϑ for different individuals (A, B,
and C in the figure).

In the experiments by Dautrebande et al. [240], which were
conducted with polydispersed dusts of carbon and Fe_2O_3 and also with
particles obtained by atomization of India ink, the value ϑ for
particles of different dimension was determined by means of
comparison of distribution curves of dimensions of particles in
inhaled and exhaled air, i.e., not a very reliable method. A
minimum of deposition was found in the entire respiratory system
at $r \approx 0.3$ µm, but in a later work by the authors a weakly expressed
minimum at $r \approx 0.12-0.15$ um. Figure 43 shows the results obtained at
a respiratory rate of 10 inhalations in 1 minute. Curve B pertains
to air, exhaled at the end of normal expiration, i.e., to deposition
in the lungs, which is thus considerably greater than the average
deposition in the entire respiratory system (curve A). A still
higher deposition takes place in the alveoli. For its determination
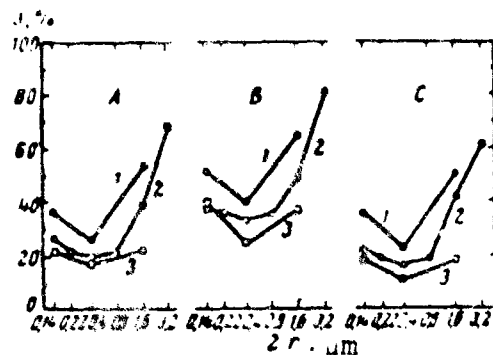
Fig. 42. Settling of aerosols in the respiratory system of three individuals: 1 — 9 inspirations a minute; 2 — 15 inspirations a minute; 3 — 21 inspirations a minute.
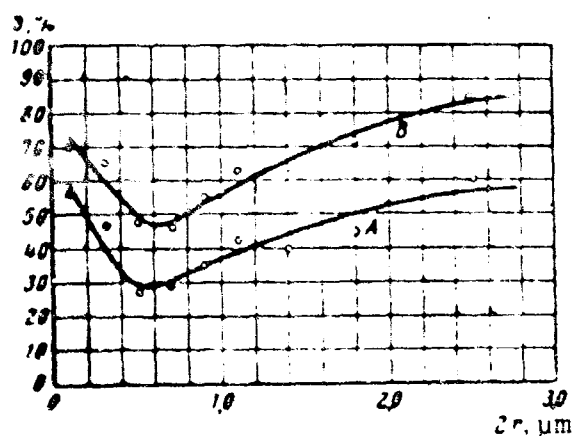
Fig. 43. Settling of aerosols in different parts of the respiratory system.

a measurement was made of particle density in the air which remained in the lungs after normal expiration. It turned out that regardless of the respiratory rate in the alveoli the following percentages of particles which penetrated there settled: ~90% of those with r = 0.1 μm; 95% with r = 0.2 μm, and 100% with r > 0.5 μm.

The data presented in the literature on the absorption of aerosols by foam [241] do not pertain to "foam apparatuses" introduced in the practice of gas purification by M. Pozin [242]. In these gases are passed at a high speed (1-3 m/s with a calculation for the entire cross section of the apparatus) through a lattice with wide openings into water without the addition of frothing agents. In this case a thin layer of foam will be formed which is very coarse and is rapidly destroyed and then formed again. Here the basic mechanism of precipitation of aerosols is undoubtedly turbulent-inertial. Therefore these apparatuses are very effective with respect to coarse aerosols, but are weakly effective during transmission through them, for example, of a fog of sulfuric acid with r = 0.1-1 μm.

Decrease in the effectiveness of absorption of aerosols during bubbling along with an increase of water temperature [243] is caused mainly by Stefan flow (p. 20).

The explanation given earlier by the author of the survey [244] favorable to the action of wetting agents during bubbling of aerosols is insufficient. It is obvious that the addition of wetting agents facilitates penetration of particles of dust into the water. We will return to this question later (pp. 155-6).

Deformation of Drops in an Electrical Field

In conclusion of this chapter we will give more exact data on the deformation of drops in an electrical field according to the calculations of O'Konski and Thatcher [245] for drops of water and dioctyl phthalate at 25°. e signifies the eccentricity of a deformed drop having the form of an elongated ellipsoid, c/a – ratio of axes, h is expressed in esu.[5]

Table 5. Deformation of drops in an electrical field.

e		c/a	rE^2 (water)	rE^2 (dioctyl phthalate)
0			0	0
0.01			--	0.043
0.02		--	0.16	0.174
0.05		1.011	1.00	1.068
0.10		1.005	4.00	4.36
0.20		1.02	15.9	17.45
0.30		1.038	35.2	39.4
0.40		1.07	61.1	70.4
0.5		1.15	93.3	110.9
0.7		1.4	139	221.6

As calculations show, at e = 0.45-0.70 for water drops (for which it is possible to take $\epsilon_K = \infty$) it is possible to approximate complex expressions for e in function rE^2, according to which Table 5 is compiled with the simple formula e = 0.003 rE^2 + 0.223. Results of the experiments by O'Konski and Gunther [246] with drops of water, suspended on thin glass filaments in a field with E = 38 esu, where e changed within limits of 0.49-0.63, agreed with this formula

with an accuracy of 1-2%, but already at e = 0.46 coincidence was noticeably worse.

Footnotes

[1] At very large τ in the above-mentioned example particles in a stream tube will move rectilinearly and evenly and their concentration will not change.

[2] The graphs obtained by Langmuir and Blodzhett are given in the article by Tribus et al. [146].

[3] Calculations for precipitation on the wings of aircraft were also carried out by L. Levin [150].

[4] In § 41 of "Mechanics of Aerosols" it is necessary to insert the following corrections· "respiratory tracts" should be "respiratory system," "lower respiratory tracts" — "lungs," "upper respiratory tracts" — "upper part of the respiratory system." Figure 62 does not give radii, but the diameters of particles.

[5] In "Mechanics of Aerosols," p. 219, it is erroneously shown that E is expressed in V/cm.

C H A P T E R   6

TURBULENT DIFFUSION OF AEROSOLS

Diffusion of Aerosols in a Turbulent Flow

Recently aerosols have been used with success for the investigation of turbulent diffusion, especially in the atmosphere. Besides it usually is assumed that movement of particles and the contents of the medium adjacent to them are identical, which is true only at sufficiently small particle dimensions. In this case the basic positions of the theory of turbulent diffusion in an uniform medium are also applicable to diffusion of aerosols and all the values examined below can pertain both to elements of the medium and to particles.

For simplicity we will limit ourselves to a case of stationary homogeneous turbulent flow in which neither the mean speed of flow nor the intensity of turbulence depend on time and spatial coordinates, and we take a system of coordinates moving with an average flow rate. Let us designate by U' the instantaneous velocity of a particle, by X the displacement of a particle (or an element of the medium) along one of the axes; in this system of coordinates obviously $\overline{U}' = 0$ and $\overline{X} = 0$. In the theory of turbulent diffusion the basic role is played by the Lograngian (temporary) coefficient of correlation

$$R(s) = \frac{\overline{U'(t)U'(t+s)}}{\overline{U'^2(t)}},$$ (6.1)

characterizing relationship between pulsational speed of the same particle in moments t and t + a, and the Lagrangian scale of turbulence

$$L = \int_0^\infty R(a)\,da.$$ (6.2)

characterizing the interval of time, upon the expiration of which pulsational movement of a particle becomes independent from initial movement.

As certain theoretical considerations and experimental data show, it is possible with a great fraction of authenticity to assume that the probability of transition of particle $w(x_0, x, t)$ [247], expressed in case of Brownian diffusion by the Gauss function, is close to this function also during turbulent diffusion. Considering, in view of the homogeneity of flow, $x_0 = 0$, we can write

$$w(x, t) = \frac{1}{(2\pi\bar{X}^2)^{1/2}}\exp\left(-\frac{x^2}{2\bar{X}^2}\right).$$ (6.3)

from which it follows that the coefficient of turbulent diffusion is expressed by the formula

$$D_t = \frac{\overline{X^2}}{2t}.$$ (6.4)

Differentiating $\overline{X^2}$ by t, we obtain

$$\frac{1}{2}\frac{d\overline{X^2}}{dt} = \overline{X(t)\,U'(t)} = \int_0^t \overline{U'(t)\,U'(t')}\,dt' = \overline{U'^2}\int_0^t R(a)\,da,$$ (6.5)

from which follows the basic formula for the theory of turbulent diffusion

$$\overline{X^2} = 2\overline{U'^2}\int_0^t (t-a)\,R(a)\,da.$$ (6.6)

With $t \gg L$, $R(a) \approx 1$

$$\overline{X^2} \approx \overline{U'^2}t^2.$$ (6.7)

With $t \gg L$

$$\overline{X^2} = 2\overline{U'^2}tL - 2t^{1/2}\int_0^\infty aR(a)\,da \approx 2\overline{U'^2}tL. \tag{6.8}$$

since the second member has a value on an order of $\overline{U'^2}L^2$, and it can be disregarded in comparison with the first member. Thus we have here a complete analogy with Brownian diffusion [248].

The idea of coefficient of turbulent diffusion acquires a definite physical meaning only at $t \gg L$, and value L in turbulent diffusion plays a role analogous to the role of value τ in Brownian diffusion. For D_t it is possible to obtain, besides (6.4), the following expression

$$D_t = \overline{U'^2}L = \frac{1}{2}\frac{d\overline{X^2}}{dt} = \overline{X'(t)\,U'(t)} \qquad (t \gg L). \tag{6.9}$$

The role of apparent average length of path [249] in this case is played by the value $(\overline{U'^2})^{1/2}\,L$.

The theory of relative diffusion of a system of particles[1] has been developed considerably worse. According to Batchelor [250], with the distance ρ between two particles exceeding the internal scale of turbulence λ_0, but small in comparison with the external (main) scale and with Re_f high numbers

$$\frac{d\overline{\rho^2}}{dt} \approx (\varepsilon\rho_0)^{1/3}t; \quad \overline{\rho^2} - \rho_0^2 \approx \varepsilon^{1/3}\lambda_0^{1/3}t^2 \tag{6.10}$$

(ε – speed of scattering of turbulent energy in 1 g of substance of the medium)[2] in the case when t is so small that relative movement of particles depends on initial distance ρ_0 between them, and

$$\frac{d\overline{\rho^2}}{dt} \approx \varepsilon t^2 \approx \varepsilon^{1/3}\overline{(\rho^2)}^{2/3} \tag{6.11}$$

at sufficiently large t. Equation (6.11) corresponds to the Richardson formula [251] for relative diffusion $D_t \approx 0.2x^{4/3}$, since $\frac{1}{2}\,\overline{d\rho^2}/dt$ can be viewed as the coefficient of relative diffusion of particles.

From equation (6.11) it is clear that speed of relative diffusion
increases with increase of distance between particles ρ, however,
with ρ exceeding the basic scale of turbulence the movements of
particles become independent and coefficient of relative diffusion
no longer depends on ρ.

A very important question concerning turbulent diffusion of
particles so large that their motion no longer could be considered
identical with movements of the medium is solved in the monograph
by Chen [85]. Proceeding from the basic differential equation of
movement (3.1) of Stokes particles, Chen proved by means of quite
complex computations that coefficients of turbulent diffusion of
particles and media are equal.[3]

Physical meaning of the Chen theorem is clear. Particles possess
smaller pulsational speed than the medium, but then their pulsational
motions are more persistent. Their temporary scale of turbulence L,
and consequently diffusion "steps" also, are greater than for
elements of the medium. Soo [252] and Liu [253] then came to an
analogous conclusion, but in a less general form.

Experimental confirmation of the Chen theorem was obtained
recently in the experiments of Soo et al. [254]. Glass beads with
$r = 57$ and 115 μm were introduced into a wind tunnel and were
photographed after specific intervals of time. Based on the
photographs calculations were made of the position of the beads in
a system of coordinates moving with an average speed of flow and
from here were calculated the values $\overline{V'^2}$, L, and D_t for particles in
longitudinal and transverse directions. Unfortunately the
corresponding values for the medium were not determined here, however,
in agreement with theory, the values D_t for beads with these two
dimensions turned out to be very close. At $\overline{U} = 25$ m/s for $r = 57$
and 115 μm D_t in longitudinal direction equaled 2.54 and 2.60 cm^2/s,
in a transverse direction 0.30 and 0.33 cm^2/s. At the same time
$\overline{V'^2}$ for bigger particles was 20% smaller than for smaller ones, i.e.,

the degree of entrainment of particles by turbulent pulsations decreased with an increase of r.

Free Aerosol Streams

There is great interest in the movement of aerosol particles in free streams, but there is very little data on this problem. N. Kubynin [253] investigated the distribution of concentrations of very polydispersed (r = 10-300 μm) coal dust in streams, released with speeds of U_0 = 22 and 38 m/s from a tube with a diameter of 5 cm. Simultaneously the profiles of speed in the stream were measured. These practically did not change with an increase in the concentration of dust from 0 to 1.15 g/g of air. It turned out that the distribution of velocities and concentrations in a stream is quite similar. This is easy to understand if one were to consider the proximity of coefficients of turbulent diffusion D_t and turbulent viscosity v_t. Near the axis of stream, however, the percentage of coarse particles is increased. Unfortunately, data for the separate fractions in the work were not obtained.

A. Chernov [257], working with dust fractions of corundum, quartz, and boric acid with $\bar{r}$ = 30-200 μm at U_0 = 17-37 m/s and nozzle diameter of 2.5 cm, confirmed independence of velocity profile on dust concentration. By photographing the moving dust particles, the author showed that their initial speed upon discharge from the nozzle V_0 practically does not depend on r; at U_0 = 28.5 m/s, V_0 = = 20-22 m/s (for the cause of this phenomenon see p. 142). Here the particles possessed a high speed of rotation, on an order of 1000 r/s, obtained by them during friction on the wall of the nozzle. Initially the velocity of particles V increases, the speed of air along the axis of the stream U decreases, at a certain distance from the nozzle they are equal, and further, thanks to inertia of particles, they move already faster than the air and the larger the particles the more the ratio V/U increases. It follows from this that the above-mentioned observations on the independence of velocity profile dust content are not fully accurate: dust should decrease airspeed near the nozzle and increase airspeed far away from it.

Precipitation of Aerosols from a Turbulent Flow

The question of distribution of dust by height in a horizontal turbulent flow has been investigated by Dawes and Slack [258]. They blew a fraction of coal dust with r = 2-20 μm through a tube with a square cross section of 30 × 30 cm at a speed of 0.5-2 m/s and measured its concentration at various heights above the bottom of the tube. For fractions with r < 8 μm the concentration was practically constant over the entire section. From the data given by the authors for fractions with r = 3-11, 11-16, and 16-22 μm, it is clear that, for example, in the second of these fractions the concentration at the bottom of the tube was 2-3 times higher than at the top. Based on the formula $\ln(n/n_0) = -V_s z/D_t$ [259] taking into account the irregular shape of coal particles (see p. 8), the coefficient of turbulent diffusion calculated by the author of the survey at U = 1 m/s for the stated fractions fluctuated from 50 to 90 cm^2/s, while based on the empirical formula of Sherwood and Woertz [260] $D_t = 0.044 \, \nu \, Re_f^{0.75}$ it should equal 11.6. If D_t is calculated by the formula $D_t = 0.7 \, U^* z$ [261], taking for z half the radius of the tube, the friction rate is determined by the well-known formula $U^* \approx 0.2 \, \bar{U}/Re_t^{\gamma}$ [262], then $D_t = 0.035\nu \, Re_t^{\gamma} = 32$ is obtained. Obviously, further analogous measurements are needed.

Let us mention two simiempirical methods for calculation of diffusion flow I toward the smooth walls of tubes during turbulent flow. Lin et al. [263] assumed that in the laminar

$$D_t - v_t = (z'/14.5)^3 \, v,$$ (6.12)

where $z^* = zU^*/\nu$, U^* — rate of friction. It follows from this that in the buffer sublayer

$$D_t = v \, (z^*/5 - 0.959).$$ (6.13)

The expression obtained from these formulas for diffuse flow, which corresponds well with experimental data, is not given here in view of its cumbersomeness.

Deissler [264] originated from the formulas which he derived earlier and which conformed excellently with experimental data, for the profile of speed during turbulent flow and arrived at the following expression, applicable at Sc > 200

$$Sh = \frac{4 \, \gamma^2 \cdot 0.124 U^* R \, Sc^{1/4}}{x \nu},$$ (6.14)

also agreeing well with data from experiments on diffusion in solutions. From formulas (6.14) and $U^* = 0.2 \, \bar{U}/Re_l^{1/8}$ [265] it follows that

$$I = \frac{n_* D^{1/4} Re_l^{7/8} \nu^{1/4}}{80 R}$$ (6.15)

in agreement with the formula of L. Landau and V. Levich [266].

In the work by Friedlander and Johnstone [267] an investigation is made of the precipitation of aerosols on walls of vertical tubes during turbulent flow. Experiments were conducted with almost spherical particles of Fe ($\bar{r} = 0.4-0.8$ μm) and Al ($\bar{r} = 2.5$ μm) in tubes with a radius of 0.27-1.2 cm. Measures were taken so that particles which precipitated on the walls were not blown off by flow (lubrication of walls). Since the rate of precipitation on the walls of the tubes exceeded by two orders that calculated by the formula (6.15) and, furthermore, increased with the size of the particles, here inertial precipitation undoubtedly took place.

Figure 44 gives the results of experiments with particles of Fe, $\bar{r} = 0.4$ μm, in a tube with R = 0.29 cm. As can be seen from the curves, a deposit will be formed not at the very entrance into the tube, but in an interval of distances x from the entrance corresponding to values $Re_x = x\bar{U}/\nu = 1.0 \cdot 10^5 - 2.5 \cdot 10^5$. Since during flow around a plate with sharp edges agitation of the boundary layer starts at $Re_x = 3 \cdot 10^5 - 5 \cdot 10^5$, then it is obvious that precipitation in these experiments was caused by agitation of the flow.
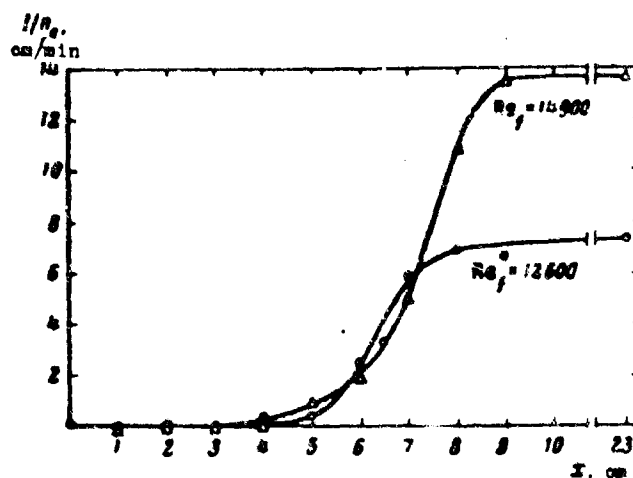
Fig. 44. Precipitation of iron particles on the walls of a tube during turbulent flow.

For a theoretical calculation of speed of precipitation the authors assumed that those particles are precipitated which approached the wall at a distance of inertial path l_1, corresponding to the mean square speed of turbulent pulsations v_r in a direction perpendicular to the wall at distance l_1 from the wall. Along with this the data from Laufer [263] were used. According to it, with an increase of z^* from 0 to ~80 v_n/U^* is increased from 0 to ~0.9 and further is not changed. For simplification of calculations the authors accepted simply that $v_n = 0.9\ U^*$. According to the hypothesis that the sublayer is purely laminar, in certain experiments precipitation in general should not have occurred, since the thickness of this sublayer $\delta_c \approx 5\nu/U^*$ was larger than l_1. With the help of formulas (6.12) and (6.13) the authors obtained the following expression for rate of precipitation of particles on 1 cm^2 of wall:

$$I = \frac{z_p U'^2}{\overline{U}[1 + U'(11.5^3/\overline{U}'^3 - 50.6)]} \qquad (l' = l_1 U'/\nu). \tag{6.16}$$

The values of I calculated from it differed by no more than twice (in both sides) from experimental. It was difficult to expect better coincidence at the existing level of our knowledge about the structure of turbulent flow near walls.

In the above-mentioned experiments by Dawes and Slack they also measured the speed of precipitation of coal dust on the bottom, and lateral and upper walls of the tube. For precipitation on the bottom of the tube they found the dependence

$$I = kr^2 n = kr^2 n_0 \exp\left(-\frac{kr^2 x}{U h}\right),$$
(6.17)

(n_0 — initial concentration of aerosol, h — height of tube, k — constant), which is easy to deduce [269], considering the concentration constant over the entire section of tube, where $kr^2 = V_s$. At $\bar{r} > 16$ μm I decreases faster than by this formula, since the concentration of aerosol, as we have seen on p.113, noticeably increases upon approaching the bottom of the tube. For the relationship β of speed of precipitation on the side walls and on the bottom of the tube the authors found the dependence β χ χ $2(2r)^{-1.35}$, where r is expressed in microns and β depends little on the speed of flow. Thus the rate of precipitation of particles on the side walls in these experiments is proportional to $\sim r^{..}$.

Pereles showed [270] that also in these experiments the rate of precipitation on the lateral and upper walls is incompatible with the hypothesis of a purely laminar sublayer. In his calculations the author disregarded inertia of particles which, as we already saw is not permissible.

Based on its basic idea the work by Owen [271] is close to the above-mentioned work by Friedlander, however, Owen takes as the basis of his calculation a more complex law for the change in the coefficient of turbulent diffusion with the distance from the wall, splitting the boundary layer into three zones. The formulas derived by him for rate of precipitation on the bottom, lateral, and upper walls of a rectangular horizontal tube agree quite well with the results of the experiments of Dawes and Slack.

Koepe [272] also conducted experiments with coal dust in a

horizontal drift with a height of 1.8 m at $\bar{U} = 1.4$ m/s and found that the number of particles settled on 1 cm^2 of bottom of drift did not depend on the horizontal distance x. This of course is an accidental result, apparently connected with the highly polydispersed state of the dust. Madisetti [273], working under the same conditions but with fractionated dust ($\bar{r} = 0.5-3$ µm), found at $\bar{U} = 50-60$ cm/s for the precipitation of each fraction on the bottom of the drift the dependence I = A exp (-kx) in agreement with formula (6.17), but a very small, in comparison with data from the experiments of Dawes and Slack, rate of precipitation on the walls. Here particles with r > 1 µm were generally not detected on the walls. It is quite difficult to explain this variance.

Diffusion of Aerosols in Free Atmosphere

Frenkiel and Katz [274] investigated the scattering in atmosphere of small clouds of powder which were released from balloons. This was done by photographing these clouds from the earth. The contours of a small cloud on photographs are determined by the fact that extinction of light rays, passing through the edges of a small cloud, is so small that it no longer is recorded by a photographic plate. The experiment lasted around 20 s, after which the small cloud vanished. By substituting the images of a small cloud into sequential instants on circles with an equidimensional area, the authors found that scattering of small clouds is described well by the formula (6.7), however, here it was necessary to accept for t = 0 not the moment of burst of the powder, but a moment 1 s later.

According to the accurate observation of Gifford [275] the scattering of small clouds is a case of relative diffusion, described not by formula (6.7), but by formulas (6.10) and (6.11). Indeed, as Gifford showed, the results of Frenkiel and Katz are accurately described by formula (6.10) at t < 10 s and formula (6.11) at t > 10 s.

In the literature theoretical works continue to appea. on the precipitation of aerosols from atmosphere. In these they either

completely disregard sedimentation of particles [276], or originate
from the Setton theory, introducing coefficients of reflection from
the earth or other artificial conditions [277]. A more correct
approach to a solution of the problem is the direct solution of
the fundamental equation of diffusion of sedimentary particles in
a flow for a linear source during a normal adiabatic temperature
gradient which is given by Rounds [278]. Approximating the
logarithmic profile of wind by exponential formula $U = U_1(z/z_0)^\alpha$
and considering $D_{tz} = \kappa U^* z$ [279], Rounds obtained for the
concentration of aerosol at the surface of the earth the expression

$$n_{z=0} = \frac{\Phi'(1 + a)\, e^{-Az}\, p^{-1}}{h U_h \Gamma(1 - p)\, A^{p-1}},\qquad (6.18)$$

in which $p = -V_S/\kappa\, U^*\,(1 + a)$; $A = h^2 U_h/D_h\,(1 + a)^2$; h — height of source,
U_h, and D_h — values of U and D_{tz} at height h, Γ — gamma function.
Rate of precipitation on the surface of the earth is then calculated
by the formula $I = V_S n_{z=0}$.

Godson [280] proposed an approximate method for the calculation
of $n_{z=0}$ on the basis of formula (6.18) in the case of a nonadiabatic
gradient. In the article by Godson curves are given for the
precipitation of aerosols on the earth (I, x) for different values
of h, a, and $V_S \bar{U}$ ($\bar{U}$ — average windspeed in interval of heights from
0 to h).

Fortak [281] gave the solution of the fundamental equation for
a case of $U = $ const and $D_{tz} = $ const.

With a point source the fundamental equation of diffusion must
be supplemented with member $\partial(D_{ty}\, \partial n/\partial y)\, \partial y$. The solution of this
equation at $U = $ const; $D_{tz} = k_1 Uz$, $D_{ty} = k_2 Ux$ is given by A. Denisov
[282], and at $U = U_1 r^n$, $D_{tz} = k_1 z$, $D_{ty} = k_3 r^m$ by L. Gandin and R. Soloveychik
[283].

Footnotes

[1] In "Mechanics of Aerosols" relative diffusion is called Lagrangian diffusion, however this term is not very fortunate.

[2] In "Mechanics of Aerosols" ε is erroneously referred not to 1 g, but to 1 cm^3 of substance of the medium.

[3] During the compilation of "Mechanic of Aerosols" the work by Chen was not known to the author, and therefore there, on p. 232, it is maintained erroneously that D_t of particles is less than D_t of the medium.

[4] Let us note that according to the observations of Hoffman [256], during measurement of speed of flow with a Pitot tube a content of dust (quartz) in the air up to 1 kg/m^3 does not affect results, if on the walls of the tube a dust deposit was not formed.

C H A P T E R 7

COAGULATION OF AEROSOLS

Brownian Coagulation of Aerosols

Let us mention first of all works on the coagulation of highly dispersed aerosols. In the work by Zebel [284] the rates of diffusion and kinetic precipitation of particles on an absorbing sphere are not equated at the distance of average apparent length of free path of particles from the surface of the sphere, as this is done by the author of the survey [285], but at the very surface. Here for the constant of coagulation is obtained the expression

$$K = K_0 / \left(1 + \frac{4D\sqrt{m}}{r\sqrt{6kT}} \right) \qquad (7.1)$$

(m — mass of particles, K_0 — value of constant, disregarding jump of concentration),[1] whereas the formula derived by N. Fuks [286], can be presented in the form

$$K = K_0 / \left(1 + \frac{3D\sqrt{m}}{r\sqrt{2\pi kT}} \right) . \qquad (7.2)$$

The opinion of Zebel that his formula is applicable also when $3D\sqrt{m}/r\sqrt{2\pi kT} \approx l_B/r \gg 1$ is incorrect. In this case approximately accurate is the formula $K = 2\sqrt{2\pi r^2 C}$ [283].

. . . . with the experiment of . . . .
. . . . dispersed aerosols with r < 0.1 μm it is possible to use
. . . that with certain reservations) only the data of Nolan and
Kennan [287], measuring the rate of coagulation of aerosols, obtained
by sublimation of platinum in filtered air. The average radius of
particles, varying within limits of $0.5 \cdot 10^{-6}$-$2.6 \cdot 10^{-6}$ cm, was
determined by diffusion method (see p.81). Particle density
was measured in a Pollak nuclei condensation counter [288], in
which the concentration of nuclei is determined based on their .
reduction of light after condensation of water vapor on them.
The average value of the ratio K/rD in these experiments is equal
to 33; deviations from it are great, but a systematic change of
K with increase of r was not observed. Without a correction for
jump of concentration this ratio for isodispersed aerosols should
equal $8\pi \approx 25$, and in view of the polydispersed state of the aerosols
increased values of K should have been expected.

Thus, from these experiments it would seem that a correction for
jump of concentration is unnecessary, however this conclusion is
not completely convincing. From experiments with horizontal channels
[289] the authors found values of 0.4-0.7 for the apparent density
of platinum particles, and this indicates that the aerosol consisted
of exceedingly friable aggregates, formed from a huge number of
primary particles and, consequently, the degree of polydispersion
in the aerosol is very great. Furthermore, on the basis of
experiments by Whytlaw-Gray [290] it is possible to assume that a
considerable share of particles has an elongated form, and both
these circumstances should have noticeably increased the constant of
coagulation and compensated for the effect of jump of concentration.
Obviously for a final solution of the problem it is necessary to
study speed of coagulation of highly dispersed weakly coagulated
aerosols.

In the new work by O'Connor [291], which was conducted in Nolan's
laboratory, for room condensation nuclei with $r = 2$-$3 \cdot 10^{-6}$ cm an
incredibly large value K/rD = 100-140 is obtained. According to

.... data about coagulation of dipolar
....ng into account the circumstance that particles
.... size have practically no more than 1 elementary charge
..., particle charges cannot be the cause of such a high constant
of coagulation.   Apparently during these measurements some serious
errors were committed.

Based on the experiments of Cawood and Whylaw-Gray [293] in an
aerosol of Fe_2O_3, obtained photochemically from vapors of Fe $(CO)_5$
added to air, at pressures of 200-760 mm Hg column the coagulation
constant increases considerably with a lowering of pressure.   This
is not surprising, since these aerosols in the first period of
their existence are undoubtedly very highly dispersed and their
coagulation constant, according to the formula (7.3), is noticeably
increased with an increase of the ratio ℓ/r.

With the help of differential counter of condensation nuclei,
which makes it possible to determine the concentration of nuclei
of different value (corresponding to different degree of
supersaturation), Yaffe and Cadle [294] qualitatively investigated
the kinetics of coagulation of highly dispersed aerosols, obtained
by heating TiO_2 and NaCl.   In agreement with theory, the number
of particles of least value with $r = 0.4-0.6 \cdot 10^{-7}$ cm decreases
rapidly from the very beginning, and the number of particles of
coarser fractions at first increased, attained a maximum, and then
decreased.

Melzak [295] proposed a method for solving the basic integro-
differential equation of coagulation

$$\frac{dn(m,t)}{dt} = \frac{1}{2} \int_0^m K(m_1, n - m_1) n(m_1) n(m - m_1) dm_1$$
$$- n(m) \int_0^\infty K(m, m_1) n(m_1) dm_1$$

with a fixed coagulation constant,[2] practically coinciding with the

122

... ... The solution of this equation with ... ... values of constants, depending on mass (or volume) of coagulating particles, is naturally much more important, but apparently is possible only by numerical methods. The first published calculation of such a kind, the kinetics of change in the factional composition of a coagulating aerosol with an assigned initial distribution of particle sizes, was performed by Zebel [298] on a computer.

In the opinion of B. Deryagin [299], in the theory of coagulation it is necessary to consider the following circumstance: in order for two approaching particles to come in contact, they have to force out the layer of medium lying between them. According to Taylor [300] the closure rate of two spheres under the action of force F is equal to

$$V = \frac{Fh}{3\pi\eta r^2}.$$
(7.6)

In the derivation of this formula it is accepted that the minimum distance between spheres h << r. As it is easy to check, it follows from it that spheres in general, cannot come in contact. In experiments with spheres which were dropping in a very viscous liquid [301], it was indeed revealed that approaching spheres do not engage, but go separate ways. Also well-known is the phenomenon, induced by the presence of an air layer, of repulsion of large water drops colliding in air, however, solid beads, as daily experience shows, mesh following collisions. For a case of large particles this problem is analyzed below. In the theory of Brownian coagulation, i.e., practically for particles with r < 1 μm, the problem is resolved more simply. Obviously in this case the Taylor formula is applicable only at values of h less than the average length of free path of gas molecules, and it is impossible to use the formula of hydrodynamics for the process of squeezing out the gas layer.

In connection with the reports by Dautrebande and his colleagues [302, 303] about the intense coagulation of silicate dust by aerosols

123

. . . is necessary to point out the following data. According
. . . experiments of Avy [304], a noticeable lowering of countable
. . . concentration of an aerosol of indigo with $\bar{r}$ = 0.1-0.15 μm and n_0 =
= $3 \cdot 10^5$ was observed during injection into it of a fog made from a
solution of NaCl with $\bar{r}$ = 2-3 μm. Here the concentration of NaCl
aerosol in the chamber was reduced to n = $2 \cdot 10^4$. After cessation
of injection coagulation of the indigo aerosol continued practically
at the same speed as in a control experiment, which should have
been expected according to the theory of Brownian coagulation.

According to Le Bouffant [305], following introduction into a
chamber with coal dust ($\bar{r}$ = 0.25 μm) of such a quantity of NaCl
aerosol with $\bar{r} \sim$ 0.1 μm that the concentration by weight of carbon
and NaCl were practically identical, no noticeable enlargement
of coal particles was observed.

Of decisive importance in these experiments is the hygroscopicity
of NaCl and, consequently, atmospheric humidity. As Walkenhorst
and Zebel [306, 307] showed, a dry aerosol of NaCl (r < 0.1 μm)
does not affect stability of coat dust. At 95-99% atmospheric
humidity rapid enlargement is observed and the precipitation of
aggregates made from particles of carbon and NaCl, due to increase
in the size of the latter induced by absorption of moisture and the
consolidation of aggregates (see p. 3). Analogous observations
were made of aerosols of SiO_2. Also understandable are the
observations by Dautrebande [308]. According to him, when
animals inhale a mixture of aerosols of SiO_2 ($\bar{r}$ = 0.35 μm) and NaCl
they are precipitated in the bronchi, but following inhalation
of a pure aerosol of SiO_2 — in the lungs. It is known that already
in the middle of trachea inhaled air becomes saturated with water
vapor [77].

According to the experiments of Fujitani [309], following
introduction of ethyl acetate vapors (up to 0.6 mM/ℓ) in a fog
made of a saturated solution of ammonium chloride with $\bar{r}$ = 0.25 μm
the coagulation constant decreases from $8 \cdot 10^{-10}$ to $3 \cdot 10^{-10}$ cm^3/s.

The same effect is produced by amyl and butyl alcohols. It is difficult to accept that here a lowering in the effectiveness of collisions takes place. Besides that, the latter of the figures cited is much nearer to the theoretical value of coagulation constant than the first. Apparently, in these experiments crystallization of NH_4Cl from drops occurred and the form of particles formed was changed (became less elongated) under the action of organic vapors.

Electrical Effects in Brownian Coagulation

We will switch to electrical effects during coagulation of aerosols. Zebel [284] gave attention to the circumstance that the effects of unipolar and bipolar charging are not symmetrical. As can be seen from the theory of coagulation of charged aerosols [210], at large absolute magnitudes of the value $\lambda_{12} = q_1 q_2 / 2rkT$ (q_1 and q_2 — charges of particles) in the case of attraction of . particles ratio of coagulation constants of charged and uncharged aerosols $\beta \approx |\lambda_{12}|$, and in case of repulsion $\beta \approx \lambda_{12} e^{-\lambda_{12}}$, i.e., the effect of unipolar charging is much stronger than bipolar. For the value β taking into account jump of concentration Zebel obtained the expression

$$\beta = \left[\frac{e^{\lambda_{12}} - 1}{\lambda_{12}} + \frac{4D}{r} \left(\frac{m e^{\lambda_{12}}}{6kT} \right)^{1/2} \right]^{-1}.$$ (7.7)

applicable, despite the opinion of the author, only at $l_0/r \lesssim 1$.

In formula $\beta = \lambda_{12}/(e^{\lambda_{12}} - 1)$ [310], by expanding $e^{\lambda_{12}}$ into a series we will obtain

$$\beta = 1 / \left(1 + \frac{\lambda_{12}}{2} + \frac{\lambda_{12}^2}{6} + \dots \right).$$ (7.8)

This formula is also cited by Gunn [311], but he has $\lambda_{12} = q_1 q_2 / rkT$.

In the experiments of Benton et al. [312] in the chamber they

... ... with r = .5-2.5 μm, obtained by atomization of 0.1-1 N
... of iron alums and KCNS. Based on the number of stained
drops in the deposit on the bottom of the chamber, the rate of
coagulation ϕ of drops of both fogs with each other was estimated.
It turned out that ϕ increases with an increase in the concentration
of solutions. The addition of cationic detergents to a solution
of alums and anionic detergents to a solution of KCNS noticeably
increases ϕ, and with the reverse combination ϕ noticeably decreases.
Since on the surface of the stated solutions ions Fe^{3+} and CNS^- are
absorbed, as well as cations of cationic detergents and anions of
anionic detergents, authors consider that double electric layers
on the surface drops influence the effectiveness of their collisions,
and namely decrease it if the drops have identical signs of surface
potential drop and increase it in the opposite case.

As is pointed out below, free charges of drops indeed noticeably
increase the effectiveness of collisions, but the mechanism of
this phenomenon is such that it cannot take place with a double
electric layer. Furthermore, electrostatic forces between two
drops which are covered by such layers are insignificantly small
even at a very close distance between drops. It is true, as
S. Dukhin and V. Deryagin showed [313], that during movement of a
drop and circulation inside drop induced by it a displacement can
take place in the charges in the double electric layer, leading
to polarization of the drop and the appearance of a quite strong
external field. However, it is most probable that the observations
of Benson are explained by the balloelectric effect. According to
G. Natanson [314], during atomization of solutions with a high
ionic strength a balloelectric effect of a second kind is observed;
the fog is charged with the sign opposite to the sign of the ions
adsorbed on the surface of the solution, i.e., positive for KCNS
and negative for alums. Additions of detergents should strengthen
this effect still more. Unfortunately, in his experiments Elton
did not measure the charges of drops.

Winkel [315] investigated kinetics of coagulation of aerosols in
a chamber, in which a uniform electrical field with an intensity

? E = 40-190 V/cm was created. In the case of f r, formed during hydrolysis of TiCl$_4$ vapors, concentration by weight was changed according to the law $c = c_* \exp(-KErt)$. In an aerosol of NH$_4$Cl the effect was much stronger and aggregates in the form of long filaments appeared. In both cases large aggregates were precipitated not on the electrodes, but on the bottom of the chamber, i.e., they possessed small free charges.[3]

Zebel [316] gives the theory of coagulation of aerosols with the particles constituting electrical or magnetic dipoles, taking into account the disorienting action of thermal motion. The basic role in this theory is played by the value $\rho_p = (P^2/kT)^{1/3}$ (P — dipole moment), expressing the distance between centers of dipoles at which the energy of interaction between them has a value on an order of kT. The author made calculations for cases of weak ($\rho_p \ll 2r$) and strong ($\rho_p \bar{>} 2.8r$) interaction. In the first case the coagulation constant increases by the factor $1 + 0.095(\rho_p/2r)^6$, in the second — by the factor $\sim \rho_p/2r$.

Sound Coagulation of Aerosols

Very little has been done in recent years on the theory of sound coagulation.[4] In the work of V. Gudemchuk et al. [317] a study was made of coagulation a fairly isodispersed fog of dioctyl phthalate with $\bar{r} = 0.28$ μm in a flow at a frequency 13 kHz. As can be seen from Fig. 20 and Table 13 of "Mechanics of Aerosols" [318], under these conditions practically complete entrainment of particles by vibrations of air takes place, i.e., coagulation by the mechanism of Khidemann was absent; nevertheless, with a sufficient intensity of sound the aerosol coagulated rapidly. Based on visual observations of the authors considerable agitation of the gaseous environment took place. For clearing up its role a system of parallel plates was placed in the coagulational column at a height of 90 cm and with intervals of 1-2 cm. These reduced the amplitude of sound oscillations comparatively little, but noticeably reduced turbulence. With the same intensity of sound in the column, in the presence of plates the speed of coagulation

... it follows from these experiments that
... is apparently a serious factor in sound
... On the other hand, turbulence paralyzes effect of
displacement of particles to antinodes of standing waves under
the action of radiation pressure [265] and the effect of asymmetry
of oscillations of particles (p. 27 of the survey) and these effects
probably do not play a noticeable role in sound coagulation. What
value there is here in the hydrodynamic effect of Oseen forces,
examined on p. 35 , will be judged only after special investigations.

Gravitational Coagulation of Aerosols

In view of the exceptional value of gravitational coagulation in
the process of formation of atmospheric precipitation, this question
has been given very much attention recently. At present it is
possible to consider it firmly established that the Langmuir model
of gravitational coagulation (a large spherical particle, falling
in an aerosol, made up of smaller particles which are not sedimenting
and do not affect its motion, at a speed equal to the difference of
actual speeds of sedimentation of large and small particles) may be
preserved only for a maximum case — a very great difference in the
value of particles. Generally speaking it is necessary to consider
the forces of hydrodynamic interaction between particles, depending
not only on the relative velocity of particles of different value,
but also from their speed with respect to the medium.

Gravitational coagulation has been studied recently by three
methods: 1) theoretically they calculate the field of flow, created
by a falling drop, and its interaction with other particles; 2) in
model experiments in a viscous liquid they investigate the
trajectories and speeds of two beads which are sedimenting at a close
distance; 3) they investigate movements and coefficients of capture
of drops in an ascending current.

Using the expression derived by him for hydrodynamic forces
$F_{||}$ and $F_{\perp}$ (see p. 31) in a Stokes approximation, Hocking [98]

simulated on a computer the trajectories and world lines of capture of freely falling water drops. It turned out here that ə > 0 only at a radius of a large drop R > 18 μm (this conclusion clearly contradicts experiment, see below). With an increase of R there is an increase both of ə and the range of values of the ratio r/R at which ə > 0 (at r/R = 1 in a Stokes approximation, as it was pointed out on p. 30, both particles possess identical speed and do not converge). Thus, at R = 20 μm this range spreads from 0.4 to 0.8, and at R = 25 μm from 0.2 to 0.9. Maximum values of ə (at r/R ≳ 0.7) accordingly are equal to 0.25 and 0.90 in these two cases.

Although during the fall drops of the stated value Re_f equals only 0.10-0.30, calculation of the coefficient of capture in a Stokes approximation can lead to large errors here, since for this it is necessary to determine trajectories of the drops, starting from such a great distance ρ between them (up to 50 R) at which ə = Vρ/ν > 1 (see p. 34).

Pearcey and Hill [319] examined this same problem in an Oseen approximation. They used a simplified form of Oseen equations for field of flow (created by a moving sphere) which is applicable at large ρ/R. The error committed here increases with approach to the surface of the sphere. The field of flow created by the movement of two spherical drops is obtained by the authors by simple summation of the fields created by each drop separately, i.e., they use the zero approximation (see p. 31) which does not satisfy exactly the boundary conditions on the surface of the drops. The error induced by this also increases with the drawing together of the drops. The opinion of the authors that drops skip past the zone in which these errors are great so rapidly that the latter have little reflection on the final results of calculations, is unconvincing.

Figure 45 depicts the field of flow around a falling drop of water with R = 73 μm (Re_f = 4). Heavy lines connect points with identical flow rate (expressed in fractions of fall rate of the
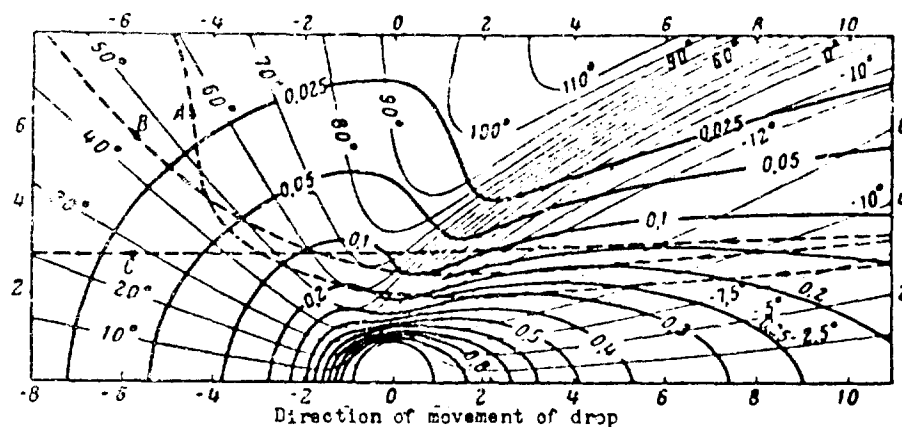
Fig. 45. Field of flow and trajectories of particles during flow around a sphere. $Re_f = 4$.

drop), thin lines — points in which the flow lines have a given angle of inclination to axis of movement, where θ < 0 if the flow lines approach the axis. As can be seen from the chart, a track will be formed behind the drop (narrowing with an increase of Re_f). In this track the rate of flow decrease comparatively slowly with an increase of distance from the drop, and the flow lines are directed toward the axis. In the front and off to the sides from the drop the speed of flow decreases considerably faster and the flow lines are directed to the sides under the greater angles. Therefore drops, moving behind a certain drop, will not only catch (see p.36), but also will be pulled into its track, i.e., will approach the axis of flow. The broken lines in Fig. 45 depict the trajectories of drops, overtaking the given drop, and the dimension of which is larger by 0.1% (A), 1.1% (B) and 11% (C) than that of the given drop. Initially (at a great distance from the given drop) these drops were found in one point: the smaller the difference in the dimensions and fall rates, the greater is the time for approach of the trajectories of both drops. Figure 46 depicts the calculations of the authors for values ν_9 in function of ratio (R - r)/r for different values R (radius of the larger drop). The rapid growth of ə with a decrease of this ratio was just explained. The growth of ə with an increase of Re_f is caused by an increase in the asymmetry of field of flow — the greater the Re_f, then the slower is the reduction in flow rate in the track with distance from the drop. The data in Fig. 46 are

130
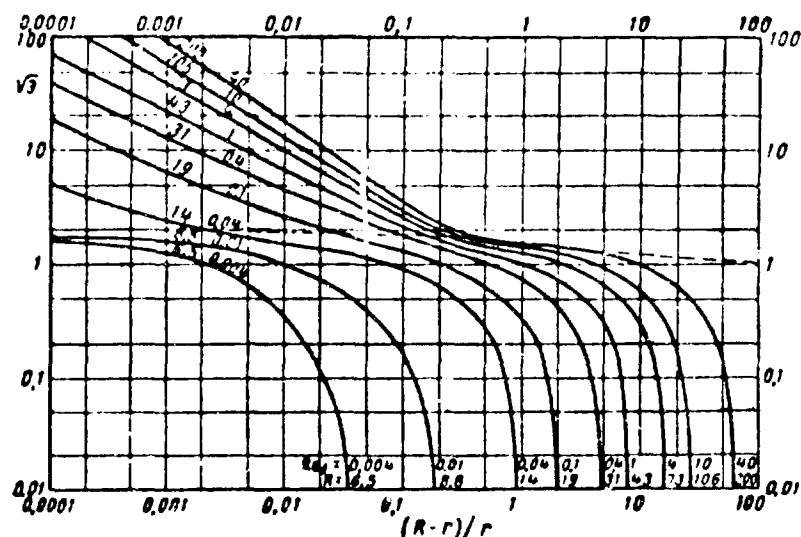
Fig. 46. Coefficient of capture during gravitational coagulation of water drops (R in μm).

calculated on the assumption that in the initial state of the drop R and r are infinitely removed from one another. Actually thanks to turbulence induced horizontal displacements of drops, and convection currents, the systematic approach of trajectories start only from a certain finite distance between them; here the value of ∂ is noticeably lowered.

The stated circumstance has specific importance for small drops (r < 10 μm), the convergence of which when there is little difference in their sizes occurs extraordinarily slowly. Therefore, the curves for such drops in Fig. 46 apparently do not have a real value.

It is clear from what has been expounded that experimental results of Tellford et al. [320] coincide with the calculations of Pearcey and Hill. For drops with r ≈ 70 μm Tellford's value ∂ = = 12 disregarding the coupling effect and ∂ = 3 taking into account this effect corresponds, according to Fig. 46, to values (R - r)/r = = 0.01-0.1, and this interval corresponds exactly to the conditions of Tellford's experiments.

Schotland [321] investigated the movement of two (for the most part identical) steel beads with r = 0.7-7 mm, sedimenting in a

131

liquid with n = 20 poises. Unfortunately, the author did not cite the results of the model experiments themselves, but recalculated them to the fall of water drops in air with the same Stk values. He considered observance of equality Re unnecessary, since he considered that the Re in his experiments was very small (for the above-indicated beads the Re changed from 0.05 to 5). Unfortunately, in the conversions the author committed an evident error, and it is impossible from the text to determine from which beads the given results were obtained.

Schotland observed the approach of two identical sedimenting beads. True contact between them did not occur due to viscous resistance of the liquid layer (see p. 123), and after convergence the beads again parted in agreement with the calculations of Pearcey and Hill. $\ni$ equaled ~ 1.7 for identical beads and considerably less than 1 for beads of various size. From these data it follows that the Re in the experiments by Schotland was not very small.

Sartor [322] also tried to transfer the results of his model experiments to graviational coagulation of fogs, however, he did not observe condition of constancy of Stk number. Furthermore, during movement of drops of water in a very viscous medium very intense circulation occurs in the drops, and this can noticeably affect the coefficient of capture. Therefore, the experiments by Sartor have only a qualitative character.

In work of Kinzer and Gobb [323] one of the drops (R) was supported at a constant height by regulating the speed (equal to V_S of this drop) of the ascending current of fog with average radius of drops $\bar{r} = 5-7$ μm and it was examined through a cathetometer. With an increase of V_S an increase of R was determined; this was induced by the capture of other drops, and from here $\ni$ was calculated. Since in these calculations the starting point was not the relative speed of drops, but V_S, i.e., it was assumed that little drops are stationary with respect to the medium, the value of $\ni$, calculated for close values of r and R, are strongly minimized.

The curve (ϑ, R) obtained by the authors has a rather complex form: at R $\gtrsim$ r $\gtrsim$ 6 µm ϑ $\gtrsim$ 1, further with an increase of R (i.e., with a decrease of r/R) ϑ decreases to ∿0.15 at R = 30 µm, which qualitatively will agree with the calculations of Pearcey and Hill. Then ϑ increases and reaches 0.9 at R = 200 µm. This part of the curve does not differ very strongly from values ϑ, calculated for potential flow; its course can be explained by the fact that with a constant r the Stk number is proportional to ∿V_S/R and increase with a growth of R [324]. With a further increase of R, ϑ again decreases to 0.15 at R = 1.5 mm. Let us note that in this range of dimensions of drops V_S/R decreases with an increase of R [96].

According to observations of Kinzer and Gobb small drops, falling into the track of a drop, which is suspended in a flow, move in little circles located in vertical planes passing through the center of the drop, obviously under the influence of vortexes formed behind the drop. The authors consider that turbulence, created by vortices forming behind all the drops of cloud, is the basic factor in gravitational coagulation. We will not expound the very complex and poorly founded theory of the authors. We will only note that during movement of a sphere in a viscous medium the formation of vortexes with dimensions equal to the diameter of the sphere begins only at Re_f $\gtrsim$ 100, and their detachment − at still higher values of Re_f [325]. Thus, for drops with R $\leq$ 300 µm this theory is hardly applicable. The matter is different during the fall of large drops: according to the observations of Oakes [326] drops with R = 1.8 mm, falling through a smoke chamber, intensively mix the aerosol contained in the chamber.

For determining coefficient of capture on moving drops of water Walton and Woolcock [327] forced drops to drop through a chamber filled with an isodispersed aerosol made of spherical particles of methlene blue (r = 1.25 and 2.5 µm), however this method turned out to be unsuccessful and the authors switched to another method. Drops of water with R = 0.25−1.0 mm were suspended on glass threads in a vertical tube, through which an aerosol was blown from bottom

133

to top with a speed corresponding V_S of the drop. Re_f comprised 70-870. The a values obtained were somewhat below those calculated theoretically by Fonda and Herne for potential flow around (Fig. 22, p. 63).

Walton and Woolcock also calculated the effectiveness of precipitation of dust with atomized water, blown in at high speed, taking into account a gradual decrease of this speed. As should have been expected, in this case the effectiveness of precipitation of small particles increases considerably.

At the present time tremendous importance has been acquired by the problem of precipitation of atmospheric radioactive aerosols with rain. As can be seen from what was stated above, in this case it is possible, without making a large error, to use for calculations the curve shown in Fig. 22 for potential flow around.

During a rain May [328] released into the atmosphere from a height of 2 m lycopodium spores labeled with J^{131} ($r = 16$ μm). Around the source on a circumference with a radius of 10 m were situated crystallizers, serving for the collection of spores, settling both independently and also washed off with rain. Some of the crystallizers were placed under umbrellas — they picke up spores, not washed by rain drops, but settling independently. Based on difference a determination was made of quantity of spores precipitated with rain drops. Unfortunately, the dimensions of the latter ($R = 0.2-2$ mm) were not determined, but were found in Best tables [329] based on intensity of rain. Satisfactory agreement was obtained between results of the experiments and theoretical calculations of precipitation in potential flow.

For determining the effectiveness of Venturi scrubbers Johnstone et al. [330] established the empirical formula

$$\vartheta = 1 - \exp(-K_3 Stk'),$$ (7.9)

where β — ratio of volumes of atomized water and purified gas, K — constant. Brink and Contant [331] confirmed this formula by experiments, set up under plant conditions, with fogs of phosphoric acid with $\bar{r}$ = 0.25-0.75 um. Here β varied from 0.8 to 0.99. Theoretically it should have been expected here that the curve obtained (β, Stk) would be the one depicted in Fig. 22 (for potential flow around a sphere). However, as it is easy to check, this curve can be easily approximated in the stated range of changes of β by the formula (7.9) by means of selecting the coefficient K.

At first glance, the conclusions of Pearcey and Hill and the experiments of Tellford et al. confirm the opinion of Boucher [332] that for a high effectiveness of the Venturi scrubber it is necessary that the sizes of drops of atomized water and particles of aerosol are close to one another, however, r particles with dimensions on an order of a micron or less these conclusions are naturally inapplicable.

Passing to influence of charges on gravitational coagulation, we will mention the work of Pauthenier et al. [333], who expanded on their previously derived formula[5]

$$ \vartheta = \left(\frac{45}{16}\right)^{\!\!\prime\!\prime\!\prime}\left[\frac{\lambda r^2 q^2}{\tau g\,(R^2 - r^2)}\right]^{\prime\prime\prime}\frac{1}{R^2} $$

(q — charge, λ — induction factor) in the case when besides gravity a vertical electrical field with intensity E is acting on the particle. In this case to member $\tau g\,(R^2 - r^2)$ one should add the member $\jmath q E/r\pi R$, where $E > 0$ if the field is directed downwards and <0 in an opposite case. The calculations by Gunn [335], who apparently did not know of the work by L. Levin on gravitational coagulation of charged fogs [336], are primitive and are not cited here.

From time to time reports appear about the positive influence of the charging of atomized water on effectiveness of precipitation of aerosols in a chamber [337, 238], however exact quantitative

... about this effect are still lacking. Charging of the aerosol itself in the corona discharge only somewhat increases its precipitation in a Venturi scrubber, to charge the atomized water in the scrubber, apparently no one has tried yet.

Since attractive force of a spherical particle with radius r to a drop, on which vapor is condensed, equal, according to the formula (2.13) $6\pi r R D_{\varepsilon} (c_{\infty} - c_S) c'/c^2$, i.e., it is changed with distance as a Coulomb force, then, as S. Dukhin and B. Deryagin noted [75], the formula of L. Levin,

$$ \Phi = \frac{3 \cdot Q q}{\pi \eta r R^2 (R^2 - r^3) g} $$

can be used for calculating the rate of gravitational coagulation of aerosol with growing drops in a supersaturated atmosphere. For this it is necessary only to replace in this formula $|Q_q|$ by $4\pi r R D_{\varepsilon} (c_{\infty} - c_S)/c'$.

In the case of evaporating drops the rate of gravitational coagulation should obviously be decreased. Therefore, the higher the humidity of the gaseous environment the more effective should be precipitation of aerosols with atomized water.

Coagulation During Agitation and in a Turbulent Flow

Gillespie [339] calculated the rate of coagulation of aerosols in a gradient flow in the presence of charges on the particles. For the rate of coagulation of spherical particles with radius r_1 and charge q_1 with particles possessing a radius r_2 and charge q_2, the following formula[6] is obtained

$$ \Phi = \frac{4}{3} [\Gamma (r_1 + r_2)^3 - 3\beta] n_2. $$

$$ \beta = \frac{q_1 q_2 (r_1 + r_2)}{6\pi \eta r_1 r_1} . $$

(7.10)

in the absence of charges formula (7.10) converts into the known formula of Smolukhovskiy [340].

136

We will review recently appearing works on the theory of turbulent coagulation. The work of Saffman and Turner [341] in principle does not differ from the work of V. Levich [342], however, the conclusions are somewhat more precise; in particular, consideration is given to the distribution of relative speeds of coagulating particles, for which normal (Gaussian) distribution is accepted. For the speed of turbulent coagulation based on the first mechanism of V. Levich, i.e., at the expense of a difference in pulsational speeds of the medium at a distance 2r, the authors obtained the formula of Levich-Tunitskiy

$$\Phi \approx k \left(\frac{\varepsilon}{v}\right)^{\gamma_2} r^3 n_0 \tag{7.11}$$

with a coefficient k = 10.4 instead of the 25 for V. Levich and 4 for N. Tunitskiy. For coagulation according to the second mechanisms, i.e., due to distinction in pulsational velocity of particles, caused by different inertia, the authors obtained formula

$$\Phi = 5.7 \, n_0 \, (r_1 + r_2)^2 \, (\tau_1 - \tau_2) \, e^{\gamma_4} v^{\gamma_4} \tag{7.12}$$

where τ_1 and τ_2 — relaxation times of coagulating particles. Here for the mean square of relative acceleration the authors accepted according to Batchelor

$$\overline{(dU'/dt)^2} = 1.3 \, \varepsilon^{\gamma_2} v^{\gamma_2} \tag{7.13}$$

From formula (7.12) it follows that the greater the difference in the value of coagulating particles the stronger the second mechanism of coagulation should be manifested. The authors calculated that in clouds at $\varepsilon = 5 \text{ cm}^2/\text{s}^3$ (this value corresponds approximately stratus clouds during a weak wind) the second mechanism predominates over the first at $r_1 - r_2 > 2.3$ µm, and at $\varepsilon = 1000 \text{ cm}^2/\text{s}^3$ (cumulus cloud with strong convection) - already at $r_1 - r_2 > 0.6$ µm.

We find a similar method of analyzing the problem for East and Marshall [343], however, they did not use an expression of the type (7.13) for mean square of acceleration of the medium and therefore could not obtain formulas for the rate of turbulent coagulation.

There is no single opinion as to whether or not it follows in coagulation by the second mechanism to consider the coefficient of capture of particles. In their calculations East and Marshall used values for ə calculated by Langmuir; in the opinion of Saffman and V. Levich [334] it is necessary to consider ə ≈ 1. Saffman is based on the model experiments of Manley and Mason [345] on coagulation in a gradient flow, but the results of these experiments pertain only to turbulent coagulation according to the first mechanism in the treatment of N. Tunitskiy [346]. According to V. Levich small particles flow around large ones and simultaneously diffuse toward them by the first mechanism. The expression obtained from this model for the effective coefficient of capture, in the opinion of V. Levich is on the order of 1, however, if $R = 10^{-3}$ cm and $\varepsilon = 1000$ cm^2/s^3 is inserted in it, we will obtain ə $= 0.05$. It is necessary to assume that the value ə essentially affects the rate of coagulation by the second mechanism. On the other hand, the value ə in this case probably differs strongly from its value during gravitational coagulation.

Frish [347] assumes that mean square of relative displacement of two particles under the action of turbulent pulsations is equal to sum of mean squares of their absolute displacements, from which it follows that the coefficient of relative turbulent diffusion of two particles is equal to the sum of coefficients of diffusion of each of them, and thus, the theory Smolukhovskiy with small changes is applicable to turbulent coagulation. These assumptions clearly contradict the theory of turbulent diffusion, and therefore the conclusions of Frish are not cited here.

As V. Levich points out [344], formulas of the type (7.11) are applicable only in the case when turbulent diffusion approximates particles up to very contact, i.e., when at any distance between

138

centers of particles up to $\rho = 2r$ $D_t \gg D$. For this, according to the formula $D_\lambda = \frac{1}{4}(\epsilon/\nu)^{\frac{1}{2}}\lambda^2$ [342], it is necessary that

$$2r \gg 2D^{\prime\prime}(\nu/\epsilon)^{\frac{1}{4}}. \tag{7.14}$$

For example, at $\epsilon = 1000$ cm^2/s^3 this condition will be observed for $r > 1$ μm. With conversion of inequality (7.14), i.e., at $r < 0.1$ μm, speed of coagulation is determined by formula of Smolukhovskiy, i.e., turbulence of medium no longer plays a role.

Effectiveness of Collisions of Solid Particles with Each Other and with Macrobodies

The most important phenomena in aerosols, their precipitation on macrobodies and coagulation, occur as a result of two processes, essentially different in their nature, convergence of particles with macrobodies or with each other and process of adhesion or merging. Convergence of particles is described by the above-examined differential equations and with an assigned field of flow and external forces can be calculated in principle with the desired degree of accuracy. Here only purely mathematical difficulties can be encountered. It is a different matter with processes occurring during collisions. Their mechanism is very complex and has been studied poorly, and at present the effectiveness of collisions (i.e., probability of adhesion or merging) cannot be calculated even in the first approximation; it can be determined only from experiment.

The mechanism of collision of solid particles with solid particles or macrobodies essentially differs from mechanisms of collision of liquid particles and bodies and they should be examined in particular. A case of collision of a liquid and a solid body occupies an intermediate position.

During collisions between solid bodies it is possible to disregard the viscous resistance of the thin gaseous layer between

the approaching bodies. Actually, let us assume that a spherical particle with radius r is moving with speed V_0 perpendicularly to a flat wall. It can be considered that the influence of viscous resistance will start to have an effect when the shortest distance h between particle and the surface reaches a certain value h_0, and from this moment a force starts to act on the particle which is obviously twice as large as in the case of a collision of two spheres (p. 123)

$$F = -\frac{6\pi\eta r^2 V_0}{h}.$$
(7.15)

In solving a differentail equation of particle movement under the action of this force, we find that the particle will stop at a point corresponding to the value

where
$$h_f = h_0 e^{-V_0 \beta},$$
(7.16)

$$\beta = 9\eta/2r\gamma.$$

If one were to take, for example, that V_0 is the free-fall velocity of a particle in the air and that $h_0 \approx 0.5$ r, then, as it is easy to calculate, h_f in all cases is less than the average length of free path of gas molecules, and with such a value for h_f it is impossible to speak of viscous resistance of a gas layer. Furthermore, in view of the microroughness of all real surfaces contact will occur already at a value of h_f on an order of height of the microprotrusions. Thus, with the possible exception of gravitational coagulation of large laminar particles which during fall are oriented parallel to each other, during collisions of solid particles with macrobodies and with each other apparently direct contact between them is always attained.

It is known from the theory of collisions between macrobodies that depending upon material, value, form, and relative speed of colliding bodies, the coefficient of restitution, i.e., ratio of relative speeds V_r'/V_r after and prior to collision can have any

value from ~1 (fully elastic collision) up to 0. The first case takes place if the maximum tension H_{max} in the zone of contact is less than a certain critical value, exceeding by several times, in view of instantaneousness of the load, the elastic limit of material at a static load. During a central elastic collision between two equal spheres or a sphere and a plane the maximum value of repulsive force equals, according to Hertz [348],

$$F_{max} = Kr^2V_r^{\frac{4}{5}}.$$ \hfill (7.17)

where K — constant, depending on elastic properties of material, and the maximum tension

$$H_{max} = K'V_r^{\frac{4}{5}}.$$ \hfill (7.18)

i.e., does not depend on r. It follows from this that with sufficiently small V_r collisions are always elastic: this conclusion is confirmed by the experiments of Raman [349] and Andrews [350] with spheres made of Al and Cu. However, for very plastic materials, Pb for example, the critical value V_r is so small that elastic collision in this case was not possible to realize.

During a slanting collision everything mentioned above pertains to a normal (directed along the line of centers) component of relative velocity V_{rn}. Data are very sparse about a change in the tangential component V_{rt}, induced by frictional force between spheres. As we will see below, the coefficient of restitution V'_{rt}/V_{rt} may be either larger or smaller than V'_{rn}/V_{rn}. We also notice that during a slanting collision spheres, under the impact of frictional force, acquire torque. Further it is known that during a slanting collision with the wall of a sphere, rotating to the same side in which it would rotate, rolling along the wall, the angle of incidence ϕ (i.e., angle between trajectory of the sphere and normal to the wall) is less than the angle of reflection ϕ'; during rotation in the opposite direction $\phi > \phi'$.

In view of the independence of H_{max} on r these regularities

141

should apparently be also observed for coarse aerosol particles at approximately $r > 0.1$ mm. At smaller r adhesional force F_{ad} starts to have an effect. In the first approximation it is proportional to r (see p. 164). Since the maximum repulsive force during an elastic collision F_{max} is proportional to r^2 [see (7.17)], then obviously the ratio F_{ad}/F_{max} increases with a decrease of r. Therefore very small particles adhere even during elastic collisions, for example, particles of an absolutely elastic substance — quartz. The more plastic the particles, then the higher the values of V_r and r at which they adhere. The condition of adhesion can be written in the form

$$\frac{mV_m'^2}{2} < \Omega_{ad}.$$ (7.19)

where V_{rn}' — normal speed of rebound of particle in the absence of adhesion force, Ω_{ad} — work of breakaway of particle [351].

Rebound of solid particles from walls plays a significant role in work of louvered dust separators (see p. 49) and in pneumatic transport of loose materials. It is known that the average velocity of particles $\overline{V}$ is considerably less than the speed $\overline{U}$ of the airstream transporting them, and during transfer upwards through a vertical tube — less than the effective velocity $\overline{U} - V_s$. Previously this phenomenon was explained exclusively by friction during slipping of material on the walls of the tube. Actually, in horizontal tubes a considerable share of the moving material can move along the bottom of the tube. In vertical tubes this can take place in the presence of a twist in the flow, and in these cases we are dealing with friction in the usual meaning of the word. However, there exists one more reason for lag of particles behind an airflow, especially in narrow tubes — the loss of tangential speed during collisions of particles with walls.

Adam [392], with the help of high speed filming, determined the trajectories and velocities of particles of quartz and CaO with
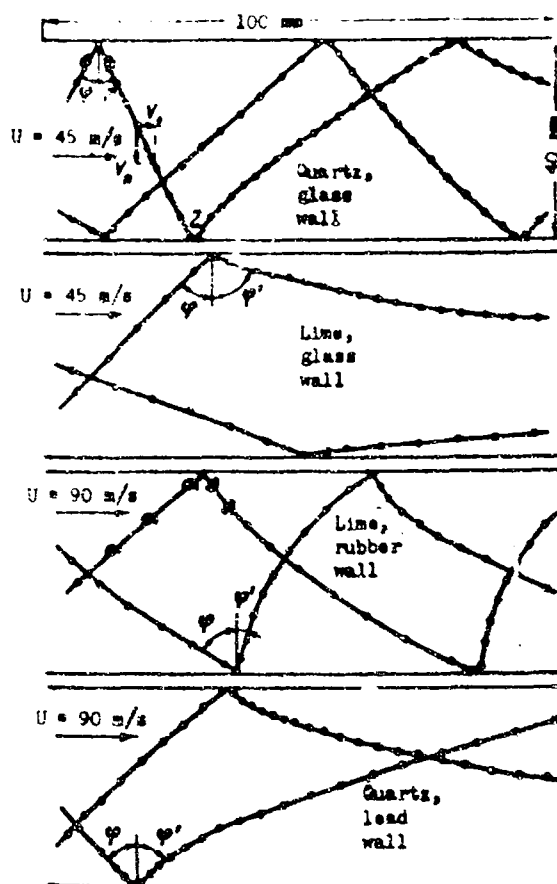
Fig. 47. Trajectories of particles of quartz in line during flow in tubes with walls made from different materials. Scale of time: distance between two points is equal to 0.000294 s.

$r = 0.1\text{-}0.5$ mm in a transparent horizontal tube with a cross section of 4×4 cm at a speed of flow of 40-90 m/s (Fig. 47). Collisions of quartz particles with glass walls usually were fully elastic (point 1); the small decrease in angle of reflection ϕ' is explained by rotation of the particles after collision with the opposite wall (see p. 141). Sometimes nonelastic collisions were observed (point 2); these were connected with destruction of particles or the wall in the zone of contact. Here V_t and V_n were considerably decreased. On lead walls all the collisions of quartz particles are nonelastic. During collisions of the more plastic particles of CaO with glass walls there is a decrease of V_t and especially of V_n, so that $\phi' >> \phi$. Therefore these particles collide much more rarely with glass walls than quartz particles. During collisions of particles of CaO with rubber walls, on the contrary, V_t is almost completely lost and V_n is preserved, i.e., $\phi' << \phi$. In this case the particles acquire especially high speeds of rotation (up to 700 r/s).

143

due to frequent collisions of quartz particles ($r = 0.25$-0.4 mm) with the walls of a tube, during which the particles lose part of their tangential speed, the mean value of the latter $\overline{V}_t/U \approx 0.5\ \overline{U}$. For particles of CaO, as it should have been expected, $\overline{V}_t/\overline{U}$ is considerably larger (~ 0.85). It is understandable that $\overline{V}_t/\overline{U}$ decreases with a decrease in the diameter of the tube.

Coefficient of resistance of the tube to flow of a dust-air mixture can be expanded to two components, corresponding to pure air and dust, where the second component λ is approximately proportional to concentration by weight of dust c. It is understandable that the greater λ then the less is $\overline{V}_t/\overline{U}$, i.e., the more energy is expended on acceleration of particles. For particles of quartz with $r = 0.25$-0.4 mm λ is almost twice as large as for particles with $r = 0.03$-0.05 mm (with that same c), since the latter are attracted to a greater degree by airflow and therefore collide more rarely with the walls. For particles of CaO with $r = 0.25$-0.4 mm λ is still less.

Many authors, in studying the precipitation of solid particles from a flow onto solid walls, considered that particles can adhere to a wall and then blown away by the flow. This undoubtedly occurs during a variable flow rate, but is improbable at a constant speed.

It is known that critical dynamic flow rate is considerably less than static [353], i.e., for blowing off a particle which is sitting on a wall a much higher speed of flow is required than that at which a moving particle can adhere to a wall. Apparently a particle colliding with a wall adheres to it only in the case when either it falls directly into a sufficiently deep potential depression, or at first rolls or slips along the wall until it reaches such a depression. Now, in order to blow off the particle again it is necessary to expend energy, considerably exceeding kinetic energy of the particle prior to collision, i.e., a higher flow rate is needed (or any other external influence).

144

Strong influence on the effectiveness of collisions of particles
with walls is exerted by the electrical charges of one and the other.
The method of photography called xerography is based on this: a
metallic plate is covered with a thin layer of selenium, to which
an electrical charge of high density is transmitted. During
illumination of plate charges flow from illuminated places and,
upon placing the plate in an airstream containing solid particles
of dye charged with the reverse sign, the particles are precipitated
only on the nonilluminated places. This explains the better adherence
of charged (unipolar) talc disinfecting powders to leaves of plants
and other objects in comparison to uncharged powders [114].

The basic method for increasing effectiveness of collisions of
solid particles with walls is the lubrication of the latter, and
this method is obligatory when working with slot instruments. In
the work of Rober which is mentioned on p. 55, the author investigated
the effectiveness of different greases. He deposited different dust
on plates through a konimeter, and then determined at what speed
of flow the deposit is blown off by a stream of pure air from the
same konimeter. In the light of what was said above from these
experiments it is impossible to make a conclusion on the
effectiveness of collisions of particles with a lubricated plate
at certain rates of flow, however, it is apparently possible to judge
the comparative effectiveness of different greases.

Particles with $r = 0.5-1.0$ μm, precipitated on clean plates,
cannot be blown off even at $U = 200$ m/s. Preventing of particles
with $r = 1-5$ μm from blowing off is possible only with proper
lubrication. Here there is great significance in the properties
of the oils used and the thickness of the layer. Lubricants which
are insufficiently viscous or applied in too thick a layer are blown
off by an airstream together with the particles of dust sitting
in them. In greases which are too thick the particles do not
penetrate and are easily blown off from the surface of the grease.
Best results are obtained with a thickness of $0.1-0.5$ μm for the

layer of lubrication; still thinner layers hold particles with r =
= 2.5-5 μm poorly. Particles with r > 5 μm, for example, lycopodium
spores, at a sufficiently high speed of stream cannot be retained
by any lubrications.

I. Dergachev [354] investigated the precipitation of coal dust
with r = 50-80 μm and at U = 25 m/s on a plate lubricated with
vaseline and located perpendicular to the flow. He found that
effectiveness of precipitation increases with an increase in the
thickness of the layer of lubrication up to ∼70 μm, i.e.,
approximately up to the value of r, and further it did not change
since it apparently reaches 100%.

In the experiments of Rozinski et al. [355] particles of ZnS with
r = 10 μm were precipitated on adhesive tapes at U = 4 m/s. It
turned out that on tape with the task of breakaway from a steel
plate at Ω = 22 g/cm 100% of the particles adhered, on the same tape
with Ω = 340 g/cm — only 11%, since it apparently had too hard a
surface. Probably during the instantaneous load at the time of
collision insufficiently soft plastics behave as solids.

Effectiveness of Collisions Between Liquid Drops

We will switch to collisions between liquid drops. The first
serious investigations of reflection colliding water drops are
attributed to Rayleigh [356]. His most interesting experiments are
with two narrow water streams, disintegrated into separate drops
under the impact of sound vibrations and encountered under different
angles. During collisions at an angle of 180°, i.e., during movement
of drops in opposite directions, they are flattened upon collision
and immediately merge. At smaller angles a crosspiece will be
formed, gradually becoming thinner with divergence of the drops.
Finally it bursts with the formation of small secondary drops or
again starts to be reduced and then merging occurs.

Such experiments are very capricious and difficult to reproduce.
The presence on the surface of drops of dust motes, drops of fat,

etc., hardly increases the percentage of effective collisions. The electrical field also facilitates merging immensely. In the opinion of Rayleigh, drops merge if any projection on the surface of the drops succeeds in pressing down the air layer during the short time of the collision. Charges on the surface of the drops promote the rapid growth of accidentally appearing projections. Extraneous particles protruding above the surface also promote the pressing of the air layer and the formation of a crosspiece between drops.

According to the observations of Rayleigh, in an atmosphere which contains a considerable quantity of gases which are highly soluble in water (SO_2, CO_2, water vapor) the effectiveness of collisions is increased considerably; apparently the gas layer is rapidly thinned out due to the dissolving of gases in the drops. An analogous effect is produced by hydrogen: obviously, in view of its poor viscosity it is easily pressed out by drops.

Based on interference colors, produced by an air layer between colliding water streams, Newall [357] determined the thickness of layer h. It decreases in the direction of flow and has a value on an order of 1 μm. An increase in the speed of streams and the angle between them leads to a decrease of h.

It is necessary to mention the experiments by Kaiser [358] with soap bubbles. These have a direct relation to the question under discussion. Kaiser pressed bubbles with a diameter of 3-6 cm with a force of 20-60 mgf to a flat soap film. In 3-25 s a merging occurred — the air layer vanished. Based on Newton's rings it was established in the layer that h in the middle of it (∿1 μm) is less than along the periphery and continuously decreases, at first quite rapidly, then more slowly to a value of 0.08 μm, after which merging occurs immediately. The process of pressing out a layer is satisfactorily described by the Stefan equation for the kinetics of forcing out a viscous liquid from a clearance between approaching parallel disks

$$\frac{1}{h_1^2} - \frac{1}{h_2^2} = \frac{4Ft}{3\pi\eta R^{4}} \qquad (7.20)$$

147

where h_0 — initial distance between disks, h — distance at moment
t, F — compressing force, R — radius of disks.

In the presence of a specific difference of potentials between
the soap bubble and film the duration of life of the bubbles is
sharply reduced, since the pressing of air from the layer is strongly
accelerated and merging occurs already at h = 0.3-0.4 μm. This
phenomenon is caused by electrostatic attraction between two films,
forming a plane capacitor. In the experiments of Kaiser the force
of this attraction exceeded by a few times the force of mechanical
pressing and, as it is easily understood, continuously increased
along with a decrease of h, i.e., an increase in the capacity of
the capacitor.

In a series of works Mahajan [359] investigated the known
phenomenon of floating of liquid drops on the surface of the same
liquid. Based on Newton's rings Mahajan established that in this
case the thickness of the air layer continuously decreases, and
the movement of this process determines the duration of life of
a drop τ. The value of τ, in general, is proportional to viscosity
of the liquid, but for certain liquids (glycerine, mercury, saturated
solution of sugar in water) τ is so small that it could not be
measured by the author. For water τ = 1-2 s, for aniline 2-3 s, for
aqueous solutions of soap 4-5 s, and for olive oil several minutes.
The influence of dust, contaminations on the surface, and electrical
field are all the same as in the experiments of Rayleigh. For
obtaining floating drops it is necessary that they fall from a
certain height: for aqueous solutions of soap from a height >1.8 cm,
which corresponds to a fall rate >60 cm/s. With a decrease of air
pressure τ decreases sharply.

M. Aganin [360] forced water drops with r = 0.5-1.2 mm to drop
on a glass plate, set at a specific angle φ to horizontal and
covered with a very thin layer of water. Merging of weakly charged
drops, formed during the grounding of the capillary tip from which
they emanated, occurred only when dropped from a height exceeding
a certain critical value H, otherwise the drops rebounded. The

experiments were easily reproduced. For drops with r = 0.75 mm, dropping on a horizontal plate, H equals 1.96 cm, which corresponds to the critical velocity of collision V_{kr} 62 cm/s. V_{kr} increases with an increase in the angle of incidence ϕ. Here the product of V_{kr} cos ϕ, i.e., critical value of normal component of speed of drop, turned out to be the value of the constant, namely 70 cm/s at r = 0.5 mm and 46 cm/s at r = 1.2 mm. According to the observations of M. Aganin during ineffective collisions the charge of drops did not change, i.e., there was no contact between the drop and the water film.

Another picture was observed when there were large charges (on an order of 0.01 esu) on the drops. In this case, as also for Rayleigh, a crosspiece appeared between the drop and the water film. It broke during rebound and part of the contents of the drop remained on the film. The magnitude of this part increased with the charge of the drop and upon achievement of a certain critical charge full merging occurred.

Analogous experiments by M. Aganin with the dropping of weakly charged drops on a fixed drop, formed on the tip of a vertical capillary, led to similar results: with r = 0.83 mm and V $\bar{>}$ 21 cm/s all the collisions were effective, at V $\bar{<}$ 18 cm/s — ineffective.

In the experiments of S. Gorbachev and Ye. Mustel [361] water drops with r = 0.65 mm moved at the moment of collision with a speed of 100 cm/s, so that their trajectories formed an angle of 2°. Planes of movement of the drops were parallel and stood at an adjustable distance Δ from each other. With an increase of Δ angle ϕ between relative speed of drops and line of centers also decreased. Here the average effectiveness of collisions decreased from 100% at Δ = 0 to zero at Δ = 4. There was no overflowing of water from one drop into another during ineffective collisions.

In the work by S. Gorbachev and V. Nikiforova [362] they used

drops with r = 0.5-0.75 mm. One drop was suspended on end of glass
capillary which was fastened to a long pendulum. The other was
placed on a paraffinized table. By shifting the table it was possible
to obtain a collision at a desired angle. Here the existence of
an upper critical speed was revealed. Above this speed collisions
were ineffective. In contrast to lower critical speed the
upper critical speed decreased with a growth of ϕ from 80 cm/s
at $\phi = 10°$ to 50 cm/s at $\phi = 50°$, and to 20 cm/s at $\phi = 70°$ (r =
= 0.75 mm). In this case during ineffective collisions overflowing
of part of the liquid from one drop into another occurred.

In the experiments of N. Tverskaya [363] water drops with
r = 0.5-1.5 mm flowed out of a capillary and fell on a fixed drop,
located on a thin metallic ring which was joined electrically with
capillary. The dependence of the upper ciritical speed V_{kr} on
the value of ϕ was measured. A determination was made of the value
V'_{kr} below which all collisions were effective, and V''_{kr} above which
all collisions are ineffective. In the interval from V'_{kr} to V''_{kr}
both were observed. Based on the opinion of the author, this is
caused mainly by pulsations of incident drops, thanks to which at
the time of collision they had a different form. With a relative
atmospheric humidity of 50%, r = 1.5 mm and sin $\phi = 0.6$, $V'_{kr} = 40$
and $V''_{kr} = 61$ cm/s, with sin ϕ .4 they are respectively 60 and 76 cm/s,
and with sin $\phi = 0.2$ 76 and 90 cm/s. The films of colliding drops
which were made by N. Tverskaya completely confirmed the visual
observations of Rayleigh which were mentioned on p. 147. At high
speeds and angles of impact the width and lifetime of a crosspiece
forming between drops are very small.

In the work by N. Tverskaya and I. Yudin [364] an important
observation was made. This was that the effectiveness of collisions
is increased considerably with a decrease in th dimensions of
the drops. Already with a decrease of r from 1.1 to 0.7 mm V''_{kr}
increases by several times. This is easy to explain: the smaller
the drops the less they are flattened during collisions: furthermore,
with an identical degree of deformation of drops the rate of
pressing out the air layer, according to equation (7.19), increases
rapidly with a decrease of r.

In accordance with the observations of P. Prokhorov and L. Leonov about the influence of atmospheric humidity on the process of merging of drops [365], the authors established that an increase of humidity sharply increases the effectiveness of collisions, especially at not very large ϕ. Thus, with r = 1.15 mm and sin ϕ = = 0.73 V''_{kr} = 25 cm/s at 36% and 50 cm/s at 93% humidity. With sin ϕ = 0.65 and 93% humidity V''_{kr} is so great that generally it cannot be determined.

As was already indicated, the process of collision of liquid drops essentially differs from collision of solid particles. First of all due to absence of microroughnesses and the light deformation of drops between an air layer is formed very easily. The greater the relative speed during collision, then the less the thickness of the layer and the greater the probability of the formation of a liquid crosspiece between drops due to microwaves on adjoining sections of their surface. This explains the existence of a lower critical speed and the rule of Aganin.

Further, during the collision of drops not only is the narrow zone near the surface of contact deformed, but the entire drop completely. The role of elastic deformation and elastic energy here is played by an increase in the surface of a drop and free surface energy. Transition of the latter back to kinetic energy occurs in such a way that flattened drops assume their initial spherical form and then repulse one another. If the air layer was not pierced during collision, divergence of drops goes on freely, if however a liquid bridge was formed, the result of a collision depends on the comparative value of kinetic energy of the diverging drops and the work of bursting the bridge. Therefore with sufficiently strong deformation, i.e., large relative speed during collision, it will be ineffective. Slanting collisions are less effective than central, since during them tangential component of speed, promoting the breaking of the bridge is preserved to a considerable degree.

151

The opinion expressed by certain authors [366] that for effectiveness of collision of drops it is necessary that the kinetic energy of their relative movement exceeds a specific share of their surface energy contradicts experiment, however with respect to collisions of drops with nonwettable solid particles this view is apparently correct (see below).

From what has been stated above it is clear that experimental material on the effectiveness of collisions between drops is rather crude and motley. A theory for a phenomenon, founded on laws of hydrodynamics and capillary physics, still does not exist. Meanwhile, this phenomenon fully merits the attention of theoretical physicists.

Effectiveness of Collisions of Liquid Drops with Solid Walls and Particles

The mechanism of collisions of liquid drops with solid walls occupies an intermediate position between the cases examined above: as can be seen from what is stated below, as a rule an air layer will not be formed here. The process of merging of two liquid volumes is absent but the mechanism of rebound, the transition of capillary energy into kinetic, in this case is the same as during the collision between liquid drops. During slanting effective collision, when capillary energy is insufficient for breaking a drop away from the wall, the drop usually slips along it.

In the experiments of Galilli and La Mer [367] a thin stream of isodispersed glycerine fog with $\bar{r}$ = 1.5-5 μm was knocked with a velocity V = 11-16 m/s against the upper side of a waterproofed glass plate, located at an angle of 40° to horizontal. The scattering drops in the deposit formed increased with a growth of V and r, whereas during full effectiveness of collisions it should have been opposite. Hence the authors made the conclusion that drops rebounded during the first collision and were precipitated in another place. The drops in this case did not slip along the surface. This is evident from the fact that with the presence on the plate of a deposit made from very fine condensed drops the latter were not

washed off by drops of the above-indicated size hitting against the plate. Drops with r = 15-20 μm did not rebound, but slid after the collision (in agreement with the experiments of Hartley described below).

Analogous experiments were conducted by Gillespie and Rideal [368] with a fog of dibutyl phthalate ($\bar{r}$ = 2.3 μm) on an untreated glass plate. At V < 2 m/s a deposit was not obtained. With an increase of V effectiveness of precipitation increased extraordinarily rapidly and a: 3 m/s reached 1. Then it also decreased rapidly, reached 0.1 at 4 m/s and again slowly increased. To explain these results is exceedingly difficult. Apparently they need verification.

(a)   (b)

Fig. 48. Effective (a) and ineffective (b) collisions of drops of dibutyl phthalate with a vertical glass plate.
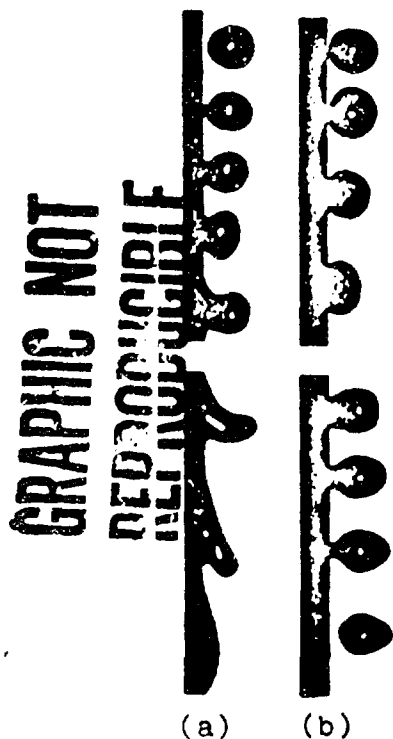
In another series of experiments drops of dibutyl phthalate (r χ 1 mm) fell vertically on a plate inclined slightly to the vertical. Films were made of them, illustrating well the mechanism of collisions (see Fig. 48, depicting effective and ineffective collision; in both cases the drops slipped along the plate downwards for a distance of 5-10 mm). Let us note that liquid will form an acute contact angle with the plate, i.e., there could not be a solid air layer here.

Further, with the help of centrifuge, the authors measured the normal force F, necessary for breaking the drops of dibutyl phthalate away from the plate and for drop with r = 6.8 μm (on surfaces these drops will form lenses with r' = 15 μm) obtained a value of F χ $5 \cdot 10^{-4}$ dynes, and for r = 1.4 μm (r' = 3 μm) $\sim 9 \cdot 10^{-6}$ dynes. These values for F are 6 orders less than the forces, calculated theoretically by the authors, necessary for breaking away of drops without their

153

deformation, since in reality the drops are deformed under the action of a detaching force with the formation of a gradually narrowing neck.

In another work by Gillespie [369] fogs, obtained by atomization of melted stearic acid with $\bar{r}$ = 1-2 μm, were precipitated on steel wire with R = 0.085 mm at rates of flow of 6-26 cm/s and an investigation was made of the distribution of deposit on surface in the function of angle θ and a frontal point. Inasmuch as the Stk number in these experiments was on an order of hundredth fractions of a unit, precipitation occurred due to coupling and electrical forces. Distribution of drops was changed significantly when thè wire was covered with silicone. This obviously indicates that the drops shifted (slipped) along the surface of the wire under the action of airflow.

In the work of Hartley and Brunskill [370] water drops of identical size (r = 25-200 μm) fell vertically with a speed of V_S on a surface located at an angle ϕ to horizontal. When the drops fell on smooth surfaces, even those waterproofed with silicone, paraffin, etc., all collisions were effective. Large drops bounced off of rough surfaces — plates, covered by layer of soot or MgO, and leaves of plants, covered by microscopic wax papillae. Thus, during the fall of drops with r < 50 μm on pea leaves all the collisions were effective, and for drops with r > 125 μm are ineffective, regardless of ϕ. In an intermediate region ∂ drops with a growth of ϕ. With a decrease of surface tension of water by means of the addition of large quantities of methanol or acetic acid, ∂ increased noticeably the the velocity of drops flying off was reduced. On plates covered with soot ∂ was still less than on leaves. Soot spots are noticeable on rebounding drops, thus indicating the presence of contact during collisions. This is also testified by the fact that a lowering of air pressure to 10 mm Hg column did not affect ∂.

Since the task of detachment of a drop lying on a surface is proportional to σr^2 and decreases rapidly with growth of contact

154

angle, and the kinetic energy of a freely falling drop is proportional
to r in a higher degree, these results are fully explicable on the
basis of the above-mentioned considerations. Hartley and Brunskill
explain the influence of microroughness of a surface by the fact
that on poorly moistened rough surfaces the contact angle of
overflowing is very great. Usually the measured static value of
this angle is probably considerably less than the instantaneous
value during collision of a drop with the surface.

Everything said above naturally pertains also to collisions of
drops with considerably larger solid particles. The opposite case
of collisions of solid particles with larger drops or with
moistened walls requires special consideration. Although this case
is of great practical interest for technology, its study up to this
time consisted mainly in the selection of moisteners, added to water
for increasing the effectiveness of collisions. The actualy mechanism
of the process has been studied very poorly.

A. Taubman and S. Nikitin a [371] allowed drops of water and
solutions of moisteners of the same magnitude ($r \approx 1$ mm) to drop
through a chamber with polydispersed dusts of quartz, talc ($r <$
< 2.5 μm), or coal ($r < 1$ μm) and determined the quantity of dust
captured by the drops. Certain solutions exhibited twice as large
a value ϑ then water, and for all three of dust. Obviously, in
order for the wettability of hydrophilic quartz by water to be
manifested a certain time is necessary, and during instantaneous
contact quartz is moistened poorly. No correlation was detected
between static surface tension of the solutions and ϑ, however, ϑ
increases with a decrease of dynamic surface tension (i.e., measured
on the freshly formed surface of liquid). It is interesting that
certain surface-active substances waterproof the surface of particles
of dust and decrease ϑ.

In the opinion of the authors, molecule of a surface-active
substance at the time of collision migrate along the surface of
a particle and make it hydrophilic or hydropholic. This is possible,

155

however, only in the case when the speed of migration is greater than the relative speed of drop and the particle at the time of collision.

P. Yermilov [372] investigated influence of moisteners on the effectiveness of trapping PbO ($r \approx 0.3$ µm) in a direct-flow cyclone with reflux walls. At high rates of flow U at the entrance into the cyclone (15 m/s) ϑ is large (0.95) even during spraying with water and is increased comparatively little (up to 0.97-0.98) with the addition of moisteners. With a decrease of U, naturally ϑ drops, but the effect of the addition of moisteners increases: at U = 1 m/s $\vartheta \approx 0$ for water and can be brought down to 0.9 by the appropriate selection of moisteners. P. Vermilov also did not detect a relationship between effect of addition of moisteners and static surface tension of solutions.

In the works of M. Pozin et al. [373] the influence is studed of the wettability of dusts on their absorption during bubbling through water and it is shown that particles of hydrophobic pyrite and hydrophilic barite with $r \overline{>} 2.5$ µm are absorbed approximately equally, and at $r \overline{<} 2.5$ µm particles of pyrite are absorbed considerably worse. Addition of a moistener hardly changes ϑ for barite and noticeably increases absorption of pyrite.

In the experiments of McCully et al. [374] a thin stream of aerosol made of glass beads with $r = 2.5-25$ µm struck against a suspended water drop. On photographs it is clearly evident that some of the beads rebounded from the drop. When the beads were waterproofed the percentage of ineffective collisions increased considerably and nonrebounding beads remained on surface of the drop, whereas untreated beads penetrated into the depths of it.

From what has been stated above it follows that the influence of wettability of particles starts to appear onl during collisions with little kinetic energy. A theory of effectiveness of collisions of drops with nonwettable particles has been proposed by Pemberton [375]. The author examines an absolutely nonwettable spherical

156

particle, on which water forms a contact angle $\theta = 180°$. As already was indicated, the instantaneous value of θ can be close to this value. It is easy to show that work of submersion of such particle is equal to $\frac{8}{3}\pi r^2 \sigma$. In the opinion of author, the collision of such a particle with a large water drop will be effective when the kinetic energy normal to the surface of the drop of the component of relative speed V_{rn} of the drop and particle exceeds the task of submersion. After using a computer to calculate value V_{rn} for potential flow around a sphere by particles, the author constructed curves (θ, Stk) for the precipitation of nonwettable particles. From this theory the influence of dynamic surface tension of a liquid on effectiveness of collisions clearly emanates, since at the time of collision the surface of a liquid is subjected to very rapid expansion.

Obviously the energy of full or partial submersion of a particle in liquid and the curve (θ, Stk) can be calculated analogously for any value of contact angle of overflow θ: it is necessary only to consider that the angle θ itself increases with relative speed during collision.

It is necessary to note that, although application of moisteners also makes it possible to lower the concentration of dust in mines during wet drilling, a radical solution of this problem is possible only with the complete elimination of air getting into blast hole [376, 377].

Footnotes

[1]$K_0 = 8\pi r D$. Usually in works on coagulation of aerosols they apply the Keningem formula for mobility, in this case

$$K_0 = \frac{4kT}{3\eta}\left(1 + A\frac{l}{r}\right). \tag{7.3}$$

[2]In "Mechanics of Aerosols," p. 271, the solution of this equation with constant K is erroneously ascribed to

157

Smolukhovskiy. In reality it was obtained by Schumann [296]. It can be written in the following simple form:

$$n(m) = \frac{ce^{-m/\bar{m}}}{(\bar{m})^2} \qquad (7.4)$$

where c — concentration by weight of aerosol, $\bar{m}$ — average mass of particles at moment t

$$\bar{m} = \frac{c}{n} = \frac{c(1 + 0.5Kn_0 t)}{n_0} \approx \frac{Kct}{2}. \qquad (7.5)$$

Schumann considered that his formula is applicable at any initial distribution of particle sizes, however, he was not able to give strict proof of this assumption.

^{3}On p. 282 and 283 of "Mechanics of Aerosols," where the theory of polarizing coagulation is expounded, the following corrections should be introduced. In formula (52.8) it is necessary to correct $5 \cdot 10^{-4}$ for $5 \cdot 10^{-5}$. On p. 282, eighth line from the bottom, it is necessary to correct 10^4-10^6 for 10^3-10^5, and on the sixth line 0.1-10 for 0.01-1. In formula (52.10) it is necessary to drop the index 1/3 at α_1.

^{4}In "Mechanics of Aerosols" on p. 289 it is incorrectly stated that sound waves which are discernible by ear do not coagulate aerosols. In reality for this purpose in practice they do not use ultrasonic, but high audio frequencies (1-10 kHz).

^{5}In "Mechanics of Aerosols" [334] this formula is written with an error.

^{6}6β stands in Gillespie's version of this formula.

158

C H A P T E R 8

TRANSITION OF POWDERS INTO AN AEROSOL

Adhesion Between Solid Particles

For the theory of breakaway and transfer of particles by an air
stream the basic and most difficult problem is that of the magnitude
of force of adhesion between contiguous solids. At present this
question still cannot be solved theoretically, mainly because the
microgeometry of surfaces in the zone of their contact is unknown.
For the same reason it is impossible to extrapolate the data of B.
Deryagin and I. Abrikosova [378] about the value of molecular forces
between noncontiguous bodies to h = 0. Experimental data, obtained
with small (on an order of 1 mm) quartz and glass beads with a
freshly fused surface unfortunately are very contradictory. Under
"pure" conditions for the experiment, i.e.,.in a vacuum or in com-
pletely dry air, in other words, in the absence of an adsorption
layer of moisture on the surface of the beads, some authors (Stone
[379], How et al. [380], McFarlane and Taybor [381]) found that the
force of adhesion is equal to zero or is very small (on the order of
hundredth fractions of a dyne), others (Bradley [382]) detected
adhesion in several tens of dynes, and still others (Harper [383],
Tomlinson [384]) indicate that adhesion sometimes is equal to zero,
and sometimes is quite large. Here almost all the authors, on the
basis of specially conducted experiments, came to the conclusion that
electrical charges on the beads do not noticeably influence adhesion.

It is possible that the cause of these disagreements is the
presence of dust motes which are difficult to remove on the surface

159

of the beads, and this prevents their contact. This is indicated by the fact that adhesion between beads which remain in the air for a certain time is usually equal to zero. If this is so, then it would follow to consider as most reliable the measurements of Bradley, according to which the force of adhesion between quartz beads ($r =$ $= 0.2$-0.5 mm) is expressed by the formula

$$F_{ad} \quad 4\pi\sigma \frac{r_1 r_2}{r_1 + r_2}$$ (8.1)

in which $\sigma = 35$ dynes/cm. However, according to the unique experimental data on adhesion of small particles [385], F_{ad} is 2 orders less than according to Bradley.
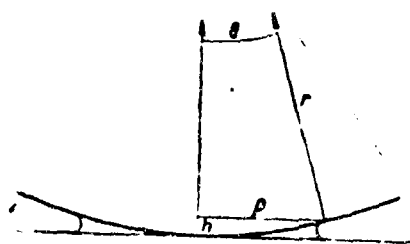
Fig. 49. Adhesion between a plane and sphere in the presence of a liquid layer.

In humid air adhesion is always considerable. According to McFarlane and Taybor [381], with an increase of atmospheric humidity from 80 to 90% the force of adhesion between a glass plate and glass beads increases from ~ 0 to $4\pi\sigma r$ (σ — surface tension of water), i.e., up to a value of adhesion, induced by negative pressure in a water layer.[1] On plates with a rough surface (and probably in the presence of dust motes) such a magnitude of adhesion is attained only in the case when the thickness of the water film is greater than the height of unevenness (or diameter of dust motes).

It is necessary to note that beads with a freshly used surface are a sample of bodies, in which the microroughness of the surface is apparently very small and the radii of curvature entering into formulas (8.2) and (8.3) are close to the radii of the beads themselves. In ordinary dust particles these radii are considerably less than the semidiameter of the particle and forces of adhesion should increase strongly during capillary condensation of moisture close to points of contact of particles.

160

Larsen [386], with the help of a centrifuge, measured adhesion between glass beads with r = 67 and 84 μm and a plate in the presence of a liquid layer and also confirmed formula (8.2). Further he derived an expression for adhesion between beads and a cylinder in the presence of a layer

$$F = 2\pi r \left\{ \frac{\rho/r}{[(\rho/r)^2 + (R/r)^2]^{1/2}} + \frac{1}{[(\rho/r)^2 + 1]^{1/2}} \right\} (1 + r/R). \qquad (8.4)$$

where R — radius of cylinder, ρ — radius of layer. This expression also conforms well with experiment. In experiments with oil lubricated vibrating glass filaments with R = 128 and 420 μm and beads with r = 55 μm, Larsen found that breakdown of the beads begins when the maximum inertial force $ma(2\pi\nu)^2$ (a — amplitude, ν — frequency of oscillations, m — mass of bead) exceeds the force of adhesion calculated by the formula (8.4), and is finished in approximately 1 minute.

Blow Off of Particles from Walls by an Air Flow

In experiments on blow off of beads (r = 8 μm) from a glass filament (R = 400 μm) without lubrication, Larsen detected a considerable (on an order) increase in adhesion with an increase of atmospheric humidity. He also investigated the shifting of beads located on oil lubricated filaments under the impact of air flow. Unfortunately, in the article by Larsen there is a number of gaps which prevent a correct evaluation of the results of these interesting experiments. Numerical data characterizing the coincidence of theory and experiment are not given, it is not clear how the hydrodynamic forces acting on the beads were calculated, etc.

The question vague remains as to what starts the breaking away of particles from walls by an air flow: are they detached directly under the impact of hydrodynamic force perpendicular to the wall (lifting), or at first do they start to roll or slip along the wall under the impact of tangential hydrodynamic force and ricochet, having run into other particles of unevenness on the surface. An exact calculation of [forces] having an effect in tangential and normal directions on particles of various form lying on the wall and recessed or raised above the laminar underlayer is very difficult.

For fairly large bodies, projecting far beyond the laminar underlayer
— cubes and spheres located in various order on the bottom of a
water tray — these forces were measured at large Re by V. Goncharov
[387], who showed that the greater the lifting force (in accordance
with the theorem of Zhukov), then the more complete is flow around
a body by flow in a vertical plane. Therefore hydrodynamic forces
decrease with a decrease in the distance between bodies: on bodies,
raised somewhat above adjoining ones, considerably greater forces act
on these than on the latter, etc. Unfortunately, numerical data
which could have been used for calculations are not given in the book
by V. Goncharov.

It is still more difficult to calculate the force necessary for
shifting small particles along a surface. For macrobodies this is the
well-known force of static friction, but already for particles with
r < 0.5 mm the angle of friction increases noticeably with a decrease
r [388]. Simultaneously there is an increase in the scattering of
values for this angle, measured for several particles of identical
size.

This is explained in the following way. Frictional force, which
in essence is a tangential force of adhesion, is proportional
(similarly to normal force of adhesion) to the area of true contact
between rubbing bodies. This area, the value of which is conditioned
mainly by plastic deformation of microprojections in points of con-
tact, in the case of macrobodies as pointed out by Bowden and Taybor
[389] is approximately proportional to normal pressing force F_N, on
which is also based the Coulomb law of friction. With a decrease in
particle dimensions F_N (force of gravity of particle) also decreases
very rapidly and all the more noticeable becomes influence of the
normal force of adhesion, also caused by deformation in the zone of
contact. In this case the area of contact, and consequently
frictional force, is proportional to the sum of both normal forces,
which was first indicated by B. Deryagin and V. Lazarev [390]. Since
the force of adhesion of particles is proportional to $\sim r$, coefficient
(and angle) of friction increase with a decrease of r.

Further, in macrobodies the differences in microroughness in zones of contact at identical F_N are more or less averaged. In the case of small particles the normal force of adhesion, and consequently the area of contact, depend to a high degree on the microgeometry of surfaces at points of contact, and therefore change very strongly from particle to particle, from one orientation of particle to another, and from one point of the wall to another. This explains why the results of all experiments on blowing away of dust are expressed by curves: the rate of flow is the % blow off particles, where the speed corresponding to complete blow off is several times greater than the speed at the beginning blowing, even with isodispersed dust [351]. The same scattering is obtained during measurement of angle of friction of dust motes. This circumstance extremely hampers the experimental study of the process blow off of dust from walls.

Cremer and Conrad [391] bypassed this difficulty, measuring the angle of friction θ not of separate particles, but of an uniform layer of different thickness of a more or less isodipersed dust which was deposited on the surface with the help of a sieve. Moreover in successful experiments the entire layer slipped as one whole, i.e., an averaged value of θ was measured.

According to what was stated above the condition of sliding is expressed by the equation

$$Mg \sin \theta = \mu\, Mg \cos \theta + H. \qquad (8.5)$$

where M — mass of dust in 1 cm^2 of layer, μ — macroscopic coefficient of friction, H — tangential force of adhesion, calculated for 1 cm^2. Placing their results in the system of coordinates (Mg sin θ, Mg cos θ), Cremer and Conrad obtained for particles of dolomite and magnesite with r > 150 μm a straight line passing through the beginning of the coordinates, i.e., in this case H ≈ 0. For r < 150 μm straight lines were also obtained, but they intersected the axis of ordinates at a point corresponding obviously to the value H. The experiments showed that the value Hr = K for the given dust (r = 30-150 μm and surface is constant and is equal to 1.4 dynes/cm for magnesite dust

163

n glass, 1.5 for iron, and 1.25 for magnesite. After heat treatment
of dust H decreases by several times.

Assuming that particles of dust in the first layer are located
close to one another and in staggered order, we find that 1 cm^2 of
layer contains $1/4r^2$ particles. This means that acting on each is a
tangential force of adhesion $F_{ad} = 4r^2 H \approx 5r$ dynes, i.e., this
force, similar to a normal force of adhesion, is approximately
proportional to r.^{2} On the other hand, Patat and Schmid [393] using
the same method found for carborundum dust on a steel plate $Hr^2 =$
$=$ const and for Al_2O_3 dust on the same plate $Hr^{0.7} =$ const, i.e., in
the first case F_{ad} does not depend on r (which is clearly incorrect),
and in the second — proportional to $r^{1.3}$.

Batel [394] found that after heat treatment of glass plate and
quartz dust in a vacuum at 300° H = 0. In experiments by Patat and
Schmid with carborundum dust on steel under these same conditions H
has a noticeable value. There is no doubt that a considerable part
of the force F_{ad} is caused by capillary action of the adsorbed water
film, as also in the case of normal adhesional force.

All the authors who used the method of Cremer and Conrad indicate
that the macroscopic coefficient of friction u increases noticeably
with a decrease of r, i.e., separation of the coefficient of friction
into macroscopic and adhesion components by this method does not
succeed. From the abundant experimental material collected by Patat
and Schmid it is possible to make only one conclusion — this was
about the great complexity of the phenomenon being studied.

We see that at present there are no theoretical calculations or
even general empirical formulas for process of breaking away of
particles by an air flow. At first glance it can appear that for this
purpose it is possible to use data about the break away and transfer
of particles by water flows, however, as Bagnold stresses [395], the
differences between these two cases are too deep for this.

According to the observations of Rumpf [396] the greater the
speed of flow during its formation the more difficult it is to blow

off a deposit of limestone dust from a vertical metallic plate, located parallel to the flow. The author explains this by the high speed of collision of particles with the plate. It is possible that here a plastic flattening of particles takes place and an increase in the area of contact. It is also possible that after collision the particles roll along the surface until they reach a potential well, i.e., a position with a great force of adhesion. The greater the velocity of a particle, thus the deeper this depression has to be, and the more durably the particle adheres to the surface.

The relationship between particle dimension and critical speed of flow has been investigated by a number of authors. A. Klimanov [397] found that for fractions of coal dust with $r = 37-52$ μm $U_{kr} = 6$ m/s, for $r = 21-37$ μm — 7 m/s, and for 0-21 μm — 10 m/s. According to Jordan [351] for blowing off (in a period of 2 s) of 50% of a deposit of quartz dust by a thin air stream perpendicular to the plate, it is required at $r = 3.5$ μm that $U = 45$ m/s, at 2 μm 95 m/s, and at 1 μm 145 m/s. These data confirm the position expressed above that for particles with $r < 50-100$ μm U_{kr} increases with a decrease of r. The data of Blomfield and Dallavalle [398], who found the opposite relationship for quartz dust beginning with $r = 5$ μm, are absolutely erroneous.

In the experiments by Dawes [399] a layer of very polydispersed powder (limestone, chalk, gypsum, shale, and light ashes with $\bar{r} = 16-40$ μm) with a thickness of 6 mm and area of 5×17 cm was deposited through a sieve on emery paper No 0, located on the bottom of a wind tunnel with a height of 7.5 cm, through which air was then blown. At $\bar{U} = 15-20$ m/s carrying away of particles (erosion) began similar to that studied by Bagnold [400]. The rate of erosion was proportional to $\bar{U}^3$ and depended to a great degree on the properties of the powder. Of the various methods for investigating the mechanical properties of powders the most successful turned out to be determination of their "cohesion" H, i.e., the force necessary for breaking a column of noncompressed powder, calculated per 1 cm^3. Erosion rate of powders with $H < 200$ dynes/cm^2 is 4-6 times greater than with $H \gtrsim 300$ and 10-15 times greater than with $H \gtrsim 700$. Value H increases with a decrease in average particle dimension and with an

increase in polydispersity of the powder, especially in the presence
of a very small fraction, and is more or less similar with the angle
of natural slope. During an investigation of atomization properties
of powders by a method similar to that of Andreasen [401], it turned
out that atomization properties in almost all cases drop with increase
of H. Relationship between H and radius of particles can be explained
successfully on the basis of the assumption that adhesion between
particles is proportional to their radius (see above).

At speeds of flow exceeding the critical value U'_{kr}, there occurs
(in fractions of a second) solid blowing away of the layer, starting
from its front edge. For different powders U'_{kr} varied from 28 to 40
m./s (it maximum value in these experiments). On a polished plate
U'_{kr} is 30% lower than on emery paper. Vibration of the sublayer also
strongly lowers U'_{kr}, without affecting the speed of erosion. Further,
U'_{kr} depends strongly on angle of slope at the front edge of the layer
– the smaller this angle, the greater U'_{kr}.

These observations, and also measurement of air pressure in
various points of the layer and theoretical calculations of the
author showed that solid blowing off is caused by an aerodynamic
force acting on the front edge of the layer. Dawes considered that
blowing off occurs when this force exceeds frictional force H_t between
the layer and sublayer. This force was determined in special experi-
ments. Here it turned out, in agreement with experiments of Cremer
and Conrad, that $H_t = H_0 + \mu p$, where p – pressing pressure. μ and H_0
– constants. However, from the tables given by the author it is clear
that the degree of correlation between values U'_{kr} and H_t for one and
the same powder is quite insignificant and the mechanism of the pro-
cess is apparently more complex.

In the opinion of author, erosion also takes place analogously.
When the tangential aerodynamic force acting on the surface of the
layer exceeds the frictional force of powder against powder, some
part of the layer shifts and is carried away. This hypothesis is
poorly confirmed by experimental data; apparently, as in the case of
thin powders, erosion takes place by the mechanism described by
Bagnold and Chepil [402].

166

The phenomena discussed here are of great interest for the theory of pneumatic transport of loose materials. This important technical process has been dealt with in a great number of works of an applied nature, however its physical bases have still been insufficiently studied.

Usually during pneumatic transport in horizontal pipes a two-phase flow is observed: along the bottom of the pipe a solid layer of material moves comparatively slowly. The speed of its movement is determined by the tangentail aerodynamic force acting on the surface of the layer and the frictional force against the bottom of the pipe. In the case of coarsely-dispersed material a considerable part of it moves by jumps, similar to the movement of natural sands. In the upper part of the pipe the particles are found in an aerosol state.[3] Small and soft particles in rather wide pipes rarely comparatively collide with the walls and their average longitudinal speed $\bar{V}_t$ differs little from the speed of air $\bar{U}$. Large hard particles in narrow pipes move by zigzags from one wall to another (see Fig. 47) and their $\bar{V}_t$ can be considerably less than $\bar{U}$. The smaller $\bar{U}$ is, the heavier the particles and the higher the concentration of transported material,

then the greater the share of it which moves along the bottom of the pipe. Since in round vertical pipes usually the flow more or less twists and material is thrown toward the walls by centrifugal force, then in this case also similar phenomena are observed.

It follows from what has been said that depending on conditions the ratio $\bar{V}_t/\bar{U}$ can be changed in very wide limits, as this is also found in a number of works. Unfortunately, only in the above mentioned (p. 142) work by Adam is such an important factor as hardness of particles considered. The observed regularities, decrease of the ratio $\bar{V}_t/\bar{U}$ with growth of particle dimensions and with a decrease in the diameter of the pipe, are well explained by the above considerations.

Pneumatic and Sound Atomization of Powdery Bodies

One of the most important and still unsolved problems in the laboratory investigation of aerosols is the thorough (aggregate-free)

atomization of powders, i.e., their conversion into an aerosol with nonaggregated particles. Thorough atomization is required mainly in two cases: in the obtaining of model aerosols with desirable properties and during laboratory reproduction of industrial aerosols with solid particles. In first case, by means of crushing and elutriation it is possible to obtain a powder with required average size and distribution of particle sizes; in the second case the powder is obtained ready for use from dust-collecting equipment. In the first case thorough atomization is required. In the second sometimes it is desirable to obtain the same degree of aggregation which was possessed by the initial aerosol, but this is easy to achieve by means of partial coagulation of a completely disaggregated aerosol.

For coarse powders (r > 20 μm) thorough atomization is not difficult to carry out with the help of an air stream, but with a decrease of particle dimensions difficulties increase. This can be seen, for example, from that fact that blowing particles with r < 10 μm out of an elutriator occurs extraordinarily slowly even in the case when such particles are introduced into the elutriator from without [404]: obviously they form aggregates instantly.

The poor atomization property of thin powders is easily explained; in the case of an aggregate moving in a gradient flow, the difference of speeds of flow in two points, separated by distance 2r, is equal to $2r\Gamma$ (Γ – gradient of speed of flow) and the force striving to sever two adhering particles is equal to

$$F_u \approx 6\pi\eta r \cdot 2r\Gamma = 12\pi\eta r^2 \Gamma. \tag{8.6}$$

The force of adhesion, as we have seen above, in first approximation is proportional to r. Certainly in addition to dimension of particles a great role is served here by their form, mechanical properties (plasticity), and density of packing, i.e., number of contacts of a particle with neighboring particles. Therefore it is especially difficult to atomize polydispersed powders, in which the density of packing is considerably greater than in isodispersed powders. A decrease in density of packing, i.e., bulk density of powder, for example under the impact of sound waves, therefore

168

essentially facilitates atomization.

According to the experiments of Davies et al. [405] a noticeable destruction of aggregates of coal dust with r on an order of 1 μm occurred when they were blown with a speed $\bar{U}$ = 170 m/s through a flat slot with a width of 2h = 0.08 mm. Since the average gradient of speed in a flat slot is equal to $(3/2)\bar{U}/h$, then according to the formula (8.6) for particles with r = 1 μm the detaching force F_M equaled $3.6\cdot 10^4$ dynes. Unique experimental data about forces of adhesion between particles of this order of magnitude, obtained by Beischer [392], lead to the formula (see p. 164)

$$F_{ad} \approx 2r.\qquad\qquad(8.7)$$

from which at r = 1 μm F_{ad} = $2\cdot 10^{-4}$ dynes, i.e., a value of the same order a F_M.

Based on this principle Eadie and Payne [406] designed on apparatus for the thorough atomization of powders in which powder, coarsely atomized by an air jet, is passed under a pressure of several (up to 30) atmospheres through a ring-shaped slot with a width of 10-250 μm. By means of air sedimentometric analysis of the aerosol obtained the authors showed that with an increase of pressure (i.e., speed of flow) the dimension of particles coming out of the slot drops only to a certain limit, and then remains constants. In the opinion of the authors, this fact indicates full disaggregation of particles, however the authors apparently did not make a micro-scopic examination and in their short article there is too little data to back up the correctness of this conclusion. It is possible, for example, to assume that in these experiments a critical speed of flow was attained which no longer increased with an increase of pressure. It is necessary, however, to recognize that disaggregation in a gradient flow is apparently the most promising path to the thorough atomization of powders. '

Another possible way is the application of oscillations. Oscillations of audio frequencies produce a double action on powders — they pack them at small amplitudes and loosen at large [407].

Loosening is accompanied by considerable reduction in cohesion in powders, by an increase of consistency, decrease in angle of slope etc. As Chin-Young Wen and Simmons showed [408], powder made of glass beads with $r = 15$ μm can be atomized with the help of oscillations of audio frequency. However, a more thorough method of atomization consists of the simultaneous action of oscillations and blowing of air through a powder.

Morse [409] worked with highly cohesive, i.e., very poorly atomized, powders of gypsum marble ($\bar{r} \approx 1$ μm), etc. During passage of air through a layer of such powder it was not loosened, and the air passed through it in the form of separate large bubbles. However, with the creation of a sound field with a frequency of 20–670 Hz and of sufficient intensity (> 110 dB) under the layer, the layer was expaned strongly (in the case of gypsum by one and a half times) and greatly improved fluidization (pseudoliquifaction) of powder occurred. In such a state with an increase of air speed a disaggregated aerosol should apparently be blown out of the powder.

In certain case it is possible to increase the atomization properties of powders by way of an insignificant addition of another highly dispersed powder   Such, for example, is the action of addition of soot to limestone dust [410]. Addition oxide magnesium is very effective. Based on the experiments of Craik and Miller [411], the addition of 1% MgO with $\bar{r} \approx 0.03$ μm to powders of starch and sugar and Nacl with $r \approx 5$ μm considerably decreases the angle of repose and, consequently, cohesion in these powders. Apparently particles MgC and soot serve the same role here as dust motes in the experiments on adhesion between beads mentioned on p. 159: they decrease the area of contact between particles of the powder.

The addition of a small amount of moisture, considerably increasing adhesion between particles, understandably produces an opposite effect. Based on the experiments of Parker and Stevens [412], with the addition of several hundredth fractions of a percent of water to powder made from glass beads with $r \approx 0.15$ mm fluidization of the powder is sharply impaired.

During the last few years very many articles on fluidization have appeared. We will dwell only on two problems.

One of the interesting properties of fluidized powders which is already utilized in technology [413] is the ability of their flow, similar to a liquid, through pipes which are slightly inclined to the horizontal. Initially a flowing system is completely homogeneous, but at a certain distance begins to break up into phases which are usual in pneumatic transport [405].
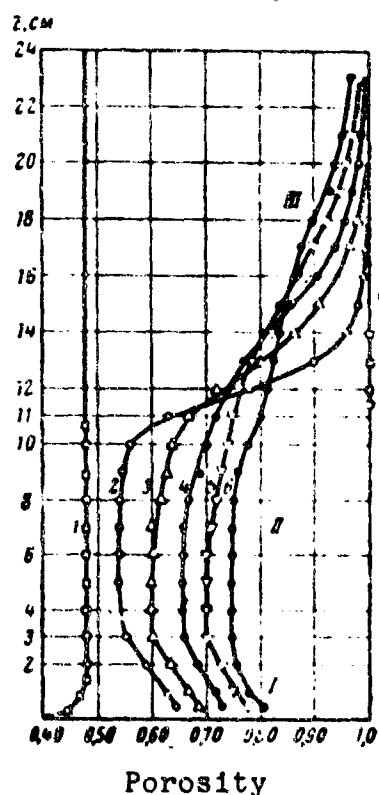
Fig. 50. Fluidization of glass beads at different speeds of air flow: 1. Beginning of fluidization; 2. U = 22.7 cm/s; 3. U = 40.7 cm/s; 4. U = 59.6 cm/s; 5. U = 78.8 cm/s; 6. U = 98.4 cm/s

Porosity

It is very difficult to determine visually what occurs in a column with fluidized powder. A great step forward in the investigation of the fluidization process was the introduction of condensing method. In different points of the system a miniature condensor is introduced and based on its capacity they determine the porosity of the powder at a given point. Figure 50 gives result of an investigation by this method of fluidization of powder made from glass beads with r ≈ 100 μm at various speeds of flow of air [414]. As can be seen from the figure, at the bottom of column there is a small zone with increased porosity, corresponding to the yield of bubbles of air

171

from the supporting system; then there is a zone of fluidized powder, the porosity of which increases with an increase of U, and, finally, on aerosol zone. Drop in concentration of the aerosol with increase of z is explained by the fact that larger particles are discarded at a certain height, but then drop back. This phenomenon was studied thoroughly by Zenz and Weil [415], and the theoretical calculations of the authors satisfactorily agree with data from experiment.

Footnotes

[1]We will examine a layer of liquid, found between a contiguous sphere and a plane (Fig. 49). With a small value for the ratio of radius of layer ρ to radius of sphere r h = r(1 − cos θ) ≈ 1/2rθ². If both surfaces are moistened by liquid, the radius of curvature of the meniscus has a value ∿h/2, based on the Laplace formula negative pressure in the layer equals 2 σ/h, and cohesive force

$$F \quad (2\sigma/h)\pi\rho^2 \approx \pi r\sigma. \qquad (8.2)$$

For two equal contiguous spheres h is twice as large and

$$F = 2\pi r\sigma. \qquad (8.3)$$

McFarlane and Taybor confirmed this formula by direct measurements of force of adherence between moistened beads.

[2]Based on the experiments of Beischer [392] the force of adhesion between particles of Fe_2O_3 with r = 0.25 μm is equal to ∿5.10⁻⁵ dynes, i.e., $F_{ad} \approx 2r$; besides, adhesion between two particles should be, according to theory, half as much as adhesion between a particle and a flat wall. Thus we obtain confirmation of the position that forces of adhesion and friction for small particles are close to one another.

[3]According to the observations of Mehta et al. [403], glass beads with r = 48 μm move at U = 5-25 m/s mainly by jumps, but beads with r = 18 μm — in the form of an aerosol.

THE MOST IMPORTANT DESIGNATIONS

B — particle mobility

D — diffusion coefficient of aerosol particles

D_g — diffusion coefficient of vapor

D_t — coefficient of turbulent diffusion

E — field intensity

$\ni$ — effectiveness of filter, intake of sample, etc.

F — force

F_M — resistance of medium

F_T — thermophoretic force

F_{ad} — adhesion force

Φ — number of particles, settling or passing over a surface in 1 s; productivity of a point source

Φ' — number of particles, settling in 1 s per unit of length of a cylinder; productivity of linear source (per 1 cm of length)

G_g — velocity of gas molecules

Γ — gradient (of velocity, temperature, etc.)

Γ_a — temperature gradient in gas

H — tension (mechanical)

I — current intensity; number of particles, settling on 1 cm^2 in 1 s

K — coagulation constant

L — length

P — dipole moment

Π — potential difference

Pe — Peclet diffusion number

Q — charge of collector, large drop

R_g — gas constant

R — radius of sphere, cylinder, large drop

Re — Reynolds number for particle

Re_f — Reynolds number for flow

Sc = ν/D — Schmidt number (Prandtl diffusion number)

Sh — Sherwood number (Nusselt diffusion number)

Stk — Stokes number

Stk_{kr} — critical Stokes number

T — absolute temperature

U — rate of flow og gas

U^* — friction rate

U_{kr} — critical flow rate

V — particle velocity

V_{kr} — critical particle velocity

V_t — tangential particle velocity

V_n — normal particle velocity

V_r — relative velocity of particle and medium

V_S — settling rate of one particle

V_S' — settling rate of a particles system

V_T — rate of thermophoresis

c — concentration by weight of aerosol, vapor

$c_v \; c_p$ — specific heat capacity of gas

c_S — speed of sound

ϑ — coefficient of settling, capture

$f(r)$ — computing distribution function of particle radii

g — acceleration due to gravity

k — Boltzmann constant

ℓ — average length of free path of gas molecules

ℓ_B — average apparent length of free path of aerosol particles

ℓ_1 — inertia range of particles

m — particle mass

m_g — mass of gas molecule

n — number of particles in 1 cm^3

n_g — number of gas molecules in 1 cm^3

p — pressure

q — particle charge

r — particle radius

r_S — sedimentational radius

r_{pr} — projected radius

r_m — median radius

t — time

t_p — period of oscillations

α — coefficient of absorption (sound), coefficient of accommodation

γ — particle density

γ_g — density of gas

ε — elementary charge; turbulent energy, scattering in 1 s 1 g of medium (dimension of cm^2/s^3)

ε_k — dielectric constant

η — viscosity of medium

θ — vectorial angle

κ — form factor

κ_1 — thermal conductivity of particle

κ_a — thermal conductivity of gas

ν — kinematic viscosity

ν_t — turbulent viscosity

ρ — distance from center, axis

σ — surface tension

τ — relaxation time

ϕ — space factor, volume concentration

χ — thermal conductivity

ψ — coefficient of drag

ω — angular frequency

Ω — energy, work

REFERENCES[1]

1. B. Vonnegut. Chem. Rev., 1949, 44, 277.
2. P. Nolan, C. O'Toole. Geofis. pura e appl., 1969, 42, 117.
3. C. Junge. J. Meteorol., 1956, 12, 13.
4. G. Herdan. Small Particles Statistics. Elsevier, 1953.
5. Physics of Particle Size Analysis, Brit. J. Appl. Phys., Suppl., № 3, 1954.
6. H. Heywood. Chem. and Ind., 1937, 56, 149.

7. I. Artemov. Dokl. AN SSSR, 1945, 50, 289; N. Fuks. Mekhanika aerozoley (Mechanics of Aerosols). str. 284.

8. J. Dallavalle, C. Orr. Physics of Particle Size Analysis, Brit. J. Appl. Phys., Suppl., № 3, 1954, 198.
9. H. Tsien. J. Aeronaut. Soc., 1946, 13, 653.
10. M. Krzywoblowski. Acta phys. austriaca, 1955, 9. 216
11. J. Mattauch. Z. Phys., 1925, 32, 439.
12. K. Schmitt. Z. Naturforsch., 1959, 14a, 870.

13. P. Epstein. Phys. Rev., 1924, 23, 710; N. Fuks. Mekhanika aerozoley (Mechanics of Aerosols). str. 32.

14. N. Gokhale, K. Gatha. Indian J. Phys., 1956, 32, 521
15. H. Faxen. Arkiv Mat Astr Fys., 1923, 17, № 27.
16. L. Bacon. J. Franklin Inst., 1936, 221, 251.

17. A. Peterlin, H. Stuart. Z. Phys., 1939, 112, 1; N. Fuks. Mekhanika aerozoley (Mechanics of Aerosols). str. 47.

18. B. Trevelian, S. Mason. J. Colloid Sci., 1951, 6, 354.
19. T. Sharkey Brit. J. Appl Phys., 1956, 7, 52.
20. R. Manley, S. Mason. J. Colloid Sci. 1952, 7, 354
21. T. Garstang. Proc. Roy. Soc., 1933 142A, 491.
22. H. Tollert. Chem.-Ingr-Techn., 1954, 26, 141.
23. A. Cruize. Engineering. 1957, 183, 366
24. Physics of Particle Size Analysis, Brit J Appl Phys., Suppl., № 3, 1954, 93.

25. V. Timbrell. Tam zhe (Ibid). pp. 93, 94.

26. K. Sawyer, W. Walton. J. Scient. Instrum., 1950, 27, 272; H. Fuks Mekhanika aerozoley (Mechanics of Aerosols). str. 125.

27. Physics of Particle Size Analysis, Brit. J. Appl. Phys., Suppl., No 3, 1954, 90, 93-95.

28. V. Timbrell Tam zhe (Ibid). pp. 12, 85.

29. N. Fuks. Mekhanika aerozoley (Mechanics of Aerosols).
str. 59.

30. G. E v e s o n, E. H a l l, S. W a r d. Brit. J. Appl. Phys., 1959, 10, 43.
31. H. F a x e n. Z. angew. Math. und Mech., 1927, 7, 79.
32. S. G u r e l, S. W a r d, R. W h i t m o r e. Brit. J. Appl. Phys.,
    1955, 6, 63.
33. K. C h o w d h u r y, W. F r i t z. Chem. Engng. Sci., 1959, 11, 92.
34. J. L u d w i g. Chem. Ztg., 195.., 79, 774.
35. P. V a n d e r L e e d e n et al. A.pl. Sci. Res., 1955, 5A, 338.

36. J. Hinze. Tam zhe (Ibid). 1949, 1A, 18.

37. Handbuch der Experimentalphyskik, 4(2). Leipzig, 1932, S. 307.

38. E. Cunningham. Proc. Roy. Soc., 1910, 83A, 357; N. Fuks.
Mekhanika aerozoley (Mechanics of Aerosols). str. 60.

39. J. H a p p e l. A. I. Ch. E. Journal, 1958, 4, 197.
40. S. K u w o b a r a. J. Phys. Soc. Japan, 1959, 14, 527.
41. H. B r i n k m a n. Appl. Sci. Res., 1947, 1A, 27.
42. P. H a w x l e y. Physics of Particle Size Analysis, Brit. J. Appl. Phys.,
    Suppl., № 3, 1954, 1.
43. H. V e r s c h o o r. Appl. Sci. Res., 1951, 2A, 155.
44. H. N o d a. Bull. Chem. Soc. Japan, 1957, 30, 195.
45 P. C h e n g, H. S c h a c h m a n. J. Polymer Sci., 1955, 16, 19.
46. T. H a n r a t t y, A. B a n d u k w a l a. A. I. Ch. E. Journal, 1957, 3,
    293.
47. R. W h i t m o r e. Brit. J. Appl. Phys., 1955, 6, 239.

48. N. Fuks. Mekhanika aerozoley (Mechanics Aerosols). str. 60.

49. R. W i l s o n. Austral. J. Appl. Sci., 1952, 3, 252.
50. H. S t r a u b e l. Z. Aerosolforsch. Therap., 1955, 4, 385.
51. R. W u e r k e r, H. S h e l t o n, R. L a n g m u i r. J. Apel. Phys.,
    1959, 30, 312.
52. L. W a l d m a n n. Z. Naturforsch., 1959, 14a, 589.

53. S. Bakanov, B. Deryagin. Kolloidn. zh., 1959, 21, 377.

54. A. E i n s t e i n. Z. Phys., 1924, 27, 1.
55. W. C a w o o d. Trans. Faraday Soc., 1936, 32, 1068.

56. P. Epstein. Phys. Rev., 1924, 23, 710; N. Fuks. Mekhanika
aerozoley (Mechanics Aerosols). str. 32.

57. P. Epstein. Z. Phys., 1929, 54, 537; N. Fuks. Mekhanika
aerozoley (Mechanics Aerosols). str. 69.

58. W. Walkenhorst. Beitr. Silikoseforsch., 1952, Heft 18.

59. N. Fuks, S. Yankovskiy. Dokl. AN SSSR, 1958, 119, 1177.

60. H. T h ü r m e r. Staub, 1960, 20, 6.
61. H. W a t s o n. Brit. J. Appl. Phys., 1938, 9, 78.
62. C. S c h a d t, R. C a d l e. J. Colloid. Sci., 1957, 12, 356.
63. E. B r u n, J. L e r o u x, P. M a r t y. J. rech. Centre nat. rech. scient.
    1955, № 31, 256.

64. N. Fuks, S. Yankovskiy. Kolloidn. zh., 1959, 21, 133.

65. H. W a t s o n. Trans. Fa y Soc., 1936, 32, 1073
66. W. Z e r n i k. " J. Ap; Phys., 1957, 8, 117.
67. E. S c h m i d t . B e c a a a a. Techn. Mechan. und Thermody-
    namik, 1939, 1. ..
68. W. K r a u s. ` ng des Temperatur- und Geschwindigkeitsfeldes bei
    freier Konvekt' ' arlsruhe, 1955.
69. M. M a i t r Ann. chim., 1933, 8, 43.

70. P. T a u z i n. C. R., 1952, 235, 1119, 1632.
71. H. R o h a t s c h e k. Acta phys. austriaca, 1955, 9, 151.
72. J. A i t k e n. Trans. Roy. Soc. Edinburgh, 1883, 32.
73. L. F a c y. Arch. Meteorol., Geophys., Bioklimatol., 1955, 8A, 269.
   C. R., 1958, 246, 102, 3161; Geofis. pura e appl., 1958, 40, № 2.

74. N. Fuks. Ispareniye i rost kapel' v gazoobraznoy srede
(Evaporation and Growth of Drops in a Gaseous Medium). M., Isd-vo
AN SSSR, 1958, § 2.

75. B. Deryagin, S. Dukhin. Dokl. AN SSSR, 1956, 111, 613.

76. K. S e m r a u, C. M a r y n o w s k i, K. L u n d e, C. L a p p l e.
   Ind. Eng. Chem., 1958, 50, 1615.
77. F. V e r z a r, F. H ü g i n, W. M i s s i o n. Pflügers Arch. ges. Phy-
   siol., 1955, 261, 219.

78. P. Deryagin, S. Bakanov. Dokl. AN SSSR, 1957, 117, 959.

79. P. Prokhorov. Doktorskaya dissertatsiya (Doctoral Disserta-
tion). In-t fiz. khim. AN SSSR, 1959.

80. B. Deryagin, S. Dukhin. Dokl. AN SSSR, 1956, 106, 851.

81. S. Dukhin, B. Deryagin. Tam zhe (Ibid). 1957, 112, 407.

82. V. Fedoseyev. A. Polyanskiy. Tr. Odessk. un-ta, fiz. mat.,
1954, 5, 95.

83. B. Deryagin, S. Dukhin. Izv. AN SSSR. Ser. geofiz., 1957,
str. 779.

84. N. Fuks. Mekhanika aerozoley (Mechanics Aerosols). str. 76.

85. T c h e n C h a n - m o u. Mean Value and Correlation Problems Con-
   nected with the Motion of Small Particles Suspended in a Turbulent Fluid.
   The Hague, 1947.
86. T. P e a r c e y, G. H i l l. Austral. J. Phys., 1956, 9, 1.
87. J. S e r a f i n i. Nat. Adv. Comm. Aeron., 1954, Rep. 1159.

88. N. Fuks. Mekhanika aerozoley (Mechanics Aerosols). str. 84.

89. R. Ingebo. Nat. Adv. Comm. Aeron., 1956, Tech. Note 3762.

90. N. Fuks. Mekhanika aerozoley (Mechanics Aerosols). str. 82.

91. F. Gucker, G. Doyle. J. Phys. Chem., 1956, 60, 989.

92. W. König, Ann. Phys. 1891, 42, 353; N. Fuks. Mekhanika
aerozoley (Mechanics Aerosols). str. 90, 91.

93. L. Landau, Ye. Lifshits. Mekhanika sploshnykh sred
(Mechanics of Continuous Media). M., Gostekhizdat, 1944, str. 37.

94. S. Dukhin. Kolloidn. zh., 1960, 22, 128.

95. P. Epstein, R. Carhart. J. Acoust. Soc. Am., 1953, 25, 553.

96. N. Fuks. Mekhanika aerozoley (Mechanics Aerosols). str. 293.

97. J. Z i n k,. L. D e l a s s o. J. Acoust. Soc. Am., 1958, 30, 765.
98. L. H o c k i n g. Quart. J. Roy. Meteorol. Soc., 1959, 85, 44.
99. H. F a s e n. Arkiv Mat. Astr. Fys., 1925, 19A, № 22.
100. M. S m o l u c h o w s k i. Bull. Acad. Sci. Cracov, 1911, 1A, 28.
101. J. B u r g e r s. Proc. Ned. Akad. Wetensch., 1941, 44, 1177.
102. M. S t i m s o n. G. J e f f e r y. Proc. Roy. Soc., 1926, 111A, 110.

103. N. Fuks. Mekhanika aerozoley, formula (13.1) (Mechanics of Aerosols, Formula (13.1).

104. J. Happel, R. Pfeffer. A. I. Ch. E. Journal, 1960, 6, 129.

105. B. Pshenay-Severin. Izv. AN SSSR. Ser. geofiz., 1957, str. 1045.

106. V. Pshenay-Severin. Tam zhe (Ibid). 1958, str. 1254.

107. C. Oseen. Neuere Methoden und Ergebnisse in der Hydrodynamik. Leipzig, 1927, § 14, 21.

108. V. Pshenay-Severin. Dokl. AN SSSR, 1959, 125, 775.

109. N. Fuks. Mekhanika aerozoley (Mechanics of Aerosols). str. 165.

110. W. Dörr. Acustica, 1955, 5, 163.

111. W. Foster. Brit. J. Appl. Phys., 1959, 10, 206.

112. W. Drozin, V. La Mer. J. Colloid. Sci., 1959, 14, 74.

113. V. Dunskiy, A. Kitayev. Kolloidn. zh., 1960, 22, 159.

114. N. Göhlich. VDI-Forschungsheft, 1958, No 467.

115. A. Robinson. Commun. Pure and Appl. Math., 1956, 9, 69.

116. L. Levin. Izv. AN SSSR. Ser. geofiz., 1957, str. 914.

117. N. Fuks. Mekhanika aerozoley (Mechanics of Aerosols). str. 109.

118. Ye. Gladkova, G. Natanson. ZhFKh, 1958, 32, 1160.

119. R. Prengle, R. Rotfus. Ind. Eng. Chem., 1955, 47, 379.

120. N. Fuks. Mekhanika aerozoley (Mechanics of Aerosols). str. 116.

121. T. G i l l e s p i e. G. L a n g s t r o t h. Canad. J. Chem., 1952, 30, 1056.
122. B. H i n k l e, C l y d e Orr, J. D a l l a v a l l e. J. Colloid. Sci., 1954, 9.
123. H. Y o s n. a w a, G. S w a r t z, J. M c W a t e r s, W. P i t e. Rev. Sci. In r., 1956, 27, 358.
124. P. N o l a n, T. O'C o n n o r. Proc. Roy. Irish Acad., 1955, 57A, 161.
125. A. G o e t z. Geofis. pura e appl., 1957, 36, 49.
126. E. F e i f e l. Forsch. Ing. Wesen, 1938, A9, 68.
127. W. B a r t h. Brennstoff-Wärme-Kraft, 1956, 8, 1.
128. W. S o l b a c h. Tonind.-Ztg., 1956, 80, 38, 298; 1958, 82, 474.

129. V. Maslov, Yu. Marshak. Teploenergetika, 1958, No 6, 63.

130. E. Walter. Staub, 1958, 18, 3.
131. H. Rumpf. Staub, 1956, Heft 47, 634.
132. T. Daniels. Engineer, 1957, 203, 358.
133. C. Stairmand. J. Inst. Fuel, 1956, 29, 58.
134. C. Yaffe, A. Hosey, J. Chambers. Arch. Industr. Hyg.
    Occupat. Med., 1952, 5, 62.
135. J. Smith, M. Gegiia. Trans. ASME, 1956, 78, 389.
136. W. Walton. Physics of Particle Size Analysis, 1954, p. 30.

137. W. Walton. Symposium on Particle Size Analysis. London,
1947, p. 136; N. Fuks. Mekhanika aerozoley (Mechanics Aerosols).
str. 143.

138. H. Watson. Am. Ind. Hyg. Ass. Quart., 1954, 15, 21.
139. S. Badzioch. Brit. J. Appl. Phys., 1959, 10, 26.
140. E. Walter. Staub, 1957, Heft 53, 880.
141. R. Dennis, W. Samples, D. Anderson, L. Silverman.
    Ind. Eng. Chem., 1957, 49, 294.
142. R. Röber. Staub, 1957, Heft 49, 41; Heft 49, 273; Heft 50, 418.
143. M. Lippman. Am. Ind. Hyg. Ass. J., 1959, 20, 406.
144. R. Brun, W. Lewis, P. Perkins, J. Serafini. Nat. Adv.
    Comm. Aeron., 1955, Rep. 1215.

145. R. Brun, H. Nergler. Tam zhe (Ibid). 1953, Techn. Note
2904.

146. M. Tribus, G. Young, L. Boelter. Trans. ASME, 1948, 70,
    977.
147. R. Dorsh, R. Brun, J. Gregg. Nat. Adv. Comm. Aeron., 1954,

148. R. Brun, H. Gallagher, D. Vogt. Tam zhe (Ibid). 1953.
Techn. Note 3047.

149. N. Bergrun. Tam zhe (Ibid). 1952. Rep. 1107.

150. I. Mazin. Fizicheskiye osnovy obledeneniya samoletov
(Physical Bases for Formation of Ice on Aircraft). M., Gidro-
meteorizdat, 1957.

151. P. Hacker, R. Brun, B. Boyd. Nat. Adv. Comm. Aeron., 1953,
Techn. Note, 2999.

152. R. Brun, J. Serafini, H. Gallagher. Tam zhe (Ibid). 1953,
Techn. Note 2903.

153. A. Fonda, H. Herne. Symposium on the Aerodynamic Capture of
    Particles. Pergamon, 1960.
154. M. Tribus, A. Guibert. J. Aeronaut. Sci., 1952, 19, 391.

155. L. Levin. Chastnoye soobshcheniye (Partial report).

156. G. Natanson. Dokl. AN SSSR, 1957, 116, 109.

157. I. Langmuir. J. Meteorol., 1948, 5, 175.

158. L. Levin. Izv. AN SSSR. Ser. geofiz., 1959, str. 422.

159. L. Levin. Dokl. AN SSSR, 1953, 91, 1329; N. Fuks. Mekhanika
aerozoley (Mechanics of Aerosols). str. 156.

160. C. Davies, C. Peetz. Proc. Roy. Soc., 1956, _34A, 269.

151. A. Thom. Tam zhe (Ibid). 1933, 141A 651.

162. H. Landahl, K. Hermann. J. Colloid. Sci., 1949, 4, 103; N. Fuks, Mekhanika aerozoley (Mechanics of Aerosols). str. 155.

163. C. Davies. Proc. Phys. Soc., 1960, 63B, 288.
164. P. Gregory. Ann. Appl. Biol., 1951, 38, 357.
165. J. Lewis, R. Ruggieri. Nat. Adv. Comm. Aeron., 1957, Techn. Note 4092.

166. V. Igmat'yev. Teploenergetika, 1958, No 3.

167. A. Amelin, M. Belyakov. Kolloidn, zh., 1956, 18, 385; Soobshch. nauchn. rab. NIUIF, 1958, vyp. 9, 58.

168. A. Amelin, M. Belyakov. Zav. lab., 1955, No 12, 1463.

169. R. Jarman. Chem. Eng. Sci., 1959, 10, 268.
170. L. Simmons, C. Cowderey. Aeronaut. Res. Council. Repts and Mem., 1945, № 2276.
171. H. Kraemer, H. Johnstone. Ind. Eng. Chem., 1955, 47, 2426.

172. G. Natanson. Dokl. AN SSSR, 1957, 112, 696.

173. R. Cochen. Rev. gén. électr., 1953, 62, 113; N. Fuks. Mekhanika aerozoley (Mechanics of Aerosols). str. 160.

174. T. Gillespie. J. Colloid. Sci., 1955, 10, 299.

175. C. Dukhin, B. Deryagin. Kolloidn. zh., 1958, 20, 326.

176. L. Levin. Izv. AN SSSR. Ser. geofiz.,1959, str. 1073.

177. N. Fuks. Ispareniye i rost kapel' v gazoobraznoy srede (Evaporation and Growth of Drops in a Gaseous Medium). M., Izd-vo AN SSSR, 1958, § 5.

178. N. Fuks. Mekhanika aerozoley (Mechanics of Aerosols). § 49.

179. I. Todorov. A. Sheludko. Kolloidn. zh., 1957, 19, 496.

180. C. Davies. Brit. J. Ind. Med., 1952, 9, 120.

181. E. Buchwald. Ann. Phys., 1921, 66, 1; N. Fuks. Mekhanika aerozoley (Mechanics of Aerosols). str. 182.

182. L. Pollak, T. O'Connor. Geofis. pura e appl., 1955, 31, 66.

183. L. Pollak, T. O'Connor, A. Metnieks. Tam zhe (Ibid). 1956, 34, 177; 1957, 36, 70.

184. R. Fürth. Tam zhe (Ibid). 1955, 31, 80.

185. J. Richardson. E. Wooding. Chem. Eng. Sci., 1957, 7, 51.

186. N. Fu's. Mekhanika aerozoley (Mechanics of Aerosols). str. 172.

187. C. Davies. Proc. Roy. Soc., 1949, 200A, 100; N. Fuks Mekhanika aerozoley (Mechanics of Aerosols). ris. 54.

188. P. Gormley, M. Kennedy. Proc. Roy. Irish Acad., 1949, 52A, 163.

189. P. Gormley. Tam zhe (Ibid). 1938, 45A, 59.

190. M. Kennedy, tsit. po P. Nolan, P. Kenny. J. Atmos. Terr. Phys., 1953, 3, 181.

191. W. DeMarcus, J. Thomas. U. S. Atom. Commiss., 1952, ORNL—1413.
192. J. Thomas. J. Colloid. Sci., 1955, 10, 246.
193. J. Thomas. U. S. Atom. Commiss.. 1951, ORNL—1648.
194. J. Thomas. J. Colloid. Sci., 1956, 11, 107.
195. L. Pollak, A. Metnieks. Geofis. pura e appl., 1957, 37, 183.
196. G. Goyer, F. Pidgeon. J. Colloid. Sci., 1956, 11, 697.
197. A. Chamberlain, W. Megaw, R. Wiffen. Geofis. pura e appl., 1957, 36, 223.

198. V. Levich. Fiziko-khimicheskaya gidrodinamika (Physical-chemical Hydrodynamics). M., Izd-vo AN SSSR, 1952, § 14; N. Fuks. Mekhanika aerozoley (Mechanics of Aerosols), str. 188.

199. S. Friedländer. A. I. Ch. E. Journal, 1957, 3, 11.

200. G. Aksel'rud. ZhFKh, 1953, 27, 1445.

201. G. Myuller. Sb. Koagulyatsiya kolloidov (Collection, Coagulation of Colloids). M., ONTI, 1936, str. 91.

202. F. Garner, R. Suckling. A. I. Ch. E. Journal, 1958, 4, 114.

203. F. Garner, R. Keey. Chem. Eng. Sci., 1958. 9, 119.

204. G. Natanson. Dokl. AN SSSR, 1957, 112, 100.

205. R. Dobry, R. Finn. Ind. Eng. Chem., 1956, 48, 1540.

206. N. Fuks. Mekhanika aerozoley, formula (34.18) (Mechanics of Aerosols, Formula (34.18).

207. Ch. Chen. Usp. khim., 1956, 25, 368.

208. L. Radushkevich, ZhFKh, 1958, 32, 282.

209. K. Tamada, H. Fujikawa. Quart. J. Mech. Appl. Math., 1957, 10, 425.
210. S. Kuwobara. J. Phys. Soc. Japan, 1959, 14, 527.
211. E. Landt. Staub. 1957, Heft 48, 9.
212. C. Stairmand t. Heat. and Ventilat Engr., 1953, 26, 342.
213. S. Friedlände.. Ind. Eng. Chem. 1958, 50, 1161.

214. N. Fuks. Mekhanika aerozoley, formula (34.18) (Mechanics of Aerosols, Formula (34.18).

215. N. Fuks. Mekhanika aerozoley, formula (40.2) (Mechanics of Aerosols, Formula (40.2).

216. I. Gallili. J. Colloid. Sci., 1957, 12, 161.

217. C. Davies. Proc. Instn. Mech. Engrs, 1952, 1B, 185; N. Fuks. Mekhanika aerozoley, formula (34.19) (Mechanics of Aerosols, Formula (34.19).

218. J. Thomas, R. Yoder. Arch. Ind. Health, 1956, 13, 545.

219. E. Ranskill, W. Anderson. J. Colloid. Sci., 1951, 6, 416; N. Fuks. Mekhanika aerozoley, ris. 59b, g (Mechanics of Aerosols, Fig. 59b, d).

220. J. Wong. W. Raaz, H. Johnstone. J. Appl. Phys., 1956, 27. 161.
221. A. Humphrey, E. Gaden. Ind. Eng. Chem., 1955, 47, 924.
222. C. Davies. J. Instn. Heat. Ventilat. Engrs, 1952, 20, 55.
223. R. Leers. Staub, 1957, Heft 50, 402.

224. N. Fuks. Mekhanika aerozoley (Mechanics of Aerosols). str 285.

225. G. Fairs. Trans. Instn. Chem. Engrs., 1958, 36, 476.
226. V. La Mer, V. Drozin. Proc. 2-nd Int. Congr. Surf. Activ, London, 1957, III, 600.
227. D. Hasenclever. Staub, 1959, 19, 37.
228. A. Rossano, L. Silverman. Heat. Ventilat., 1954, 51, 102.
229. A. Winkel. Staub, 1955, Heft 41, 469.
230. D. Thomas. J. instn. Heat. Ventilat. Engrs., 1952, 20, 35.
231. T. Gillespie. J. Colloid. Sci., 1965, 10, 299.
232. C. Billings, R. Dennis, L. Silverman. U. S. Atom. Commiss., 1964, NYO — 1592.
233. J. Fitzgerald, C. Detweiler. Arch. Ind. Health, 1957, 16, 3.
234. W. Walkenhorst. Staub, 1959, 19, 69.
235. C. Snyder, R. Pring. Ind. Eng. Chem., 1955, 47, 960.

236. N. Yeliseyev. Sbornik materialov po pyleulavlivaniyu v tsvetnoy metallurgii (Collection of Materials on Dustcatching in Nonferrous Metallurgy). M., Metallurgizdat, 1957, str. 251.

237. J. Thomas, R. Yoder. Arch. Ind. Health, 1956, 13, 550.

238. P. Morrow, E. Mehrhof, L. Casarett, D. Morken, Tam zhe (Ibid). 1958, 18, 292.

239. B. Altshuler et al. Tam zhe (Ibid). 1957, 15, 293.

240. L. Dautrebande, H. Beckmann, W. Walkenhorst. Tam zhe (Ibid). 1957, 16, 179.

241. N. Fuks. Mekhanika aerozoley (Mechanics Aerosols). str. 215.

242. M. Pozin, I. Mukhlenov, E. Tarat. Pennyy sposob ochistki gazov ot pyli, dyma i tumana (Foam Method of Purification of Gases from Dust, Smoke and Fog). M., Goskhimizdat, 1953.

243. H. Remy, H. Finnern. S. anorg. Chem., 1926, 159, 241.

244. N. Fuks. Mekhanika aerozoley (Mechanics of Aerosols). str. 215.

245. C. O'Konski, C. Thatcher. J. Phys. Chem., 1953, 57, 955.

246. C. O'Konski, R. Gunther. J. Colloid. Sci., 1955, 10, 563.

247. N. Fuks. Mekhanika aerozoley (Mechanics of Aerosols). § 37.

248. N. Fuks. Mekhanika aerozoley, formuly (35.1), (35.7) (Mechanics of Aerosols, Formulas (35.1), (35.7).

249. M. Smolukhovskiy. Sb. Brounovskoye dvizheniye (Collection, Brownian Movement). M., ONTI, 1936, str. 150; N. Fuks. Mekhanika aerozoley (Mechanics of Aerosols). str. 163.

250. G. Batchelor, A. Townsend. Surveys in Mechanics, Cambridge, 1956, p. 352.

251. L. Richardson. Proc. Roy. Soc., 1923, 104A, 640; N. Fuks. Mekhanika aerozoley (Mechanics of Aerosols). str. 245.

252. S. Soo. Chem. Engng. Sci., 1956, 5, 57.

253. Vi-Cheng Liu. J. Meteorol., 1956, 13, 399.

254. S. Soo, C Tien. V. Kadambi. Rev. Sci. Instr., 1959, 30, 821.

255. N. Kubynin. Izv. Vses. teplotekhn. in-ta, 1951, No 1.

256. W. Hoffmann. VDI-Ber., 1955, 7, 15.

257. A. Chernov. Izv. AN KazSSR, Ser. energ., 1955, vyp. 8, str. 82.

258. J. Dawes, A. Slack. Saf. Mines Res. Est., Rep., No 105, 1954.

259. N. Fuks. Mekhanika aerozoley (Mechanics of Aerosols). str. 232.

260. T. Sherwood, B. Woertz. Ind. Eng. Chem., 1939, 31, 1034; N. Fuks. Mekhanika aerozoley (Mechanics of Aerosols). str. 233.

261. N. Fuks. Mekhanika aerozoley (Mechanics of Aerosols). str. 237.

262. Sovremennoye sostoyaniye gidroaerodinamiki vyazkoy zhidkosti (Contemporary State of Hydroaerodynamics of a Viscous Liquid). M, IL, 1948, § 155, formula (20).

263. C. Lin, R. Moulton, G. Putnam. Ind. Eng. Chem., 1953, 45, 636.

264. R. Deissler. Nat. Adv. Comm. Aeron., 1955, Rep. 1210.

265. N. Fuks. Mekhanika aerozoley (Mechanics of Aerosols). str. 83.

266. V. Levich. Fiziko-khimicheskaya gidrodinamika (Physical-chemical Hydrodynamics). M., Izd-vo AN SSSR, 1952, gl. 3; N. Fuks Mekhanika aerozoley, formula (46.33) (Mechanics of Aerosols, Formula (46.33)).

267. S. Friedländer, H. Johnstone. Ind. Eng. Chem., 1957, 49, 1151.

268. J. Laufer. Nat. Adv. Comm. Aeron., 1954, Rep. 1174.

269. N. Fuks. Mekhanika aerozoley formula (46.2) (Mechanics of Aerosols, Formula (46.2)).

270 E. Pereies. Sai. Mines Res. Est. Rep., № 144, 1958.
271 P. Owen. Sympo Aerodyn. Capture of Particles, Peragmon, 1960.
272. P. Koepe. Staub, 1952, Heft 28, 39.
273. A. Madis tti. Staub, 1956, Heft 47, 652.
274. .. Frenk el. Katz. J. Meteorol., 1956, 13, 388.
275 F. Gifiod. J. Meteorol., 1957, 14, 410.
276. R. Trappenberg. Staub, 1955, Heft 39, 5; Heft 40, 189; M. Dem, R Trappenberg. Forsch. Ber. Nordrhein-Westf., 1957, S. 380.
277. G. Czanauy. Aus al. J. Phys., 1955, 8, 546; 1957, 10, 558.
278. W. Rou s. Trans. Amer. Geophys. Un., 1955, 36, 395.

279. N. Fuks. Mekhanika aerozoley, formula (47.20) (Mechanics of Aerosols, Formula (47.20))

280. W. Godsun. Arch. Meteorol., Geophys. und Bioklimatol., 1958, 10A, 305.
281. H. Portak. Z. Meteorol., 1957, 11, 19.

282. A. Denisov. Izv. AN SSSR. Ser. geofiz., 1957, str. 834.

283. L. Gandin, R. Soloveychik. Tr. GGO, 1958, vyp. 77, str. 84.

284. G. Zebel. Kolloid Z., 1958, 157, 37.

285. N. Fuks. Mekhanika aerozoley, § 49 (Mechanics of Aerosols, § 49).

286. N. Fuks. Mekhanika aerozoley, formula (49.20) (Mechanics of Aerosols, Formula (49.20)).

287. P. Nolan, E. Kennan. Proc. Roy. Irish Acad., 1938, 46A, 171; P. Nolan, E. Koffel. Geofis. pura e aopl., 1955, 31, 97.

288. J. Pollak. T. Murphy. Geofis. pura e appl., 1955, 30, 136.

289. . Nolan, N. Guerrini. Trans. Faraday Soc., 1936, 32, 1175; N. Fuks. Mekhanika aerozoley (Mechanics of Aerosols). str. 187.

290. R. aytlou-Grey, Kh. Patterson. Dym (Smoke). M., Goskhimizdat, 1934, p. 10.

291. T. O'Connor, Geofis. pura e appl., 1955, 31, 107.

292. N. Fuks. Mekhanika aerozoley (Mechanics of Aerosols). str. 114.

293. W. Cawood, R. Whytlaw-Gray. Trans. Faraday Soc., 1936, 32, 1059.
294. I. Yaffe, R. Cadle, J. Phys. Chem., 1953, 62, 510.
295. Z. Melzak. Quart. Appl. Math., 1953, 11, 231.
296. T. Schumann. Quart. J. Roy. Meteorol. Soc., 1940, 66, 195.

297. N. Tunitskiy. ZhETF, 1938, 8, 418; N. Fuks Mekhanika aerozoley (Mechanics of Aerosols). str. 271.

298. G. Zebel. Kolloid.-Z., 1958, 156, 102.

299. D. Deryagin. Dokl. AN SSSR, 1956, 109, 967.

300. Tsit. po W. Hardy, I. Bircumshaw. Proc. Roy. Soc., 1925, 108A, 12.

301. R. Schotland. J. Meteorol., 1957, 14, 381.
302. L. Dautrebande, H. Kahler, B. Lloyd, E. Mitchell. Arch. Intern. Pharmacodynam. Therap. 1949, 80, 413.
303. L. Dautrebande, H. Beckmann, W. Walkenhorst. Beitr. Silikoseforsch., 1954, Heft 31.
304. A. Avy. Staub, 1953, Heft 32, 147.
305. L. Le Bouffant. Rev. Ind. Miner., 1955, 36, 62.
306. W. Walkenhorst, G. Zebel. Beitr. Silikoseforsch., 1956, eft 44, 53.
307. W. Walkenhorst. Z. Aerosolforsch. Therap., 1955, 4, 538.

308. Tsit. po W. Walkenhorst. Tam zhe (Ibi). 1958, 7, 157.

309. Y. Fujitani. Bull. Chem. Soc. Japan. 1957, 30, 683.

310. N. Fuks. Mekhanika aerozoley (Mechanics of Aerosols). § 51.

311. R. Gunn. J. Colloid. Sci., 1955, 10, 107.

312. D. Benton, G. Elton, E. Peace, R. Picknett. Intern. J. Air Pollut., 1958, 1, 44.

313. S. Dukhin, B. Deryagin. Dokl. AN SSSR, 1958, 121, 503.

314. G. Natanson. Kolloidn. zh., 1958, 20, 705.

315. A. Winkel. Staub. 1955, Heft 41, 469.

316. W. Zebee. Staub. 1959, 19, 381.

317. V. Gudemchuk, B. Podoshevnikov, B. Tartakevskiy Akust. zh., 1959, 5, 246.

318. N. Fuks. Mekhanika aerozoley (Mechanics of Aerosols) str. 07, 165.

319. T. Pearcey, G. Hill. Quart. J. Roy. Meteorol. Soc., 1957, 83, 77.

320. J. Tellford, N. Thorndike, E. Bowen. Quart. J. Roy. Meteorol. Soc., 1955, 81, 241; N. Fuks. Mekhanika aerozoley (Mechanics of Aerosols). str. 293.

321. R. Schotland. J. Meteorol., 1957, 14, 381; Artificial Stimulation of Rain, Pergamon, 1957, p. 170.

322. D. Sartor. J. Meteorol., 1954, 11, 91; N. Fuks. Mekhanika aerozoley (Mechanics of Aerosols). str. 293.

323. G. Kinzer, W. Gobb. J. Meteorol., 1956, 13, 295; 1958, 15, 138; Artificial Stimulation of Rain, Pergamon, 1957, p. 167.

324. N. Fuks. Mekhanika aerozoley (Mechanics of Aerosols). Table 9.

325. L. Torobin, W. Gauvin. Canad. J. Chem. Eng., 1959, 37, 167.

326. R. Oakes. Symp. Aerodyn. Capt. Particles, Pergamon, 1960.

327. W. Walton, A. Woolcock. Tam zhe (Ibid).

328. F. May. Quart. J. Roy, Meteorol. Soc., 1958, 84, 451.

329. A. Best. Tam zhe (Ibid). 1950, 76. 16.

330. H. Johnstone, R. Field, H. Tassles. Ind. Eng. Chem., 1954. 46, 1601.

331. J. Brink, C. Contant. Ind. Eng. Chem., 1958, 50, 1157.

332. P. Boucher. Chal. et Industrie, 1952, 33, 363.

333. M. Gauthenier, R. Cochet. J. Dupuy. Comptes rend., 1958, 246, 2233.

334. N. Fuks. Mekhanika aerozoley, formula (54.3) (Mechanics of Aerosols, Formula (54.3)).

335. R. Gunn. J. Meteorol., 1955, 12, 511.

336. L. Levin. Dokl. AN SSSR, 1954, 94, 467; N. Fuks. Mekhanika aerozoley (Mechanics of Aerosols). str. 298.

337. V. Tkach Sb. Voprosy gigiyeny truda i profzabolevaniy v gornorudnoy, khimicheskoy i mashinostroitel'noy promyshlennosti (Collection. Questions of Work Hygiene and Professional Diseases in Mining and the Chemical and Machine-Building Industry). Kiyev, Gosmed'zdat USSR, 1958, str. 9.

338. I. Chizhov. Sbornik materialov po pyleulavlivaniyu v tsvetnoy metallurgii (Collection of Materials on Dustcatching in Nonferrous Metallurgy). M., Metallurgizdat, 1957, str. 361.

339. T. Gillespie. Proc. Roy. Soc., 1953, 216A, 569.

340. M. Smolukhovskiy. Sb. Koarulyatsiya kolloidov (Collection. Coagulation of colloids). M., ONTI, 1936, str. 28; N. Fuks. Mekhanika aerozoley, formula (55.4) (Mechanics of Aerosols, Formula (55.4)).

341. P. Saffman, J. Turner. J. Fluid Mechan., 1956, 1, 16.

342. V. Levich. Dokl. AN SSSR, 1954, 99, 809, 1041; N. Fuks. Mekhanika aerozoley (Mechanics of Aerosols). str. 304.

343. T. East, J. Marshall. Quart. J. Roy Meteorol. Soc., 1954, 80, 26.

344. V. Levich. Fiziko-khimicheskaya gidrodinamika, izd. 2-e (Physical-chemical Hydrodynamics, Edition 2). M., Fizmatgiz, 1959, gl. 5.

345. R. Manley, S. Mason. J. Colloid. Sci., 1952, 7, 354; N. Fuks. Mekhanika aerozoley (Mechanics of Aerosols). str. 303.

346. N. Tunitskiy. ZhFKh, 1946, 20, 1136; N. Fuks. Mekhanika aerozoley (Mechanics of Aerosols). str. 304.

347. H. Frish. J. Phys. Chem., 1956, 60, 463.

348. A. Dinnik. Izbrannyye trudy (Selected Works). M., Izd-vo AN SSSR, 1952, 1, gl. 5.

349. C. Raman. Phys. Rev., 1918, 12, 442.

350. J. Andrews. Philos. Mag., 1930, 9, 593.

351. D. Jordan. Physics of Particle Size Analysis, 1954, p. 194.

352. O. Adam. Chem.-Ingr.-Techn., 1957, 29, 151.

353. N. Fuks. Mekhanika aerozoley (Mechanics of Aerosols). str. 317, 319.

354. I. Dergachev. Izv. Vses. teplotekhn. in-ta, 1949, No 6.

355. J. Rosinski, C. Nagamoto, A. Ungar. Kolloid.-Z., 1959, 164, 26.
356. J. Rayleigh. Proc. Roy. Soc. 1882, 34, 130; Philos. Mag., 1899, 48, 321.
357. H. Newall. Philos. Mag., 1885, 20, 30.
358. E. Kaiser. Ann. Phys., 1894, 53, 667.
359. L. Mahajan. Kolloid.-Z., 1933, 65, 20; 1931, 59, 16; Philos. Mag., 1929, 7, 247; 1930, 10, 383; Z. Physik, 1932, 79, 389; 1933, 81, 605; 1934, 84, 676; 1934, 90, 663.

360. M. Aganin. Zh. geofiz., 1935, 5, 408; Izv. AN SSSR, Ser. geogr. geof., 1940, 3, 305.

361. S. Gorbachev, Ye. Mustel'. Kolloid.-Z. 1935, 73, 21.

362. S. Gorbachev, V. Nikiforova. Tam zhe (Ibid). str. 14.

363. N. Tverskaya. Tr. GGO, 1954, vyp. 47, str. 112.

364. N. Tverskaya. I. Yudin. Tr. Leningr. gidromet. in-ta, 1956, vyp. 5-6.

365. P. Prokhorov, L. Leonov. Kolloidn. zh., 1952, 14, 66; N. Fuks. Mekhanika aerozoley (Mechanics of Aerosols). str. 311.

366. G. Browne, N. Palmer, T. Wormell. Quart. J. Roy. Meteor. Soc., 1954, 80, 291.
367. J. Gallili, V. La Mer. J. Phys. Chem., 1958, 62, 1296.
368. T. Gillespie. E. Rideal. J. Colloid. Sci., 1955, 10, 281.
369. T. Gillespie. J. Colloid. Sci., 1955, 10, 266.
370. C. Hartley, R. Brunskill. Surface Phenomena in Chemistry and Biology, Pergmon, 1958, p. 214.

371. A. Taubman, S. Nikitina. Dokl. AN SSSR, 1956, 110, 600, 816; 1957, 116, 113.

372. P. Ermilov. Uch. zap. Yaroslavsk. tekhnol. in-ta, 1956, 1, 111; 1957, 2, 93; Izv. Vyssh. uch. zav., Khim., khim. tekhn., 1959, 2, 134.

373. M. Pozin, N. Mukhlenov, V. Demshin. ZhPKh, 1955, 28, 841; N. Mukhlenov, V. Demshin. Tam zhe (Ibid). str. 922.

374. C. McCully et al. Ind. Eng. Chem., 1956, 48, 1512.
375. C. Pemberton. Symp. Aerodyn. Capt. Particles, Pergamon, 1960.
376. M. Landwehr, R. Kortner, W. Walkenhorst, E. Bruckmann. Staub, 1957, Heft 53, 841.

377. V. Kaganer. Byull. NIGRI, Krivoy Rog, 1958, vyp. 4.

378. B. Deryagin, I. Abrikosova. Trans. Faraday Soc., Discussion 1954, 18, 36; N. Fuks. Mekhanika aerozoley (Mechanics of Aerosols). str. 280.

379. W. Stone. Philos. Mag., 1930, 9, 610.
380. P. How, D. Benton, I. Puddington. Canad. J. Chem., 1955, 33, 1375.
381. J. McFarlane, D. Tabor. Proc. 7-th Intern. Congr. Appl. Mech. 1948; p. 335; Proc. Roy. Soc., 1950, 202A, 224.
382. R. Bradley. Philos. Mag., 1932, 13, 853.
383. W. Harper. Proc. Roy. Soc., 1955, 231A, 388.
384. G. Tomlinson. Philos. Mag., 1928, 6, 695.

385. N. Fuks. Mekhanika aerozoley (Mechanics of Aerosols). str. 333.

386. R. Larsen. Am. Ind. Hyg. Ass. Quart., 1958, 19, 265.

387. V. Goncharov. Issledovaniye dinamiki ruslovykh potokov (Investigation of Dynamics of Channel Flows). M., GIMIZ, 1954.

388. R. Fowler, W. Chodziesner. Chem. Engng. Sci., 1959, 10, 157.
389. F. Bowden, D. Tabor. Friction and Lubrication of Solids, Oxford, 1956.

390. B. Deryagin, V. Lazarev. Kolloidn. zh., 1935, 1, 295.

391. E. Cremer, F. Conrad, T. Kraus. Angew. Chemie, 1952, 64, 10; E. Cremer. Staub, 1951, Heft 37, 427.
392. D. Beischer. Kolloid.-Z., 1939, 89, 214.
393. E. Patat, W. Schmid. Chem.-Ingr.-Techn., 1960, 32, 8.
394. W. Batel. Chem.-Ingr.-Techn., 1959, 31, 343.

● ... . Mekhanika ...
    8 ...

    ... ... Tr. Mосk. хим. техн. Inst., 19..., No
. ...

    3... ... ...orfield, J. Dallavalle, Publ. Health Bull., 1935
No ...

    3... ... Dawes. Safety in Mines Res. Establ., Res. Rep., No 36
and ..., 19..; J. Dawes, A. Wynn. Tam zhe, Res. Rep., No, 46, 1952.

    ... A. Bagnold. The Physics of Blown Sand and Desert Dunes.
...nion, 1941; N. Fuks. Mekhanika aerozoley (Mechanics of Aerosols).
...tr. 317.

    4... A. Andreasen. Kolloid.-Z., 1939, 86, 70; N. Fuks. Mekhanika
...zoley (Mechanics of Aerosols). str. 332.

    4... N. Fuks. Mekhanika aerozoley (Mechanics of Aerosols). § 57.

403. N. M e h t a, J. S m i t h, E. C o m m i n g s. Ind. Eng. Chem., 1957,
     49, 986.
404. A. R e i f, C. W h y t e, M. G i b l i n. Arch. Ind. Health, 1956, 14.
     442.
405. C. D a v i e s, H. A y l w a r d, D. L e a c e y. Arch. Ind. Hyg. Occ·
     Med., 1951, 4, 354.
406. F. E a d i e, R. P a y n e. Iron Age, 1954, № 10, 99.
407. W. K r o l l. Chem.·Ingr·Techn., 1955, 27, 33.
408. C h i n · Y o u n g W e n, H. S i m o n s. A. I. Ch. E. Journal, 1959,
     5, 264.
409. R. M o r s e. Ind. Eng. Chem., 1955, 47, 1170.

    410. F. Tideswell, R. Wheeler. Trans. Instn. Mining Engrs.,
1938, ..., 176; N. Fuks. Mekhanika aerozoley (Mechanics of Aerosols).
...tr. 332.

411. D. C r a i k, B. M i l l e r. J. Pharmacol. and Pharmacy, 1958, 10, Suppl.,
     136.
412. H. P a r k e r, W. S t e v e n s. A. I. Ch. E. Journal, 1959, 5, 314.
413. F. D'A r c y · S m i t h. Ind Chemist., 1957, 33, 181.
414. P. B a k e r, P. H e e r t j e s. Brit. Chem. Eng., 1958, 3, 241.
415. F. Z e n z, N. W e i l. A. I. Ch. E. Journal, 1958, 4, 472.

Footnotes

[1]The book by the author "Mechanics of Aerosols" M., Publishing
house AN SSSR, 1955, is designated N. Fuks. Mechanics of Aerosols.

R. Bagnold. The Physics of Blown Sands and Desert Dunes. 2nd Ed., Methuen, 1954, p. 72, 163.
396. H. Rumpf. Chem.-Ingr.-Techn., 1953, 25, 317; VDI-Berichte, 1955, 6, 17.

397. A. Klimanov. Sb. nauchn. tr. Mosk. gorn. in-ta, 1955, No 15, str. 101.

398. J. Blomfield, J. Dallavalle. Publ. Health Bull., 1935 No 217.

399. J. Dawes. Safety in Mines Res. Establ., Res. Rep., No 36 and 49, 1952; J. Dawes, A. Wynn. Tam zhe, Res. Rep., No, 46, 1952.

400. A. Bagnold. The Physics of Blown Sand and Desert Dunes. London, 1941; N. Fuks. Mekhanika aerozoley (Mechanics of Aerosols). str. 317.

401. A. Andreasen. Kolloid.-Z., 1939, 86, 70; N. Fuks. Mekhanika aerozoley (Mechanics of Aerosols). str. 332.

402. N. Fuks. Mekhanika aerozoley (Mechanics of Aerosols). § 57.

403. N. Mehta, J. Smith, E. Commings. Ind. Eng. Chem., 1957, 49, 986.
404. A. Reif, C. Whyte, M. Giblin. Arch. Ind. Health, 1956, 14, 442.
405. C. Davies, H. Aylward, D. Leacey. Arch. Ind. Hyg. Occ. Med., 1951, 4, 354.
406. F. Eadie, R. Payne. Iron Age, 1954, № 10, 99.
407. W. Kroll. Chem.-Ingr.-Techn., 1955, 27, 33.
408. Chin-Young Wen, H. Simons. A. I. Ch. E. Journal, 1959, 5, 264.
409. R. Morse. Ind. Eng. Chem., 1955, 47, 1170.

410. F. Tideswell, R. Wheeler. Trans. Instn. Mining Engrs., 1938, 97, 176; N. Fuks. Mekhanika aerozoley (Mechanics of Aerosols). str. 332.

411. D. Craik, B. Miller. J. Pharmacol. and Pharmacy, 1958, 10, Suppl., 136.
412. H. Parker, W. Stevens. A. I. Ch. E. Journal, 1959, 5, 314.
413. F. D'Arcy-Smith. Ind. Chemist., 1957, 33, 181.
414. P. Bakker, P. Heertjes. Brit. Chem. Eng., 1958, 3, 241.
415. F. Zenz, N. Weil. A. I. Ch. E. Journal, 1958, 4, 472.

Footnotes

[1] The book by the author "Mechanics of Aerosols" M., Publishing House AN SSSR, 1955, is designated N. Fuks. Mechanics of Aerosols.

U. S. BOARD ON GEOGRAPHIC NAMES TRANSLITERATION SYSTEM

Block		Italic		Transliteration	Block		Italic		Transliteration
А	а	*А*	*а*	A, a	Р	р	*Р*	*р*	R, r
Б	б	*Б*	*б*	B, b	С	с	*С*	*с*	S, s
В	в	*В*	*в*	V, v	Т	т	*Т*	*т*	T, t
Г	г	*Г*	*г*	G, g	У	у	*У*	*у*	U, u
Д	д	*Д*	*д*	D, d	Ф	ф	*Ф*	*ф*	F, f
Е	е	*Е*	*е*	Ye, ye; E, e*	Х	х	*Х*	*х*	Kh, kh
Ж	ж	*Ж*	*ж*	Zh, zh	Ц	ц	*Ц*	*ц*	Ts, ts
З	з	*З*	*з*	Z, z	Ч	ч	*Ч*	*ч*	Ch, ch
И	и	*И*	*и*	I, i	Ш	ш	*Ш*	*ш*	Sh, sh
Й	й	*Й*	*й*	Y, y	Щ	щ	*Щ*	*щ*	Shch, shch
К	к	*К*	*к*	K, k	Ъ	ъ	*Ъ*	*ъ*	"
Л	л	*Л*	*л*	L, l	Ы	ы	*Ы*	*ы*	Y, y
М	м	*М*	*м*	M, m	Ь	ь	*Ь*	*ь*	'
Н	н	*Н*	*н*	N, n	Э	э	*Э*	*э*	E, e
О	о	*О*	*о*	O, o	Ю	ю	*Ю*	*ю*	Yu, yu
П	п	*П*	*п*	P, p	Я	я	*Я*	*я*	Ya, ya

* ye initially, after vowels, and after ъ, ь; e elsewhere.
When written as ё in Russian, transliterate as yë or ë.
The use of diacritical marks is preferred, but such marks
may be omitted when expediency dictates.

FOLLOWING ARE THE CORRESPONDING RUSSIAN AND ENGLISH

DESIGNATIONS OF THE TRIGONOMETRIC FUNCTIONS

Russian	English
sin	sin
cos	cos
tg	tan
ctg	cot
sec	sec
cosec	csc
sh	sinh
ch	cosh
th	tanh
cth	coth
sch	sech
csch	csch
arc sin	$\sin^{-1}$
arc cos	$\cos^{-1}$
arc tg	$\tan^{-1}$
arc ctg	$\cot^{-1}$
arc sec	$\sec^{-1}$
arc cosec	$\csc^{-1}$
arc sh	$\sinh^{-1}$
arc ch	$\cosh^{-1}$
arc th	$\tanh^{-1}$
arc cth	$\coth^{-1}$
arc sch	sech^{-1}
arc csch	csch^{-1}

---

rot	curl
lg	log